FUEL OIL ATOMIZATION

by

JOHN PLOEGER LONGWELL

B.S., University of California

1940

Submitted in Partial Fulfillment of the

Requirements for the Degree of

DOCTOR OF SCIENCE

from the

MASSACHUSETTS INSTITUTE OF TECHNOLOGY

1943

Signature of Author.....

Department of Chemical Engineering, May 10, 1943

Signature of Professor in Charge of Research Signature Redacted .....

Signature of Chairman of Department Committee on Graduate Students Signature Redacted .....

Chem. engg
Thesis
1943

M.I.T. Graduate House
Cambridge, Massachusetts
May 10, 1943

Professor George W. Swett
Secretary of the Faculty
Massachusetts Institute of Technology
Cambridge, Massachusetts

Dear Sir:

I take pleasure in submitting the attached thesis, entitled "Fuel Oil Atomization," in partial fulfillment of the requirements for the degree of Doctor of Science in Chemical Engineering.

Very sincerely yours,

John P. Longwell

ACKNOWLEDGMENT

The author wishes to express his appreciation for the help and advice of Professor Hottel and of Mr. Hulse, of the Standard Oil Development Company of New Jersey.

This work was made possible by the financial support of the Standard Oil Development Company of New Jersey.

TABLE OF CONTENTS

SUMMARY

This investigation of atomization by pressure atomizing nozzles was undertaken as part of a program devoted to the study of combustion of fuel oils. Previous workers in the field have studied the atomization and flow characteristics of particular nozzles, but the picture was incomplete and there was no attempt at generalization of the results in terms of nozzle design. The object of this work was to obtain data on the effect of design and operating conditions on the performance of this type of nozzle and to generalize these data so that they will be of use in the design of oil burning equipment.

The standard technique for studying drop size distribution consists of determining the size of a large number of individual drops and is extremely time-consuming. It was felt that the development of a more satisfactory method of studying drop size distribution was almost a prerequisite to obtaining sufficient data for generalization. The technique decided upon consisted of collecting the drops in a stream of flowing fluid which was at room temperature. This stream of fluid, in which the drops were immiscible, removed the drops from under the collecting orifice so that they would not fall on each other.

It was allowed to flow far enough so that the drops would regain their spherical shape after being deformed by impact on the fluid surface. The stream of fluid then fell into a container of alcohol kept at dry ice temperature-low enough to freeze the drops solid. The drops were then sieved while still cold, to separate them into different size groups. The relative sizes of the various fractions were determined by dissolving the oil in a known volume of benzene and comparing the color/density with a colorimeter.

The distribution could be described by a form of the Rosin Equation $= \ln 0.5$

$$R = e^{-.693 (D/D_o)^n}$$

where R is the fraction of a sample above a size D

D_o is the weight median drop diameter

n is a constant

Although it is more common to use a weight mean drop diameter as a characterizing drop dimension, the weight median drop diameter was used since this mean is just as useful in interpreting the results, and is much more convenient to find from the type of data taken.

High-speed photography indicated that under some conditions the spray cone was subject to rapid fluctuations of approximately sonic frequency. The effect of these fluctuations was to increase the drop size above what it would have been if the fluctuations had not occurred. Under some conditions these fluctuations would change frequency with a very small change of operating conditions. Such a change would cause a sudden variation in the drop size given by the nozzle. It was found that the effect of the fluctuations was less serious as the atomizing pressure was increased and the viscosity of the fluid was decreased.

The performance of nozzles of the above type may be considered properly correlated when the discharge rate, the particle size, the size distribution, and conditions under which a conical spray will be formed can be predicted.

The particle size and size distribution depend on the properties of the medium in which the atomization takes place, the energy of the fluid as it leaves the nozzle, the physical properties of the fluid being atomized, and the dimensions of the spray cone. Time did not permit the study of all of these variables.

Those studied were the pressure of atomization, the viscosity of the fluid, and the cone dimensions. The commercial nozzle used by Kolupaev in a study of this same problem permitted such a narrow range of viscosities at which the fluid would be properly atomized that it was difficult to study the effect of viscosity on atomization. For this reason a series of nozzles was built which had a considerably wider range of operating viscosities.

It was found, for conditions where no violent fluctuations of the spray occurred and the cone was well formed, that $\frac{D_o \sin \alpha/2}{r_o}$ was constant for a given atomizing pressure and viscosity. (D_o = weight-median drop diameter, r_o = radius of nozzle orifice, α = spray cone angle.) The effect of pressure and viscosity on this group can be summarized by the empirical equation:

$$\frac{D_o \sin \alpha/2}{r_o} = 0.72 \frac{e^{.705\nu}}{p^{.375}} \qquad (12)$$

p is the pressure in p.s.i.

ν is the viscosity in Stokes

The constant "n" of the Rosin Equation, which is a measure of the closeness of the distribution, was

found to depend on D_o alone and to increase as D_o increases. This means that the larger the drops the more nearly the same size they will be, and that knowledge of D_o alone is sufficient to describe the spray (at least for the nozzle type herein studied).

It should be noted that, while the weight-median drop size, D_o, decreases with increasing pressure, cone angle, and decreasing viscosity, the variable which has the most effect is the radius of the orifice. This fact indicates that to obtain good atomization small nozzles should be used.

For the nozzles built in the laboratory a discharge coefficient based on the area of the orifice was found to be independent of pressure and viscosity over a large portion of the range where good atomization was obtained. The discharge coefficient at zero viscosity is useful in comparing various nozzles and can be predicted by the equation:

$$(14) \quad c_o = \sqrt{1-bc_o^2} - abc_o^2\sqrt{a^2-1} - bc_o^2 \ln\left(\frac{1+\sqrt{1-bc_o^2}}{\sqrt{bc_o^2}\left(\sqrt{a^2-1}+a\right)}\right)$$

where

c_o is the discharge coefficient at zero viscosity

$$b = \frac{\pi^2 r_o^4}{A_s^2}\left(\frac{r_s}{r_o}\right)^2$$

$$a = \frac{r_c}{r_{ip}}$$

r_s is the average radius of a particle as it enters the swirl chamber

r_o is the radius of the orifice

r_i is the radius of the vortex at the orifice

r_{ip} is the radius at which all of the energy of a particle would be in the form of rotational energy

A_s is the combined area of the tangential slots

This equation was obtained from an approximate analysis of flow in the nozzle.

The value of "a" which depends on the size of the vortex formed is difficult to measure so an empirical correlation of this variable was resorted to. A satisfactory correlation was obtained by plotting "a" against $\frac{r_s L}{A_s}$ where L is the distance from the back of the swirl chamber to the orifice of the nozzle.

The cone angle is of interest since it affects the drop size distribution and the shape of the spray. Over most of the range of good atomization the cone angle decreases with increasing viscosity but does not change with pressure. All of the nozzles built in the laboratory had the same sort of variation with viscosity; the cone angle divided by the cone angle at zero viscosity was found to be the same func-

tion of viscosity for all the nozzles of the series.

The cone angle at zero viscosity can be estimated to within about five degrees from the equation (15) $\cos \alpha_o/2 = \frac{C_o}{1 - a^2 C_o^2 b}$

"a" can be found from a plot of "a" against $\frac{r_s L}{A_s}$ for different values of $\frac{L}{r_o}$. Although this method of estimating the cone angle is based on an approximate analysis of the flow in the nozzle, the analysis was useful primarily in indicating the factors which should enter. A correction factor in the form of different values of "a" than would be used to obtain the discharge coefficient was necessary to make the estimated cone angles agree with the measured ones.

If the jet which issues from the orifice does not form a cone, the atomization will be poor since the jet will break up into sheets, the edges of which will form large drops. The conditions under which a cone will be formed can be estimated from a graphical correlation of the data obtained in terms of the pressure above which a cone will be formed, the viscosity, the discharge coefficient, and the ratio $\frac{L}{r_o}$.

Under some conditions after a smooth cone

is formed, it will be drawn together by the surface tension of the oil. When this occurs good atomization is not expected since the cone breaks up unevenly under these conditions. The pressure above which a diverging cone will be obtained can be estimated by the empirical equation:

$$(17) \quad P_d = .39\left(\frac{\nu}{c r_o^2 \cos \alpha/2}\right)^{.78}$$

where

P_d is the pressure below which a diverging cone will not be formed in p.s.i.

ν is the viscosity in Stokes

c is the discharge coefficient

r_o is the radius of the orifice

α is the cone angle

If this pressure is not lower than that necessary to obtain a cone, there will be no region of formation of a converging cone.

Since for given values of nozzle pressure drop and fluid viscosity the ratio $\frac{D_o \sin \alpha/2}{r_o}$ is a constant, small values of the weight median drop size are obtained by making $r_o/\sin \alpha/2$ as small as possible. At a given flow rate, with pressure drop still fixed, the value of r_o will vary inversely as the

square root of the discharge coefficient; so for a given flow rate it is desirable to have as high a value of $\sqrt{C} \sin \alpha/2$ as possible. The values of the cone angle and the discharge coefficient at zero viscosity are a good criterion of the nozzle performance $\sqrt{C_o} \sin \alpha/2$ consequently will be referred to as the "atomization criterion." Since this criterion is not a function of the absolute size of the nozzle, two nozzles that are geometrically similar will have the same value of $\sqrt{C_o} \sin \alpha_o/2$ and nozzles of different size and type similar to those studied can be compared by noting the relative magnitude of $\sqrt{C_o} \sin \alpha_o/2$ The atomization criterion can be estimated either by using the correlations so far presented or by direct measurement of the cone angle and the discharge coefficient using a fluid of low viscosity such as water.

The more important effects of the design variables on the operation of the nozzle can be summarized by the following statements, based on the correlations previously mentioned:

1. As As/r_o^2 is decreased from a large value the cone angle increases and probably goes through a maximum, the discharge coefficient decreases, $\sqrt{C_o} \sin \alpha_o/2$

goes through a maximum, the viscosity for cone formation goes through a maximum, and the viscosity for diverging cone formation decreases.

2. As L/r_o is increased at one value of As/r_o^2 the cone angle decreases, the discharge coefficient increases, the viscosity for cone formation decreases markedly, and the viscosity for diverging cone formation increases slightly.

3. As r_s/r_o increases the cone angle increases, the discharge coefficient decreases, there is little effect on the viscosity of cone formation, the viscosity for the formation of a diverging cone decreases, and the value of As/r_o^2 for the same value of $\sqrt{C_o}$ sin $\alpha_o/2$ increases.

4. The radius of the orifice affects only the viscosity of diverging cone formation which is much less as the radius becomes smaller.

It is evident that L/r_o should be as small as possible for this type of design, and it was found that

its value for most commercial nozzles was unnecessarily high. Since the maximum of the curve of $\sqrt{Co}\ \sin \alpha_o/2$ vs A_s/r_o^2 is not at the same value of As/r_o^2 as the maximum for the viscosity of cone formation, a choice of As/r_o^2 depends on whether range of atomization or quality of atomization is the primary consideration. A nozzle which would be a compromise and would have good atomization and good range, but could be slightly improved in either respect, at the expense of the other, would have the following dimensions:

A_s/r_o^2 20

L/r_o 3

r_s/r_o 3

The discharge coefficient would be about 0.53, and the cone angle would be about 77°. When the value of r_o becomes less than 0.03 cm, the viscosity of oil which can be atomized is limited by the fact that the cone tends to converge.

INTRODUCTION

This work is part of a program at M. I. T. which is devoted to the study of combustion in oil furnaces. It is hoped to be able to combine knowledge of the rate of combustion of individual drops in terms of their size, composition, temperature, and surrounding atmosphere with knowledge of the process of mixing diffusion and heat transfer in the combustion chamber in such a way as to make possible the prediction of furnace behavior in terms of the geometry of the combustion chamber, the various flow rates, and the equipment used. This thesis is concerned with the problem of estimating the particle size distribution of the spray as it enters the combustion chamber as a function of the properties of the oil and of the atomizing equipment used.

The pressure or mechanical atomizer has extensive application both in industrial and domestic furnaces, and was chosen as the first type of atomizing equipment to study. The atomizing action of this type depends on giving a jet of fuel a high rotational velocity so that as it leaves the orifice of the nozzle it takes the form of a thin conical sheet. This sheet then breaks into particles which are much smaller than

would be obtained if a jet with no rotation had been used at the same pressure.

Rotation is given to the jet by bringing the fluid tangentially into a swirl chamber which precedes the orifice. The radius of the swirl chamber is larger than that of the orifice, and as the particles of fluid are forced to rotate in a path of smaller radius they gain in rotational energy at the expense of the pressure head. By making use of this principle large amounts of rotational energy can be obtained without the necessity of using very small tangential passages. A disadvantage of this type of atomizer is that since the flow rate varies as the square root of the pressure, and since proper atomization is not obtained at low pressures, large variations in flow rate can not be obtained without going to very high pressures. Some special types of mechanical atomizers have been developed which have a high turn-down ratio, that is, a large variation of flow rate within a relatively narrow pressure range. One type of high turn-down ratio nozzle bleeds fluid from the back of the swirl chamber to decrease the flow rate, and another bleeds fluid from the front of the swirl chamber at the orifice for the same purpose. Time was not available in which to study all

of the types so the investigation was confined to the simplest form with no bleeding. Figures 2 and 3 in the section on apparatus and procedure are drawings of nozzles studied.

Although previous workers (1), (2), (3), (4), have obtained data on various types of nozzles, it was not possible to use their data to predict the performance of a nozzle other than the specific type tested under their test conditions. One of the objects of this work was to generalize the results on various nozzles. In order to do this in a reasonable amount of time it was necessary to develop a technique of studying drop sizes which was less laborious than the previously used technique of collecting the drops on a plate and then counting and measuring individual drops. Information was also lacking as to the effect of nozzle dimensions on discharge rates, cone angles, and maximum viscosity at which a diverging cone could be obtained at a given pressure. Since these variables are also of interest to the furnace designer, they were investigated as well as the drop size distribution.

APPARATUS AND PROCEDURE

Study of Size Distribution

The equipment used to supply the oil under pressure to the nozzle and to confine the spray was the same as that used by Kolupaev (1). Figure 1 is a diagrammatic sketch of this apparatus. The oil was contained in a pressure chamber of approximately one gallon capacity, which could be held at the desired temperature. A calibrated thermocouple was in the chamber near the point of exit of the oil, and the oil was constantly stirred when held at a temperature different than that of the room. The pressure, supplied by compressed nitrogen, was measured and held constant by a pressure regulator on the nitrogen cylinder. In order to assure constant pressure throughout the run, before turning on the spray, nitrogen was bled from the cylinder at approximately the same rate at which it would flow during the run. When the spray was turned on the bleed valve was shut off so that there was no change in the nitrogen flow rate and, therefore, no variation of pressure. If this precaution was not taken the pressure would drop as much as ten pounds during a run. The spray was turned off by a plug valve which was placed just before the nozzle. The temperature of the nozzle holder was measured and held at the same temperature as the oil.

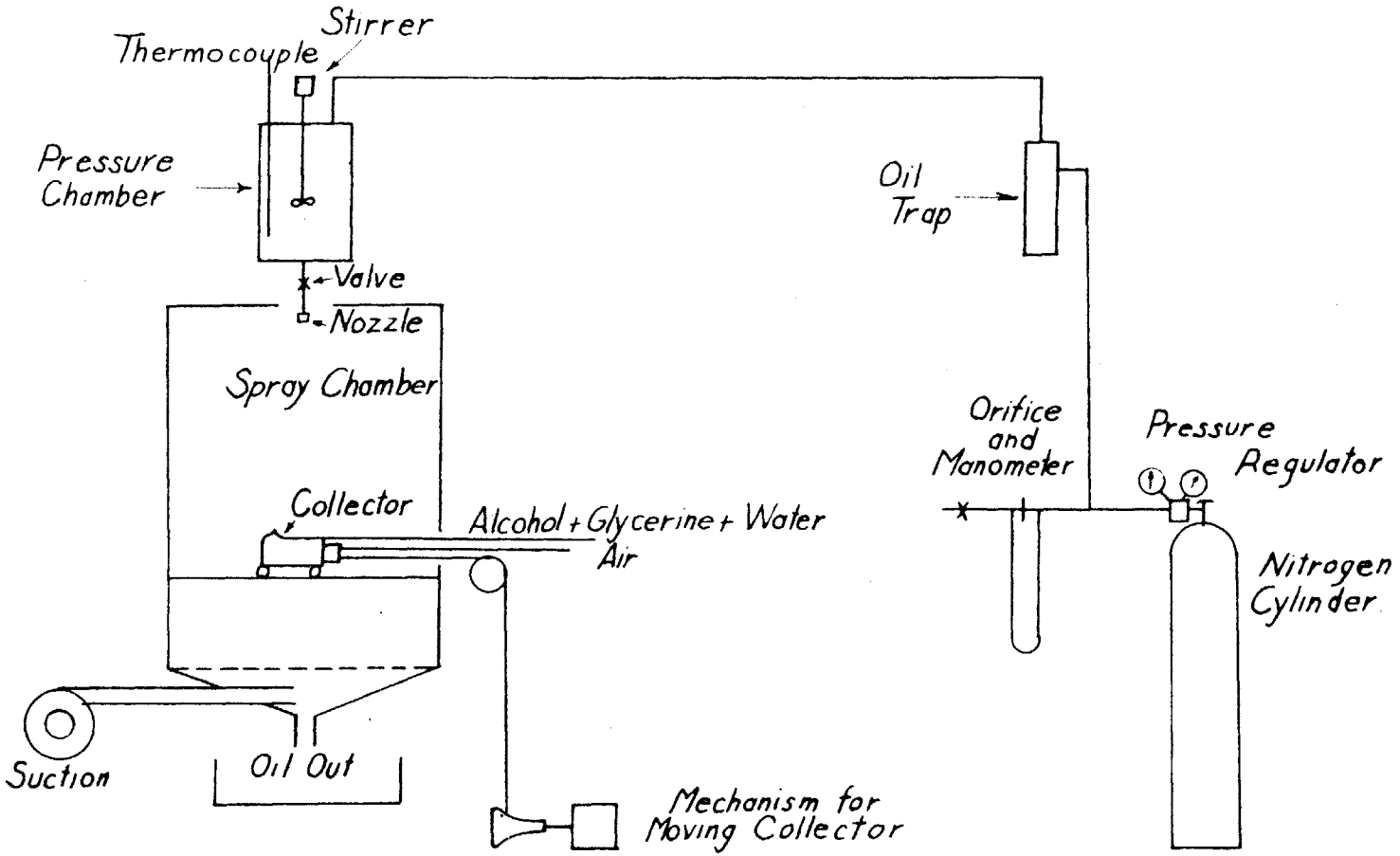
Stirrer
Thermocouple
Pressure Chamber
Valve
Nozzle
Spray Chamber
Collector
Alcohol + Glycerine + Water
Air
Suction
Oil Out
Mechanism for Moving Collector
Oil Trap
Orifice and Manometer
Pressure Regulator
Nitrogen Cylinder

Fig. 1

Air was drawn through the chamber by a vacuum cleaner blower in order to increase the falling rate of the smaller particles. The oil spray landed on a mat of steel wool, and was collected on a pan beneath the spray chamber. This oil was discarded in the runs where it was heated since it tended to change viscosity on long heating, and its viscosity was taken from a viscosity-temperature curve for fresh oil. The oil that was sprayed at room temperature was re-used since its viscosity was measured before each run with a Saybolt viscosimeter.

The device used to hold the nozzles was the same as that used by Kolupaev, as was the Todd 58 x 40 burner tip. The nozzle and nozzle holder are shown in Fig. 3. Fig. 2 gives the dimensions and shape of the nozzles used in the greater portion of the work of this thesis. These nozzles were manufactured in the laboratory and will fit in the same holder as the Todd 58 x 40. They are made in two parts so that a number of combinations of slots, swirl chambers, and orifices could be studied without building a nozzle for each type. The reason for not using commercial nozzles was that a wider range of nozzle types could be studied this way, and that this type of nozzle gave considerably better performance in regard to the range of viscosity at

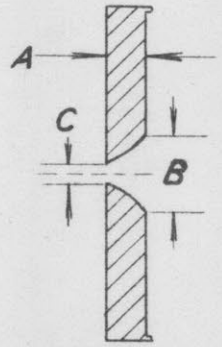

CROSS-SECTION
OF NOZZLE

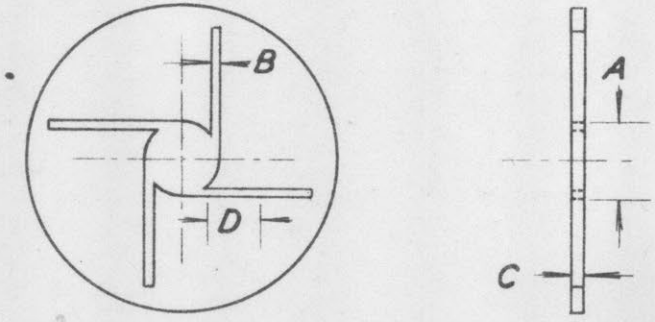

PLATE

NOZZLE	A	B	C
8	.030	.115	.0565
10	.044	.110	.0490
11	.058	.170	.0910
12	.060	.130	.0315
14	.049	.170	.0440
18	.060	.200	.111
10	.044	.110	.0525
15	.005	.047	.047

PLATE	A	B	C	D
1	.205	.016	.034	.2
2	.205	.029	.034	.2
3	.125	.023	.044	.06
5	.120	.016	.044	.02
6	.250	.047	.064	.17
D IS THE LENGTH OF SLOT THRU WHICH THE FLUID MUST FLOW				

FIG. 2

ALL DIMENSIONS IN INCHES

BURNER TIP 10X3 MEANS NOZZLE NO. 10 COMBINED WITH PLATE NO. 3

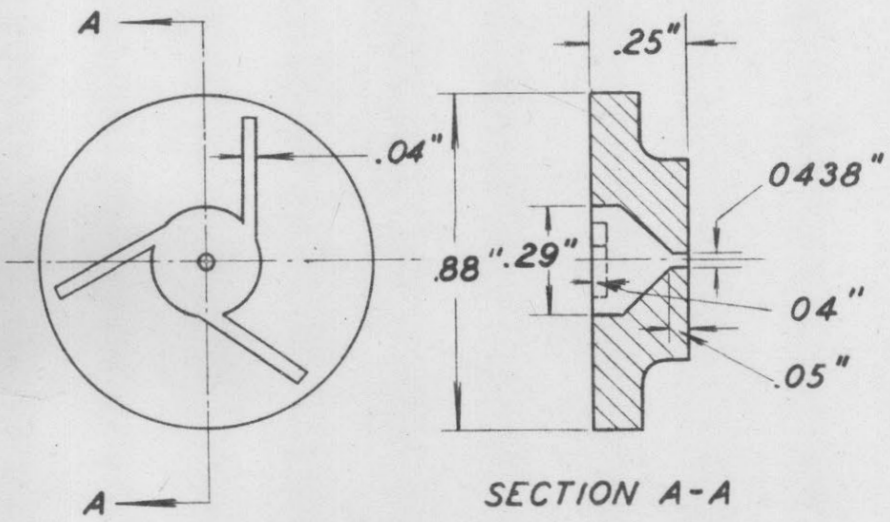

TODD 58 X 40 BURNER TIP

FIG 3

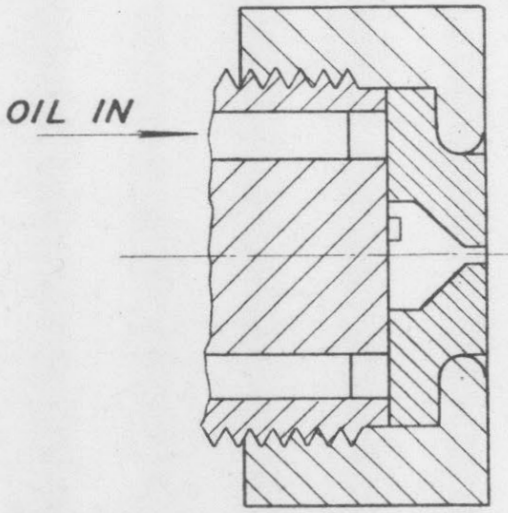

SECTION OF TODD 58 X 40 BURNER TIP AND PART OF HOLDER TWICE ACTUAL SIZE

which successful atomization could be obtained.

Considerable work was done with the Todd 58 x 40 nozzle used by Kolupaev before it was discovered that the orifice was chipped. When this was noticed another similar nozzle was obtained from the Todd Company. The nozzle used by Kolupaev will be referred to as T 58x40 #1 and the other one as T58x40 #2. Photographs of the orifices of these nozzles are shown in Fig. 4. In both cases the orifices were slightly out of round so that neither of them could be considered perfect. The nozzles made for this work had carefully polished orifices, which were periodically checked for roughness. The reason that orifice 10' is slightly larger than orifice 10 is that some notches were found in 10 and their removal entailed the enlargement of the orifice. These nozzles will be referred to by the following system: 10x3 would designate orifice No. 10, and plate No. 3 as shown in Fig. 2.

Although the drop size and flow rate varies along any radius of the spray cone, it was felt that at this stage of the investigation the added value of knowing these quantities at every point in the spray was not sufficient to merit the additional labor of obtaining the data. For this reason average values were obtained by taking the samples of drops along a radius.

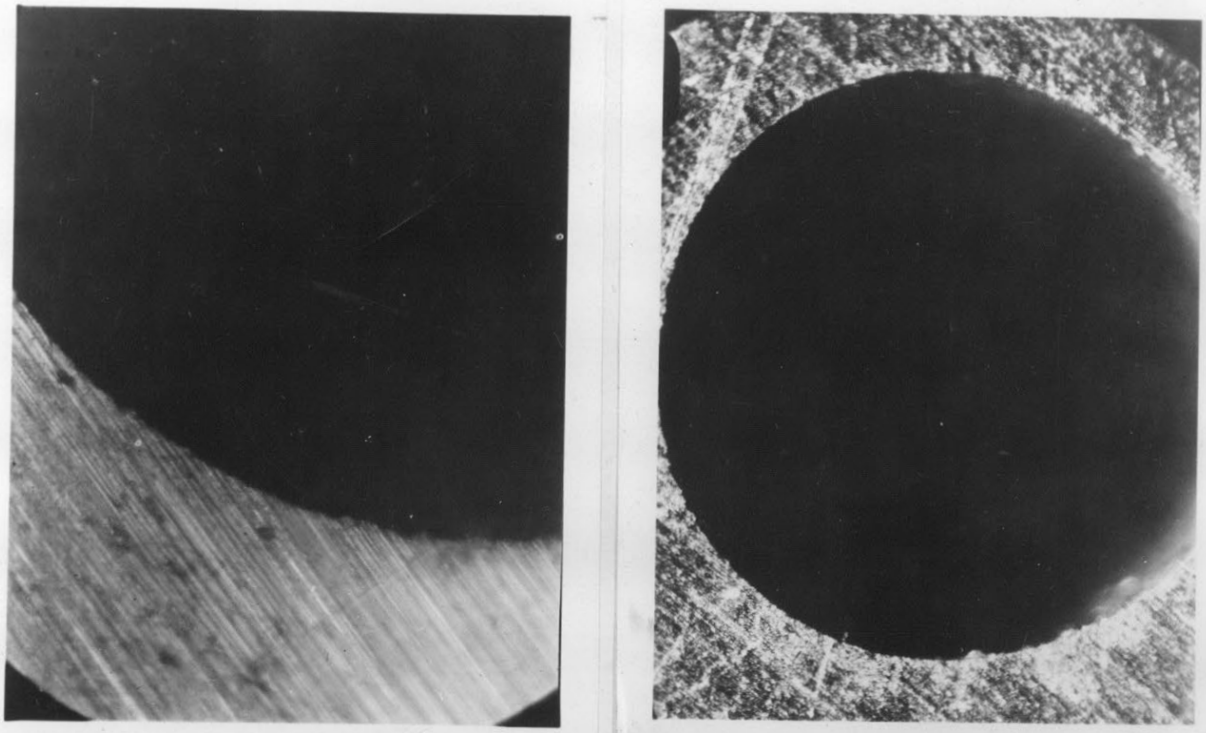

PHOTOGRAPHS OF TODD 58x40 #2 NOZZLE
AVERAGE DIAMETER .0438 INCHES

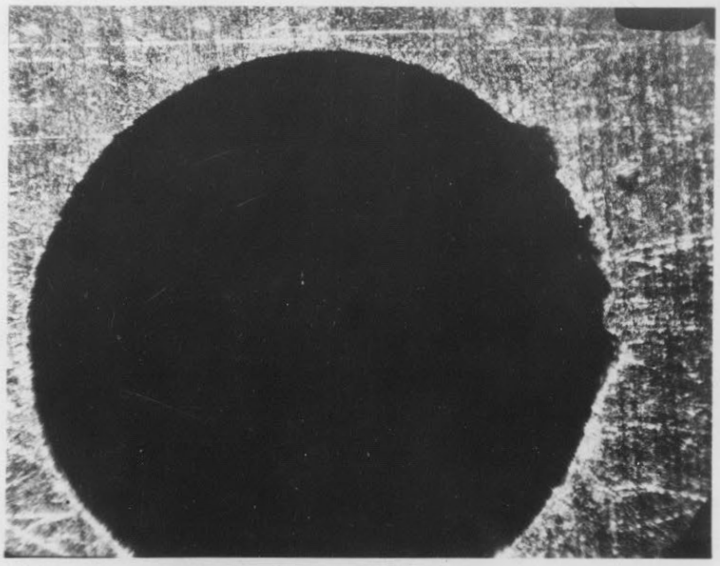

PHOTOGRAPHS OF TODD 58x40 #1 NOZZLE
AVERAGE DIAMETER .0418 INCHES

Fig. 4

If it is assumed that the area of the sampler is small, a representative sample of the spray will be obtained if the sampler is moved along a radius at a velocity inversely proportional to the radius. This type of motion can be obtained by winding a string on the surface of a rectangular hyperbola of revolution which is rotated at a constant angular velocity. In the actual apparatus it is not possible to have the collector going at the required velocity at the center of the spray; however it was felt that a reasonable approximation to the representative sample was obtained with the apparatus constructed. The sampling was found to be satisfactory by comparing the results of an integration of point samples with the results given by the sampler when drawn across the spray with the apparatus constructed.

The spray was allowed to run at least twenty seconds before the sample was taken to make sure that the small drops had a chance to reach the point of collection.

A cross section of the sampler is shown in Fig. 5. It was so constructed that it could be opened and shut by compressed air at the proper points along a radius of a spray cone. When it was open the drops of oil would fall in the opening upon a glass plate over

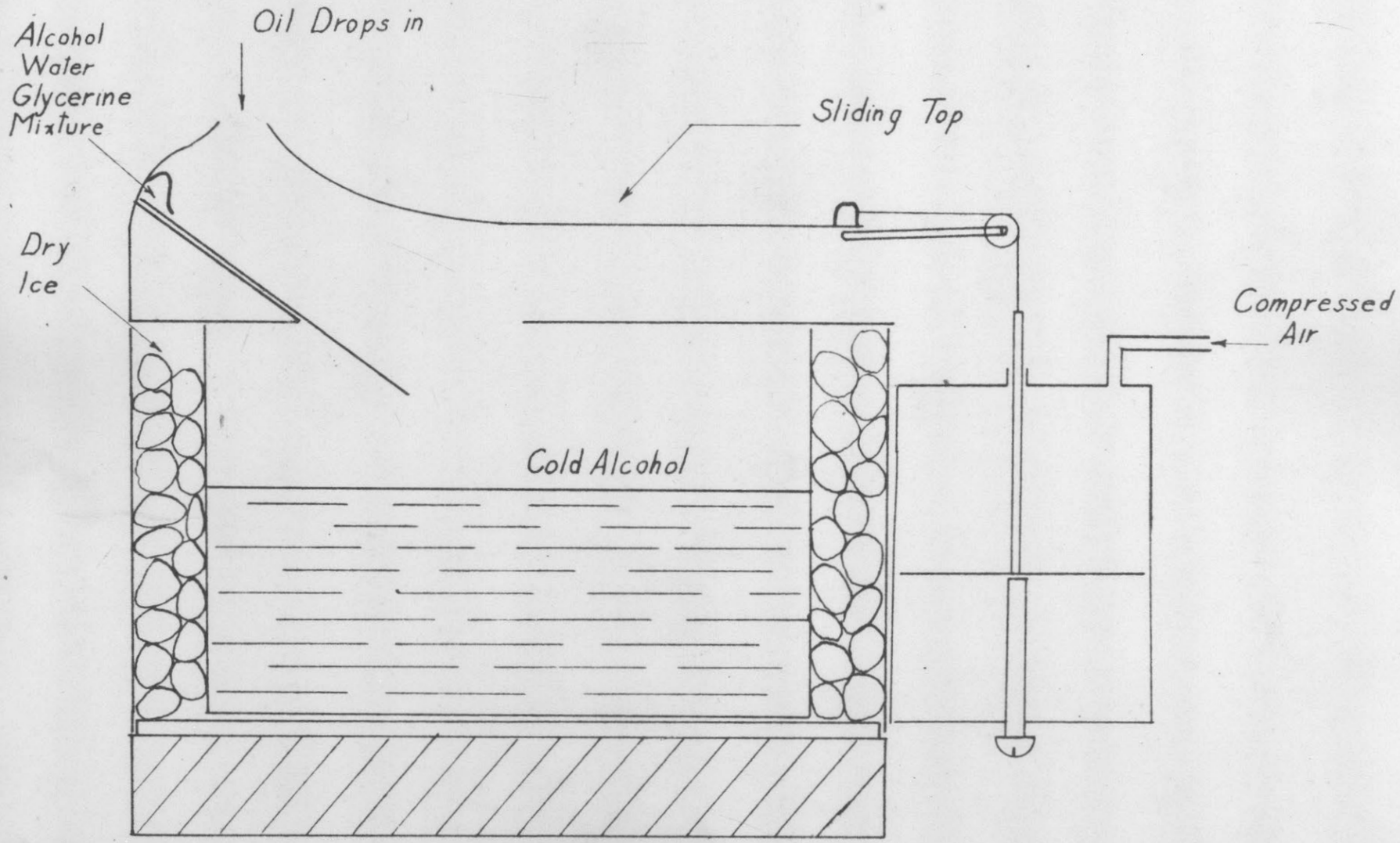

DROP SAMPLER

Full Scale

FIG. 5

which a mixture of alcohol, water, and glycerine was flowing. This stream of fluid was at room temperature and served the purpose of allowing the drops to regain their spherical shape after impact with the fluid surface, and of moving them from under the opening of the sampler so that the concentration of drops in the liquid wouldn't become high enough to make agglomeration serious. The mixture of fluid and oil drops then fell into a container of alcohol which was approximately the temperature of dry ice. This froze the drops and the sample could be handled without fear of agglomeration. The sample, after being collected in this manner, was then transferred to a previously chilled beaker which contained lumps of dry ice, where it was kept until sieved.

A cross section of the apparatus used for sieving is shown in Fig. 6. This apparatus consists of a series of sieves mounted above each other so that the liquid carrying the frozen oil drops will flow from one to the other. The smallest drops are filtered out by glass wool and the liquid is drawn out by an aspirator. Usually four sieves were used which gave four points on a distribution curve. The whole system is kept cold by the surrounding layer of dry ice. After

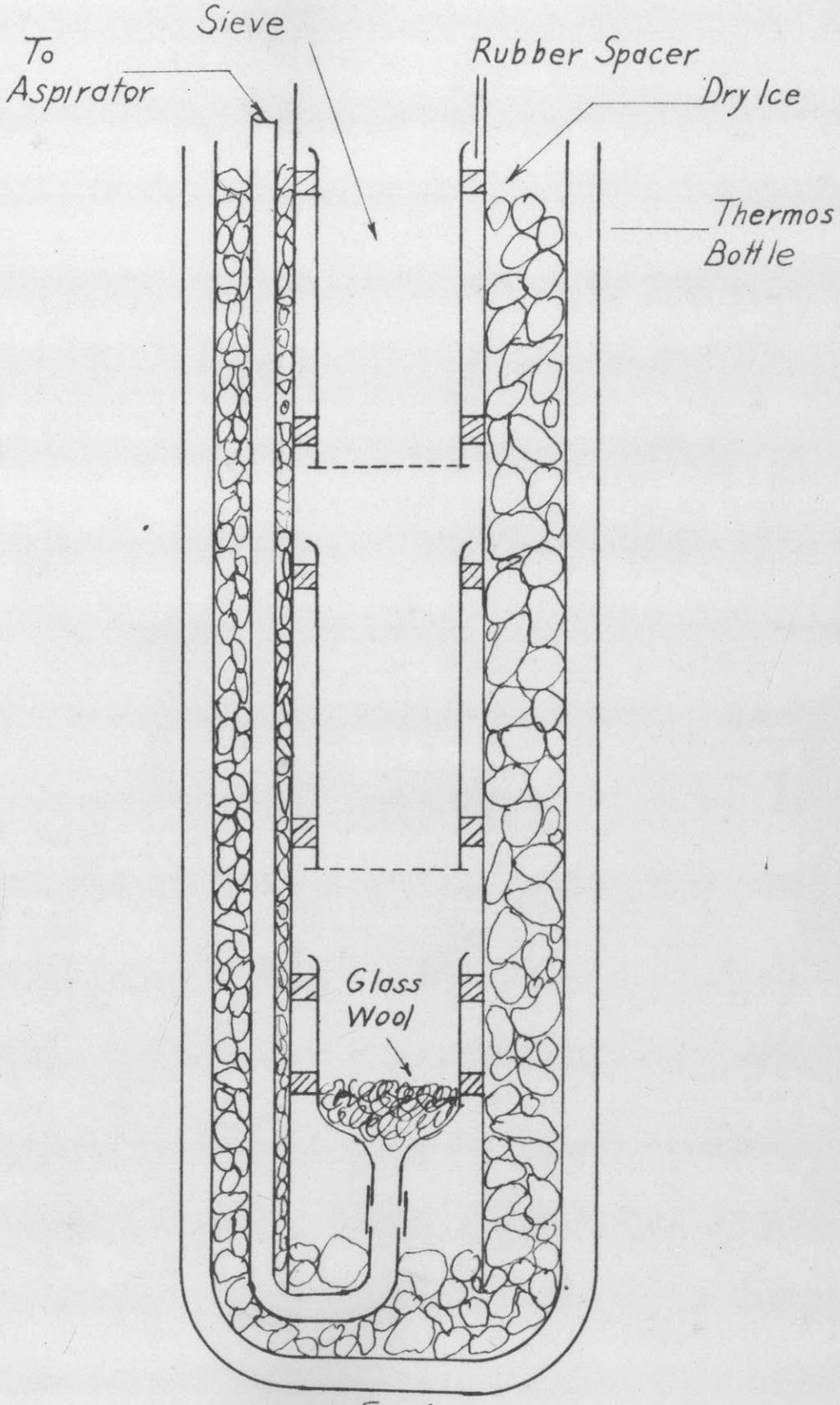

Fig. 6
SIEVING APPARATUS
Full Scale

all of the liquid and oil drop mixture has been poured through the sieves, the sieves are washed with cold alcohol to work the drops down to their proper sieve. It was found that about fifty cc. was sufficient for each sieve if it was poured quite slowly and from a height of about one foot. The impact caused by the fluid falling from this height helped to force the small drops through their holes. When the washing was completed the sieves were removed and allowed to dry. In order to obtain the drop size distribution knowledge of the relative weights of the oil on the various sieves and on the glass wool filter is necessary. These relative weights were obtained by dissolving the oil in benzene, measuring the volume of the solution, and comparing the color of the solution with a colorimeter. The color density of the solution was found to be proportional to the concentration, so enough information was available to find the relative weights.

Some of these techniques are new and required considerable investigation. A more complete discussion of the problem of freezing and sieving oil drops is given in the Appendix.

Discharge Rates

The discharge rates at various pressures and viscosities were measured by collecting a sample in a bottle for about ten seconds. The spray was started and stopped by opening and shutting the plug valve. It is not believed that an appreciable error was introduced by the inertia of the system since no trend of discharge rates was found with shorter times of collection of sample. The apparatus used in Fig.1 was used only in the study of size distribution; for other work a desk-mounted apparatus was used to supply the oil under pressure making observations of the spray more convenient. With the exception of the relative sizes and positions of the various parts, the apparatus was the same as that mounted on the spray chamber, consequently no further description will be given. The time was measured with a stopwatch and the volume collected was measured with a graduated cylinder.

Cone Angle and Vortex Measurements

The cone angles were measured by two techniques. Some of the measurements were taken from photographs of the spray cone and others by direct measurement of the cone angle with a bevel gauge. The lighting for the photographic work was supplied by high-speed flash ap-

paratus. Some of the pictures of the T 58X40 nozzle were taken using an apparatus which gave a short enough flash so that the motion seemed to be entirely stopped, but the majority of them were taken with an apparatus which did not give a short enough flash to show any detail of the formation of drops. The vortex in the nozzle was studied by taking photographs of lucite models.

The Formation of a Cone

At a given fluid viscosity as the pressure is increased the jet of liquid will change from an irregular shape to a smooth cone. This point is of interest since good atomization cannot be expected until a smooth cone is formed. Fig. 7 illustrates this change. The pressure at which this change occurs was found by increasing the pressure of atomization until the cone was formed.

Formation of a Diverging Cone

When the smooth cone is formed the surface tension of the fluid may pull it together. The pressure at which the drops formed no longer seemed to converge was judged visually as a function of pressure and viscosity. Fig. 8 illustrates a cone which breaks up before com-

HIGH SPEED PHOTOGRAPHS OF LUCITE NOZZLE

The nozzle is on the right, the spray cone in the center, and the collecting bottle on the left of the photograph.

Lucite Model of 10x3
Viscosity .85 $cm^2/sec.$
Pressure 80 p.s.i.

Cone not formed.

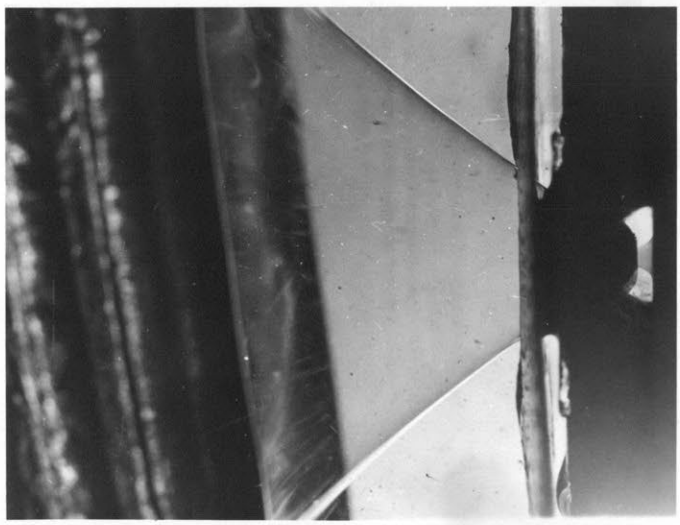

Lucite Model of 10x3
Viscosity .85 $cm^2/sec.$
Pressure 120 p.s.i.

Cone formed but no vortex core. Increase of one angle is caused by the bottle

Lucite Model of 10x3
Viscosity .85 $cm^2/sec.$
Pressure 160 p.s.i.

Beginning of vortex core is visible.

FIG. 7

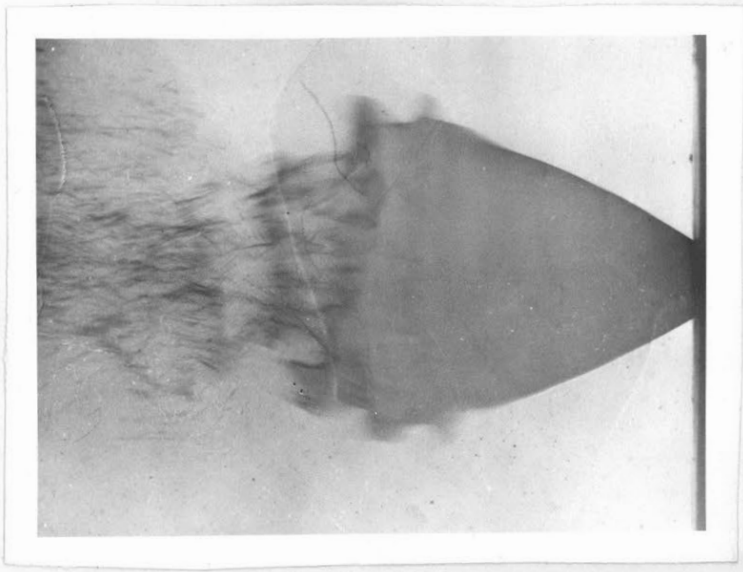

CONE JUDGED AS CONVERGING

12x3 Nozzle Viscosity .16 Poises Pressure 21 p.s.i.

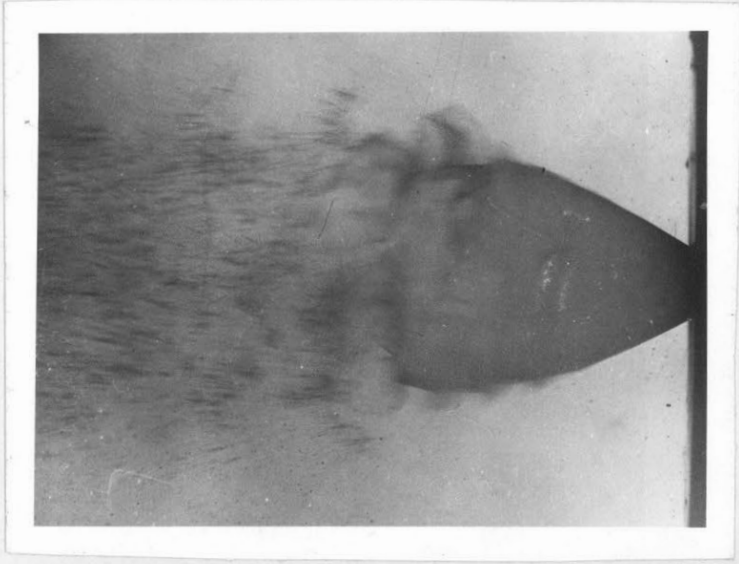

CONE JUDGED AS NOT CONVERGING

12x3 Nozzle Viscosity .16 Poises Pressure 25 p.s.i.

FIG. 8

pletely converging but in which the drops converge, and one which was judged barely satisfactory.

Oils Used

For those runs in which a heated oil was desired, a Bunker C oil, #DBY-6958 obtained from the Colonial Beacon Oil Co., was used. A few runs were made using some heavy oils obtained from the Standard Oil Development Co. of New Jersey. The oils used are noted with the corresponding runs in Table 5. The unheated oils were coumpounded from locally obtained materials.

RESULTS AND DISCUSSION

Drop Size Distribution

The data taken on drop size distribution are values of R, the fraction of the total weight above a certain size of drop D. Typical results are given in Fig. 7 where R is plotted as a function of D. The size D is the diameter of a circle which could be placed in 25% of the sieve openings, the rest being too small. A more detailed discussion of this choice will be found in the Expansion of Procedure which is given in the Appendix. To use this information on size distribution it is desirable to know the weight of a drop which will just be held back by the sieve opening of size D. It is felt that, for the work on unheated oil, this weight can be taken as the weight of a solid sphere of oil diameter D.

When frozen drops of Bunker C oil were examined under the microscope, it was found that while some of the drops appeared to have not included air many of them did contain air bubbles. This amount of air varied from a very small fraction of the total volume to drops which appeared as mere shells of oil. Values of drop density based on the diameter of the spheres varied between .5 and .85 for this oil. No effort was made to obtain good sampling in these measurements and probably the average density for those particular runs lies somewhere between the two values. A more

detailed discussion of these measurements is given in the Appendix. Examination of the frozen drops obtained with oil which was atomized at ambient temperature indicated that very little air was included in this case. It is estimated that the amount for the worst condition examined was the order of 5%*. Since the oil which was atomized at room temperature does not change in viscosity as it falls, and as it strikes the liquid surface in the collector, the bubbles are more easily broken than is the case for the Bunker C oil which probably has a very high viscosity by the time it has fallen through the air very far. Examination showed that the amount of included air did increase as the atomizing viscosity of the oil was increased. The discussion of atomization given in this section is based on the atomization of room temperature oil which can, within the experimental error, be treated as spheres of solid oil.

If the data on size distribution is to be handled mathematically in the study of combustion, it is necessary to represent it by some sort of an equation. The empirical equation,

$$(1) \quad R = e^{-b(D)^n}$$

where R is the fractional weight above a particle size D

e is the logrithmic base, and

b, n are constants

has been successfully used by other investigators (1) (6)

* This estimate was made by inspection of frozen drops under the microscope. The worst condition was for =.6 cm./sec. P=120 p.s.i.

to represent particle size distribution. It is commonly known as the Rosin equation.

The work of Kolupaev (1) established the value of the Rosin equation in representing data for this type of atomization. His work covered values of R from .01 to .999, and although a single value of n would not cover the whole curve if high values of R were included, it would for values of R between .01 and .99. Values of n for this work varied between 2.2 and 4.9 for R less than 0.5. A single value of 2.8 was recommended for use in this range. Houghton (4) reported some data on drop sizes for the atomization of water in a similar type of nozzle. It was found that this data was also quite well represented by the Rosin equation.

Most of the values of R obtained in this work fell between limits of .10 and .85. In general the results fitted the Rosin equation quite well. This equation will give a straight line of ln ln 1/R is plotted against ln D. Fig. 7 is such a plot. n corresponds to the slope of the line on this plot, and is a measure of the spread of the distribution. A high value of n corresponds to a closely sized group of particles. It is desirable to express the constant b in terms of a mean particle size so that the size of different groups can be easily compared. The most common method of doing this is to use a mean drop diameter defined by the equation

$$(2) \qquad Dm = \int_0^1 D\,dR$$

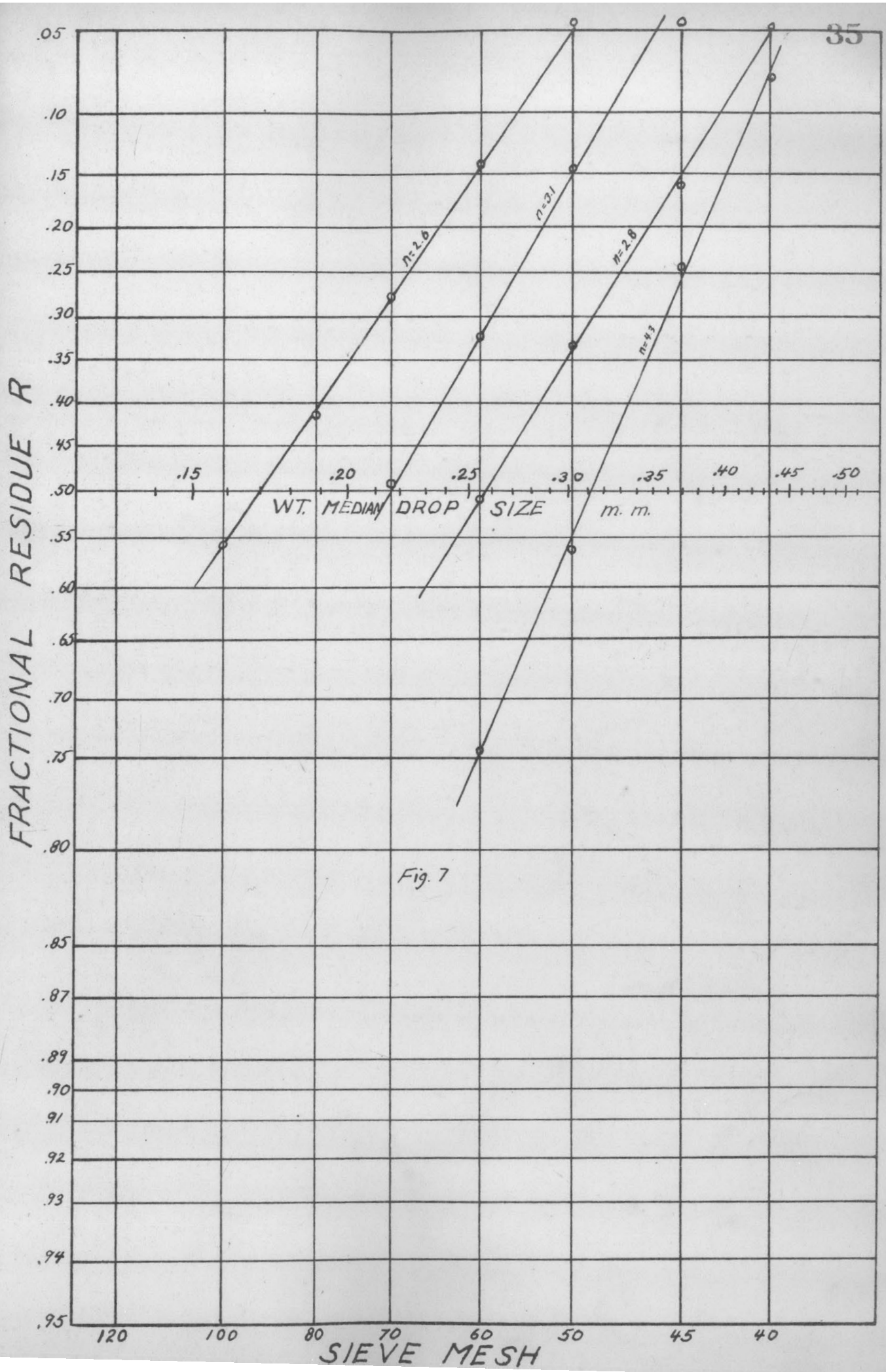
FRACTIONAL RESIDUE R
.05
.10
.15
.20
.25
.30
.35
.40
.45
.50
.55
.60
.65
.70
.75
.80
.85
.87
.89
.90
.91
.92
.93
.94
.95
n=2.6
n=3.1
n=2.8
n=4.3
.15
.20
.25
.30
.35
.40
.45
.50
WT. MEDIAN DROP SIZE m. m.
120
100
80
70
60
50
45
40
SIEVE MESH

Fig. 7

When this integral is evaluated b can be eliminated to give the equation:

(3) $$R = e^{-\left(\frac{1}{n}! \; D/Dm\right)^n}$$

In this work the characteristic size that will be used is the size at which the value of R is 0.5. This value, which will be called Do, is very convenient to use because it can be found directly from a graph like Fig. 7. When b is eliminated by using the definition of Do, the Rosin equation becomes

(4) $$R = e^{-\frac{\ln .5}{Do^n} D^n} \qquad R = e^{-.693\left(\frac{D}{Do}\right)^n}$$

This equation has the advantage of being somewhat simpler in form than Eq. (3). Do and Dm have very nearly the same value and will coincide at one value of n. at $n = 2$, $Do/Dm = .94$; $n = 4$, $Do/Dm = 1.005$

A median value is defined as that value which divides a distribution so that an equal number of items are on each side of it. If the word item is defined as a certain weight of oil it can be seen that Do could be called the weight median drop diameter as contrasted with Dm which is the weight mean drop diameter.

All the data on drop size were handled by plotting as in Fig. 7 to determine the median drop size Do and the exponent n of the Rosin equation. The original data appear in Table V. Runs 1 to 34 were taken with the T58x40 #1 nozzle. The pressure was varied between 80 and 145 p.s.i., and the viscosity was varied between .14 and .50 poises by heating

the Bunker C oil which was used. In runs 35 to 59 the T 58x40 #2 was used. The atomizing pressure was 105 p.s.i., and the viscosity variation was from .095 to .88 poises which was also obtained by heating a Bunker C oil. The 10x3 nozzle was used in runs 60 to 98 in which a variety of oils were used; the pressure varied between 30 and 170 p.s.i., and the viscosity range was .09 to .76 poises. Runs 99 to 129 in which the affect of nozzle design was studied as well as the affect of pressure and viscosity made use of a number of different nozzles. A mixture of #2 fuel oil, paraffin, and Bunker C was used. The range of pressures was 50 to 300 p.s.i., and the range of viscosities was from .082 to .83 poises.

Runs 99 to 131 warrent discussion here, and the rest will be discussed in the Appendix.

The variables which might be expected to affect the size distribution and size can be classified as follows:

1. Properties of the surrounding atmosphere and chamber.
2. Design of the nozzle.
3. Physical properties of the fluid being atomized.
4. Pressure drop through the nozzle.

1. Properties of the surrounding atmosphere and chamber.

The surrounding atmosphere can have an effect due to its physical properties, and due to its effect as a heat transfer medium which may change the phsysical properties of

the oil as it is breaking into drops. In all cases air from the room was used and the chamber was at room temperature so that there was very little change in either heat transfer characteristics or physical properties. When Bunker C was atomized its temperature at the orifice was of the order of 100°C. Since the change in density of the oil is small with temperature changes of this magnitude, viscosity and surface tension would be expected to be the variables whose change should have the most effect. Both of them increase as the temperature is lowered, and since drop size increases with their increase it would be expected that a greater drop size would be found for the case of an oil sprayed into an atmosphere of colder air than if it had been sprayed into an atmosphere of the same temperature. As has already been noted, the amount of air inclusion is greater for the case of spray being cooled by the atmosphere. This would also cause the drop size, as measured by the technique used in this work, to appear larger. Fig. 8 illustrates the result of spraying hot oil as compared to that of spraying cold oil. It can be seen that the curves approach each other at low viscosities. This could be due to the fact that viscosity has little effect on atomization at low values of viscosity, and that the viscosity changes less with temperature in the range of .1 poises than at higher viscosities, or it could be due to less entrapment of air at low viscosities, if such was the case. However, there is no evidence as to

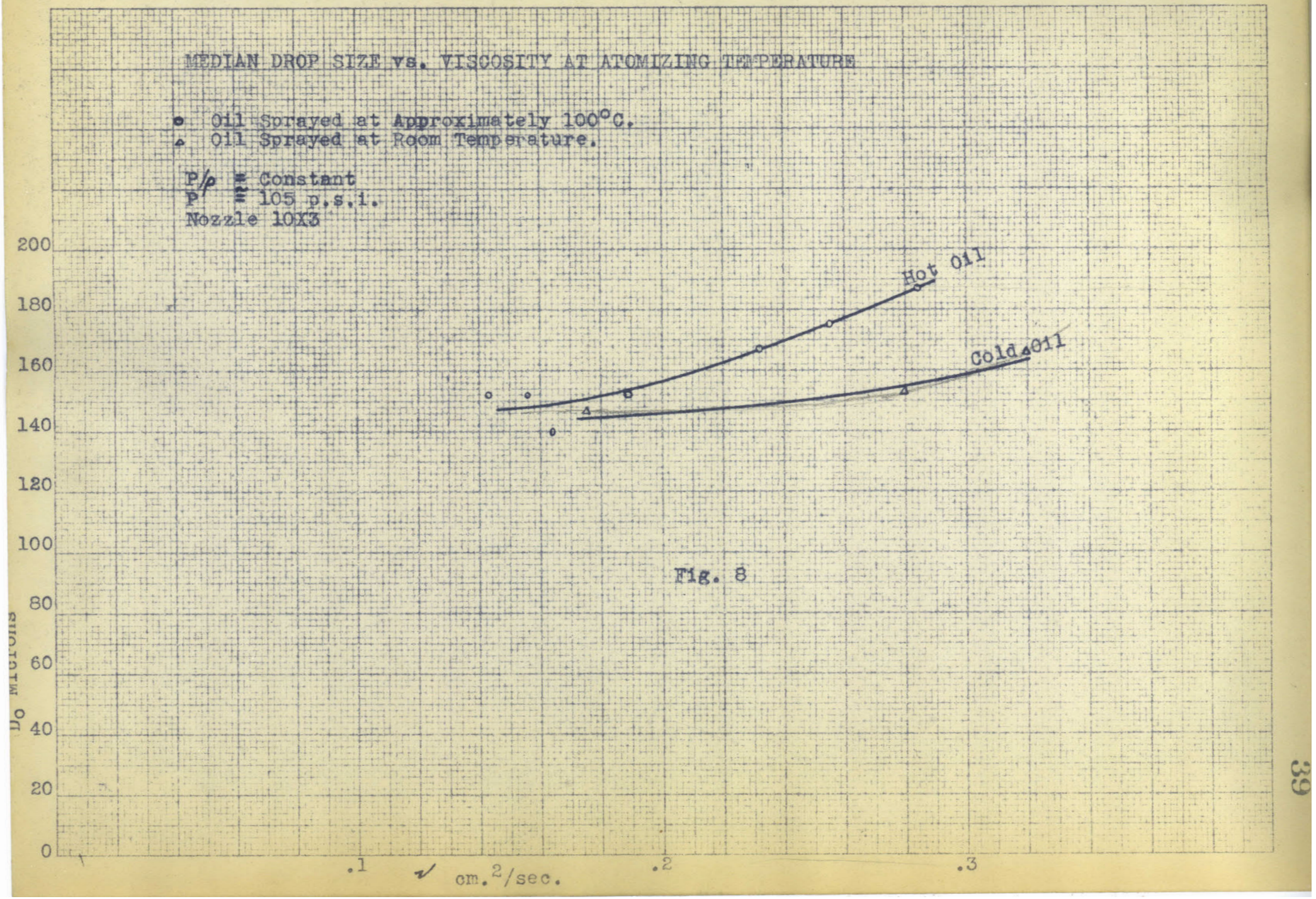
MEDIAN DROP SIZE vs. VISCOSITY AT ATOMIZING TEMPERATURE
o Oil Sprayed at Approximately 100°C.
Δ Oil Sprayed at Room Temperature.
P/ρ = Constant
P = 105 p.s.i.
Nozzle 10X3
Hot Oil
Cold Oil
200
180
160
140
120
100
80
60
40
20
0
.1
.2
.3
ν cm.²/sec.
Do Microns

Fig. 8

the separate mechanisms. The same effect was noted with the T 58x40 #2 nozzle, heated oil giving a Do of 160 microns at .1 stokes, and 105 p.s.i. while the value that would have been expected from work on room temperature oil was 145 microns.

Since the heat transfer conditions in a furnace are not comparable to those in the spray chamber used, and since using room temperature oil eliminated the variables of air entrainment and temperature difference, it was decided to shift to the room temperature oil after some work had been done on heated oils.

2. The design of the nozzle

The function of the nozzle is to eject the fluid in a conical sheet. The design of a particular nozzle will determine the angle of the cone and the thickness of the sheet of fluid as it leaves the orifice for given fluid properties and energy. The nozzle dimensions which determine these variables will be discussed in detail in the section on nozzle design.

There are certain regions of operation in which some of these nozzles give cone angles and film thicknesses which fluctuate periodically. The frequency of these fluctuations varies from below sonic up through the sonic range, and a nozzle will often give a clear musical note. The high-speed photographs on the next page illustrate the nature of

30 p.s.i.

60 p.s.i.

90 p.s.i.

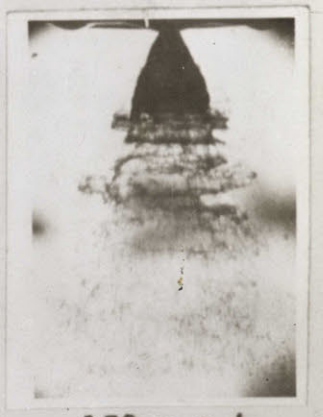

130 p.s.i.

VISCOSITY EQUALS 0.19 STOKES

70 p.s.i.

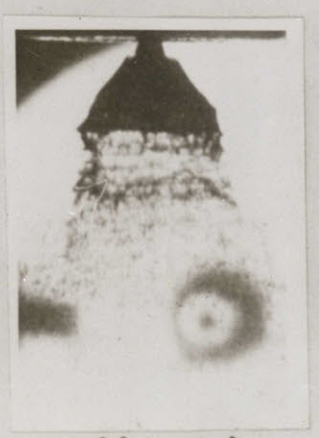

90 p.s.i.

105 p.s.i.

130 p.s.i.

VISCOSITY EQUALS 0.28 STOKES

HIGH SPEED PHOTOGRAPHS OF TODD 58x40 #2 NOZZLE

pages interchanged. See next page here

When this happens the edges of the pieces probably have a chance to draw together, and thus form large drops. The drop size for cases in which there were vibrations did not correlate with the drop size obtained for the other cases, and in general it can be said that the more violent the vibrations the greater the deviation from the correlation. For low viscosities the effect is less pronounced since the cone breaks up much sooner. Increasing the pressure also shortens the length of the cone and reduces the effect of the fluctuations. This is borne out by the fact that the correlation is much better at high pressures and low viscosities than at low pressures and high viscosities.

A characteristic history of the cone, for a nozzle which gives fluctuations, as the pressure is increased at constant viscosity is as follows: When the cone is first formed it is long and smooth; as the pressure is increased the cone becomes shorter, and at certain pressure it will shorten suddenly and will vibrate. As the pressure is further increased the frequency of the vibrations increase but the amplitude decreases. It was found that at the point where the vibrations first started the drop size would change suddenly. Also the frequency of the vibration may suddenly change as is the case with the T 58x40 producing a discontinuity in drop size. This nozzle and the 10x3 were studied in more detail than the others and a more complete discussion

skip to 2nd page following.

this fluctuation. There is evidence that these fluctuations originate within the nozzle itself. First, some of the pictures show the change in cone angle starting very near the orifice of the nozzle, and second, when the fluctuations are of sonic frequency interferring with the cone mechanically does not change the pitch of the sound given off. If these fluctuations were caused by the action of the atmosphere on the sheet it would be expected that the frequency would change. Judging from the pictures, it would seem that any cross-section of the cone at right angles to the axis of the cone would be circular. The evidence for this is that in general both sides of the cone change at the same time. If the cross-section were not circular this would not be the case since the orientation of the nozzle is random, and the cone would be unsymmetrical from some view. Such a condition could be caused by the size of the vortex in the orifice of the nozzle changing periodically with time. The analysis given in the section on nozzle design indicates that such a fluctuation would produce the effects which are indicated by the high-speed photographs. That is, if the size of the vortex decreases the cone angle will increase, other things being equal.

It was found that the general effect of these vibrations is to increase the drop size, since the cone is then broken up into larger pieces than would have been the case if contact with the air had performed all of the disintegration.

Back to previous page

of these special cases is given in the Appendix. All of the nozzles tried gave some vibrations under certain conditions, but in many cases the amplitude was small and no apparent affect on the drop size was noted. 10' x 3 gave the most serious vibrations and 12 x 3 was also bad in certain regions. Since the amount of data that could be taken was limited, conditions that gave bad fluctuations were avoided in most of the work. The problem of what causes these vibrations and of what to do to stop them remains unsolved.

If a furnace were operating in a range where there was a tendency to change frequency of vibration or to change from no vibration to vibration, sudden changes in flame dimensions might be expected. The solution of this problem is to move out of the region by a change in viscosity or pressure. A method of avoiding the problem is to atomize at viscosities of the order of .1 Stokes and a pressure over 100 p.s.i. Under these conditions the jet breaks up so soon that the fluctuations do not seem to have much affect.

A series of runs were made at essentially constant pressure and viscosity to study the effect of nozzle dimensions on atomization. These data (runs 100 to 110) indicated that the most important variable was the radius of the orifice. Fig. 9 shows Do plotted as a function of r_o. The data can be quite well represented by plotting in this manner. However, inspection indicated that for the same r_o, as the cone angle

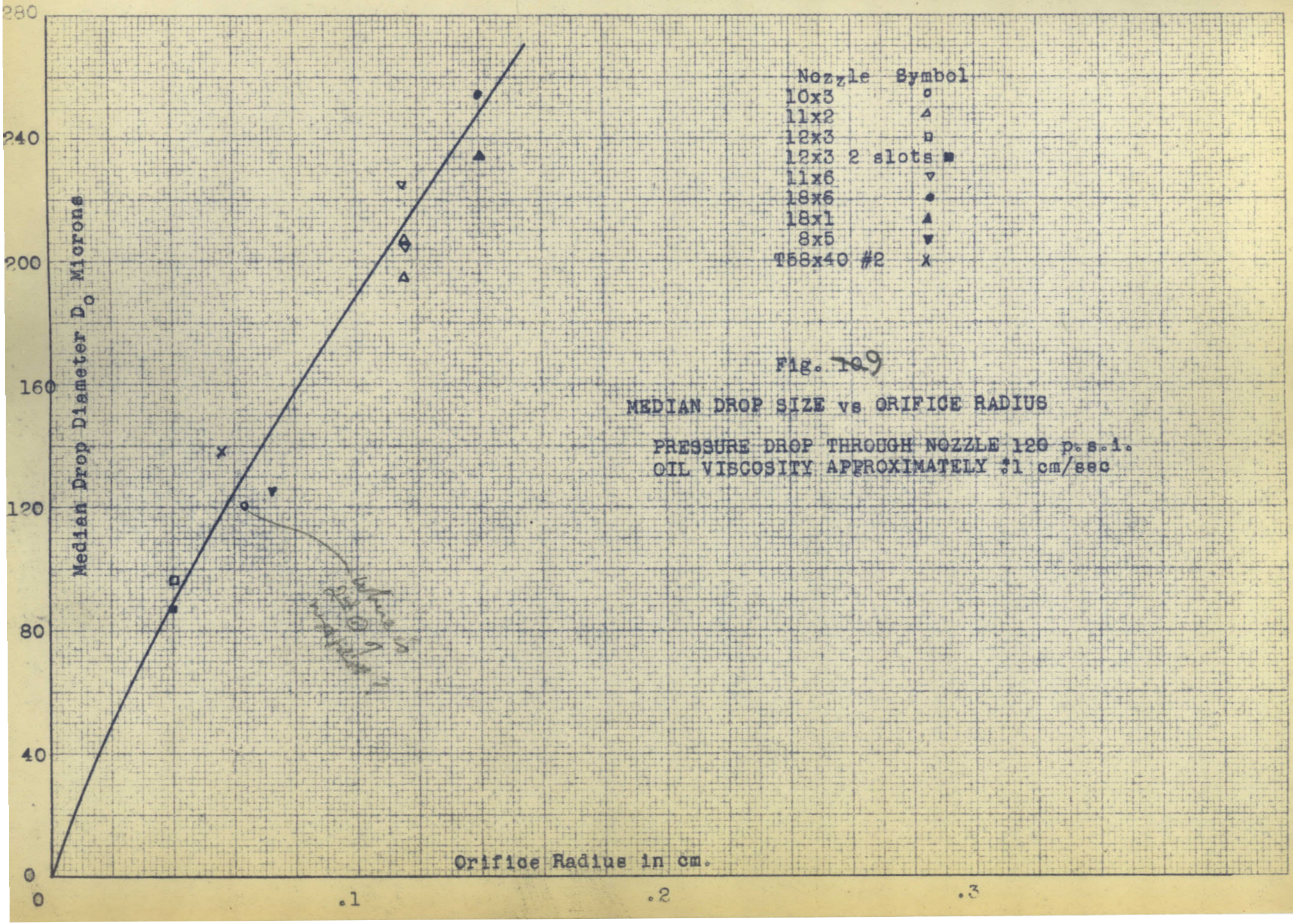

Fig. 29

MEDIAN DROP SIZE vs ORIFICE RADIUS

PRESSURE DROP THROUGH NOZZLE 120 p.s.i.
OIL VISCOSITY APPROXIMATELY .1 cm/sec

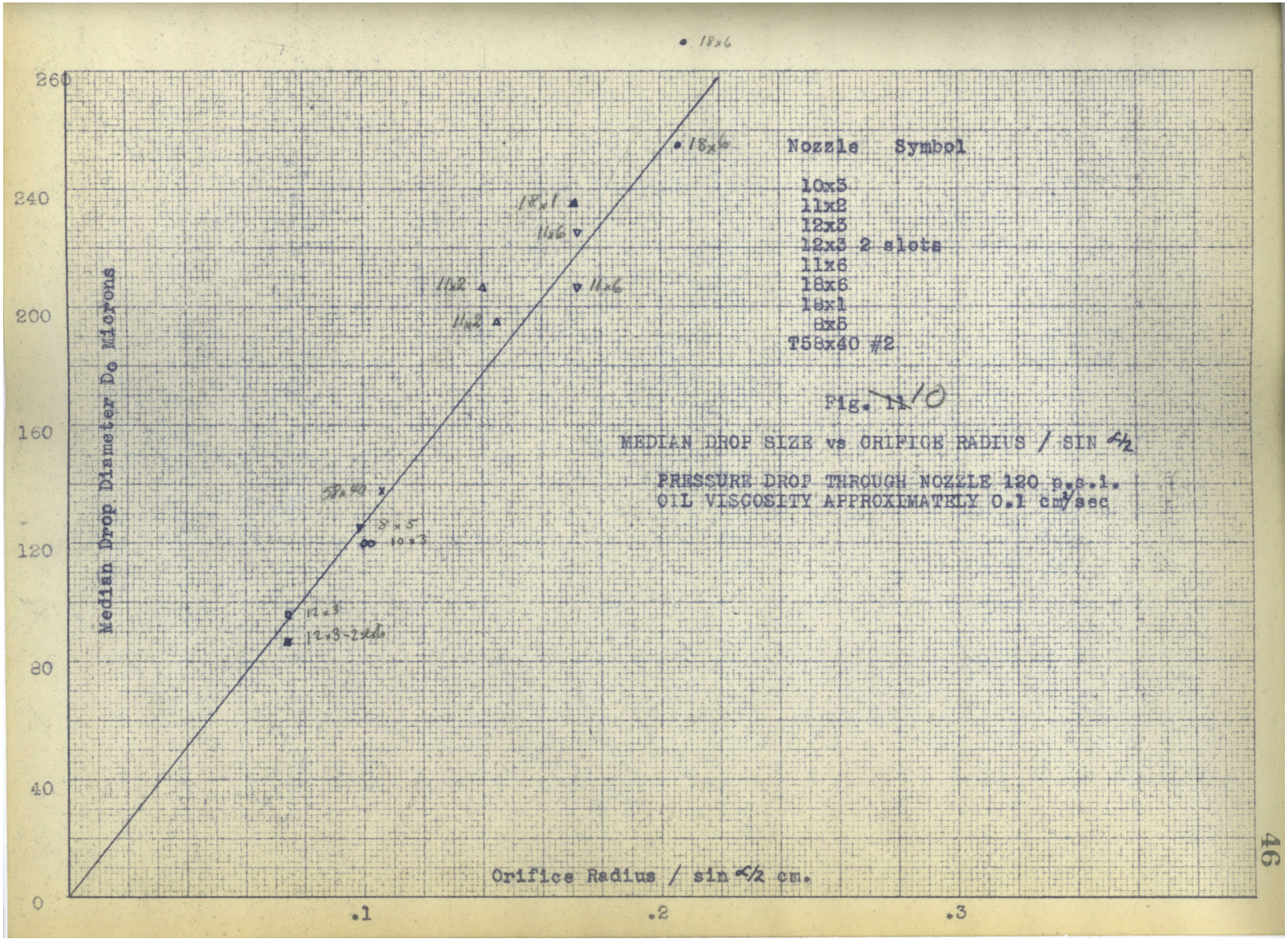

Fig. 11/0

MEDIAN DROP SIZE vs ORIFICE RADIUS / SIN $\alpha/2$

PRESSURE DROP THROUGH NOZZLE 120 p.s.i.
OIL VISCOSITY APPROXIMATELY 0.1 cm^2/sec

increased the value of Do decreased. Plotting Do against $r_o/\sin \alpha/_2$ as in Fig. 10 improves the correlation somewhat. This method of plotting is supported by the following considerations.

For one fluid and set of operating conditions it would seem reasonable to assume that the thickness of the oil film at the place where the film breaks up would largely determine the drop size and distribution; so the characteristics of the cone which determine the film thickness at this point should be of interest. If it is assumed that the film of oil does not slow down appreciably before it breaks up and that the cone angle is constant, it can be said that the area of fluid at any plane at right angles to the axis of the cone is constant. This statement can be written:

(5) $$\pi(r^2 - r'^2) = \pi(r_o^2 - r_o'^2)$$

where r is the radius of the outside of the cone at the point of breakup

r' is the radius of the inside of the cone at the point of breakup.

Subscript o refers to conditions at the orifice.

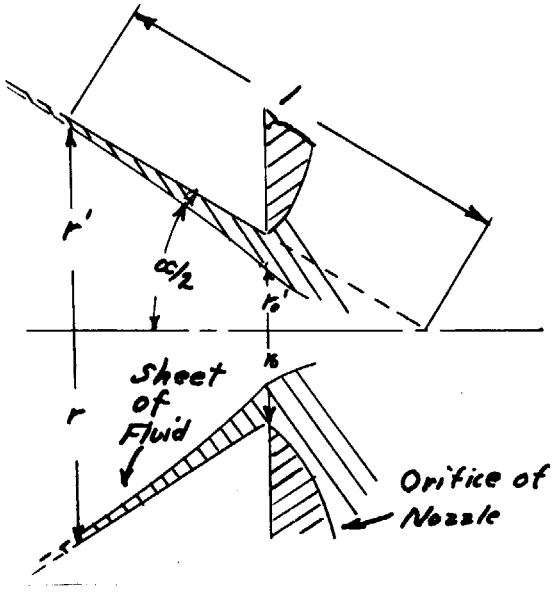

Since the thickness of the film can be written:

(6) $t = (r - r') / \cos \alpha/2$

where α is the cone angle.

By combining Eq. 5 and 6 the following equation is obtained:

(7) $\frac{t}{t_o} = \frac{r_o + r_o'}{r + r'}$

or approximately

(8) $\frac{t}{t_o} = \frac{r_o}{r}$

for thin sheets of fluid. If the expression $r = l \sin \alpha/2$ is substituted in Eq. 8 one obtains:

(9) $\frac{t}{t_o} = \frac{r_o}{l \sin \alpha/2}$

where l is the length of the cone to the point of breakup.

Making the heuristic assumption that drop size is proportional to the thickness, t, of the sheet of fluid at the point of breakup one obtains from Eq. 9 the condition that

(10) $\frac{D_o \sin \alpha/2}{r_o} \cdot \frac{l}{t_o} = \text{const.}$

is constant for given pressure and physical properties. The term, l/t_o the cone length measured in units of the thickness of its base may tentatively also be assumed constant. If such is the case then Do is proportional to $r_o/\sin \alpha/2$. Fig. 10, which shows Do plotted against $r_o/\sin \alpha/2$, indicates that, within the accuracy of the data, this is the case. As is demonstrated by Fig. 11 this relationship between Do,

r_o, and α is valid at other values of viscosity and pressure, and is very useful in correlating the data. The relationship breaks down for the case where violent fluctuations of the cone occur as in runs 126 and 127. It also broke down for the case of runs 128 and 129. The nozzle in these runs could have been operating in a region where the vortex was not perfectly formed. The relation between the cone angle and sheet thickness would then be different from that for a nozzle operating in the region of good vortex formation.

3. The Physical Properties of the Fluid Atomized

The physical properties of the fluid which would be expected to affect the atomization are the density, the surface tension, and the viscosity.

Density is probably as important a variable as the others, but it changes so little for the oils studied that any effect of its change was not detected. Runs 60 to 65 which are plotted in Fig. 8 were done with oils of a density variation of 8%; that they all fall on a smooth curve suggests that the effect of density, at least over this small range of variation, is not a profound one.

The effect of surface tension on atomization is probably quite important in the atomization of fluids other than hydrocarbon oils. However, the surface tension of these oils does not vary over a large enough range to allow any conclusions to be drawn on its effect.

Houghton (4) published some drop sizes for similar nozzles atomizing water. It was found that these results could be expressed quite well by the Rosin equation. For purposes of comparison with the data on oils a cone angle of 60° was assumed. The values of Do for his work were about twice that which would have been expected from the work on oil. The method used to obtain the data on water was to pass a plate under the spray and to photograph the plate and the water drops collected on the surface. The drops were then counted and measured and a correction factor applied to obtain the equivalent sphere of fluid. There may be some error in comparing the results obtained by the two methods, but it is safe to say that it is definitely indicated that an increase in surface tension has considerable effect in increasing the drop size.

The viscosity of the oil affects the cone angle, the thickness of the film, and the breakup of the film. It was found that a different value of $\frac{D_o \sin \alpha/2}{r_o}$ was obtained for different viscosities. Fig. 11 shows the variation of this ratio with viscosity at constant pressure. The points shown are from runs 99 to 124. No runs were included where the cone was seen to fluctuate badly or where the nozzle was operating near the viscosity where a good cone was not formed. The effect of viscosity on $\frac{D_o \sin \alpha/2}{r_o}$

under these conditions can be represented by the equation:

$$(11) \qquad \frac{D_o \sin \alpha/2}{r_o} \propto e^{.705\nu}$$

where ν is the viscosity in cm^2/sec.

The effect of viscosity on the cone angle must be known if Do is to be found. The cone angle as a function of viscosity is given in Fig. 20, and is to be discussed later.

4. The Effect of Pressure Drop Through the Nozzle

The data of Table 8 indicates that in the region where the vortex is well formed the cone angle and the film thickness are not functions of the atomizing pressure. Fig. 11 then illustrates the effect of pressure on Do. As would be expected, the higher the pressure the smaller the value of Do. Over the pressure range studied the effect can be represented by the equation

$$(12)_a \qquad \frac{D_o \sin \alpha/2}{r_o} \propto \frac{1}{p^{.375}}$$

Probably the head of fluid is the correct variable to use in this case, but since the density changed so little the use of pressure is just as representative of this series of runs.

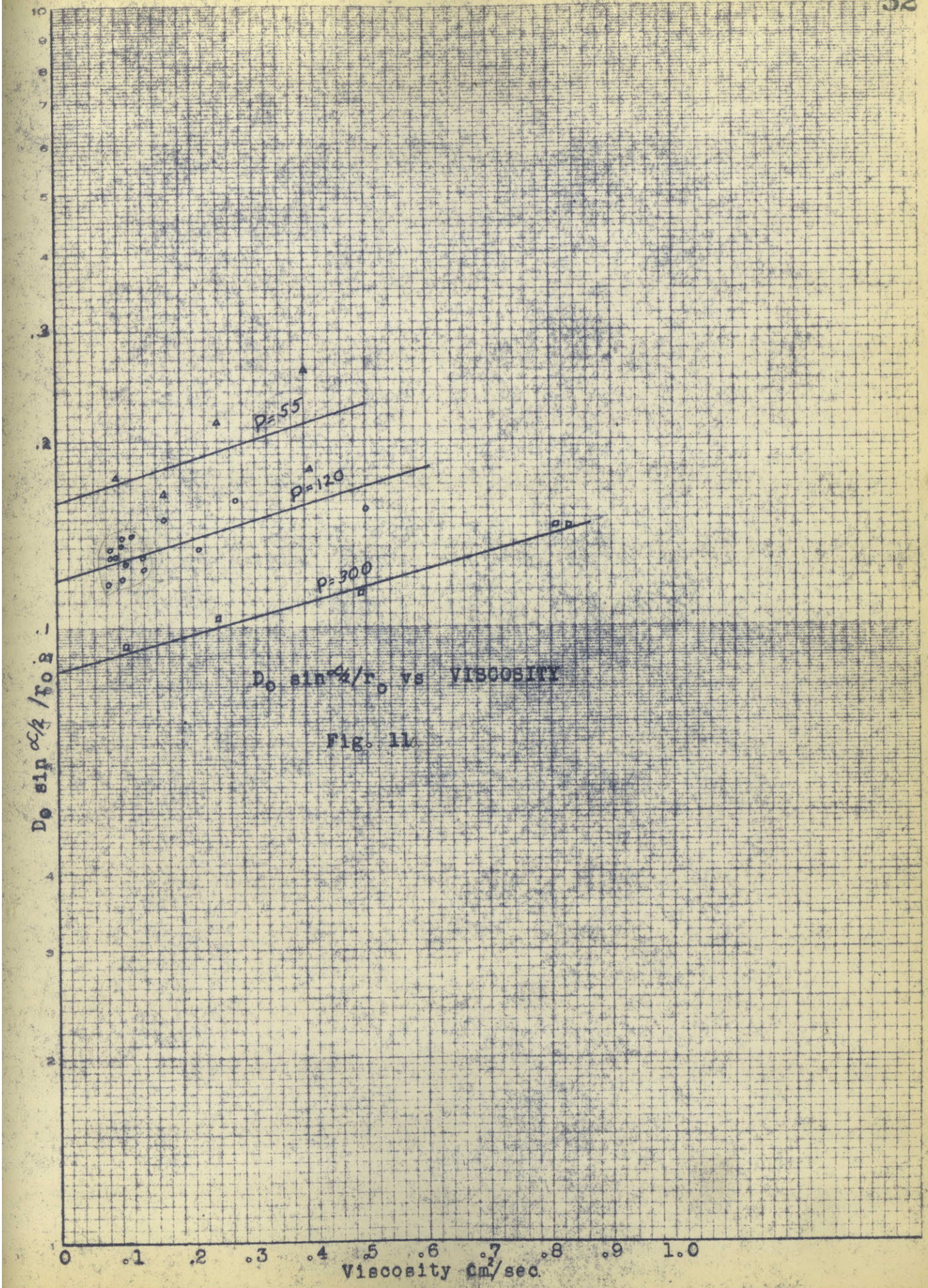

$D_o \sin \alpha/2 / r_o$ vs VISCOSITY

Fig. 11

The effect of pressure and viscosity can be combined into one empirical equation,

$$(12) \qquad \frac{D_o \sin \alpha/2}{r_o} = 0.72 \frac{e^{.705\nu}}{P^{.375}}$$

where P is the pressure in p.s.i.

ν is the viscosity in $cm^2/sec.$

The range of data represented by this equation is shown by Fig. 11.

The above equation, together with the reduction of deleterious effect of fluctuations of the cone at low viscosities, both indicate the advisability of using an oil of low viscosity. However, there does not appear to be much advantage in going below a viscosity of .1 $cm^2/sec.$ It is also apparent that a nozzle should be operated at as high a pressure as possible for both of the above reasons. However, if a large decrease in drop size is desired, small nozzles should be used since the drop size depends directly on the radius of the orifice. Using several small nozzles would offer greater flexibility of operation and better atomization than one large nozzle of capacity equal to the capacity of the small ones.

As is explained in the section on nozzle design, there is a narrow range of cone angles and discharge

coefficients which will give the best performance. A number of commercial nozzles could be improved in this respect, and these variables should be considered in choosing a nozzle.

Commercial nozzles are available which accomplish a large variation in flow rate at one pressure by bleeding oil from the orifice or from the back of the nozzle. No radical departure from the constancy of $\frac{D_o / \sin \alpha/2}{r_o}$, for one set of operating conditions, is anticipated. It would then be expected that the use of a nozzle of this type would give larger drops than if a bank of small nozzles were used to obtain flexibility of operation. For small variations in flow rate this type of nozzle gives better results than would be obtained with a single nozzle of the ordinary type which adjusted the oil flow rate by changing the pressure of atomization. The added inconvenience and difficulty of keeping the nozzles in good condition involved in using a number of small nozzles would have to be balanced against the advantage of improved combustion obtained from the better atomization.

The above discussion was based on the factors which determine D_o. The constant n must also be evaluated in order to describe the spray. It was found that values of n were best correlated by plotting them as a function of Do. This curve is shown in Fig. 12. The data for this correlation was taken from runs 99 to 124. The root mean square deviation of data points from the curve was found to be $\pm$10%. The fact that n increases with Do means that the distribution is much closer for a spray which has a large weight median drop size than for a curve which has a small one.

The fact that a ten percent deviation is probable in the values of n means that it is possible for nozzles which give the same Do to have a spray with different combustion characteristics. The reason for these deviations is not clear since usually the lines drawn through the data points could not be varied this much and still be representative of the data.

Discharge Rates

Figures 14 and 15 show the discharge rate plotted against the viscosity at constant pressure drop through the nozzle for nozzles T58x40 and 10x3. At low values of viscosity the discharge coefficient

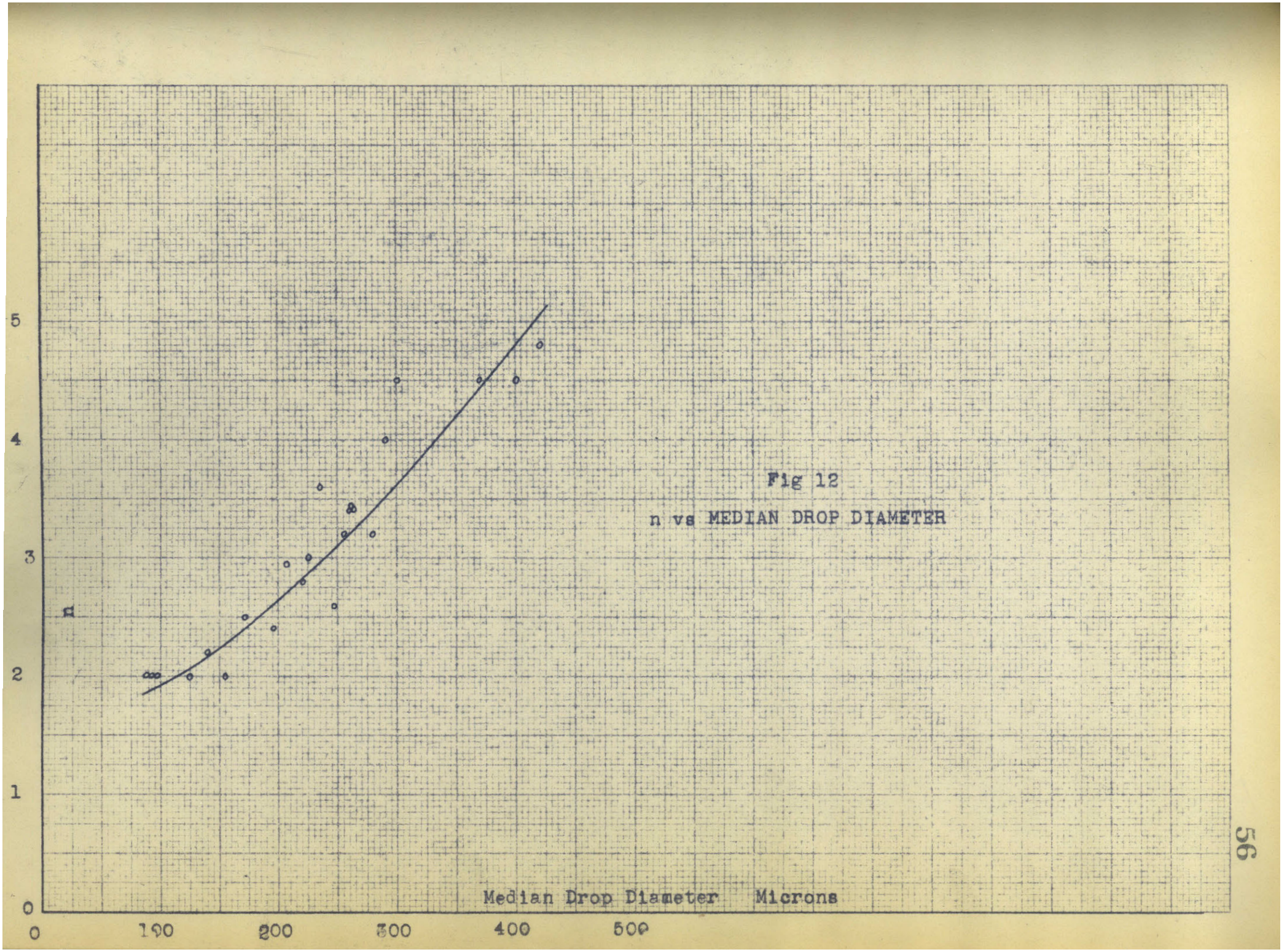

Fig 12

n vs MEDIAN DROP DIAMETER

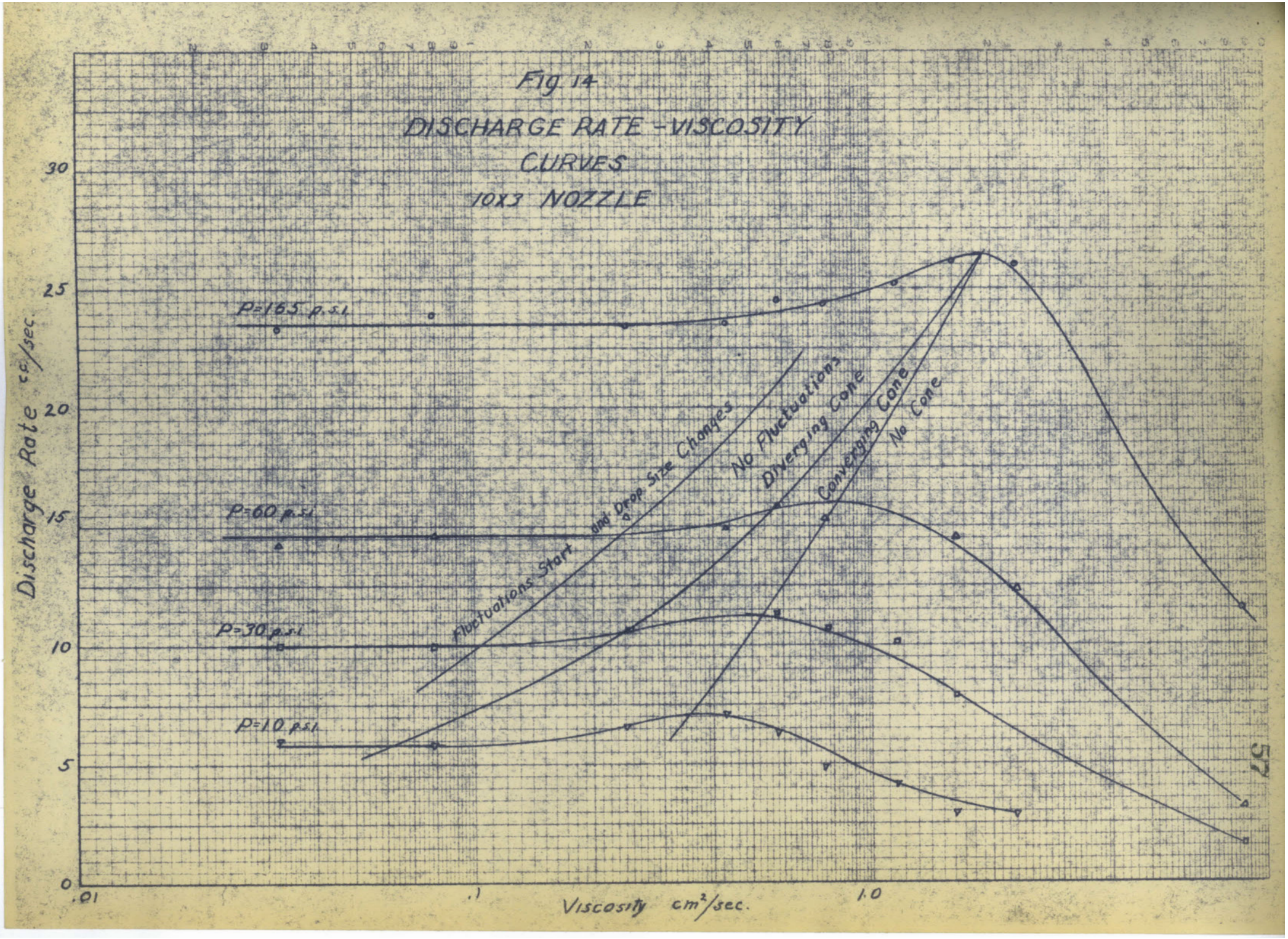
Fig 14
DISCHARGE RATE - VISCOSITY
CURVES
10X3 NOZZLE
Discharge Rate c.c./sec.
30
25
20
15
10
5
0
P=165 p.s.i.
P=60 p.s.i.
P=30 p.s.i.
P=10 p.s.i.
Fluctuations Start
Drop Size Changes
No Fluctuations
Diverging Cone
Converging Cone
No Cone
.01
.1
1.0
Viscosity cm²/sec.
57

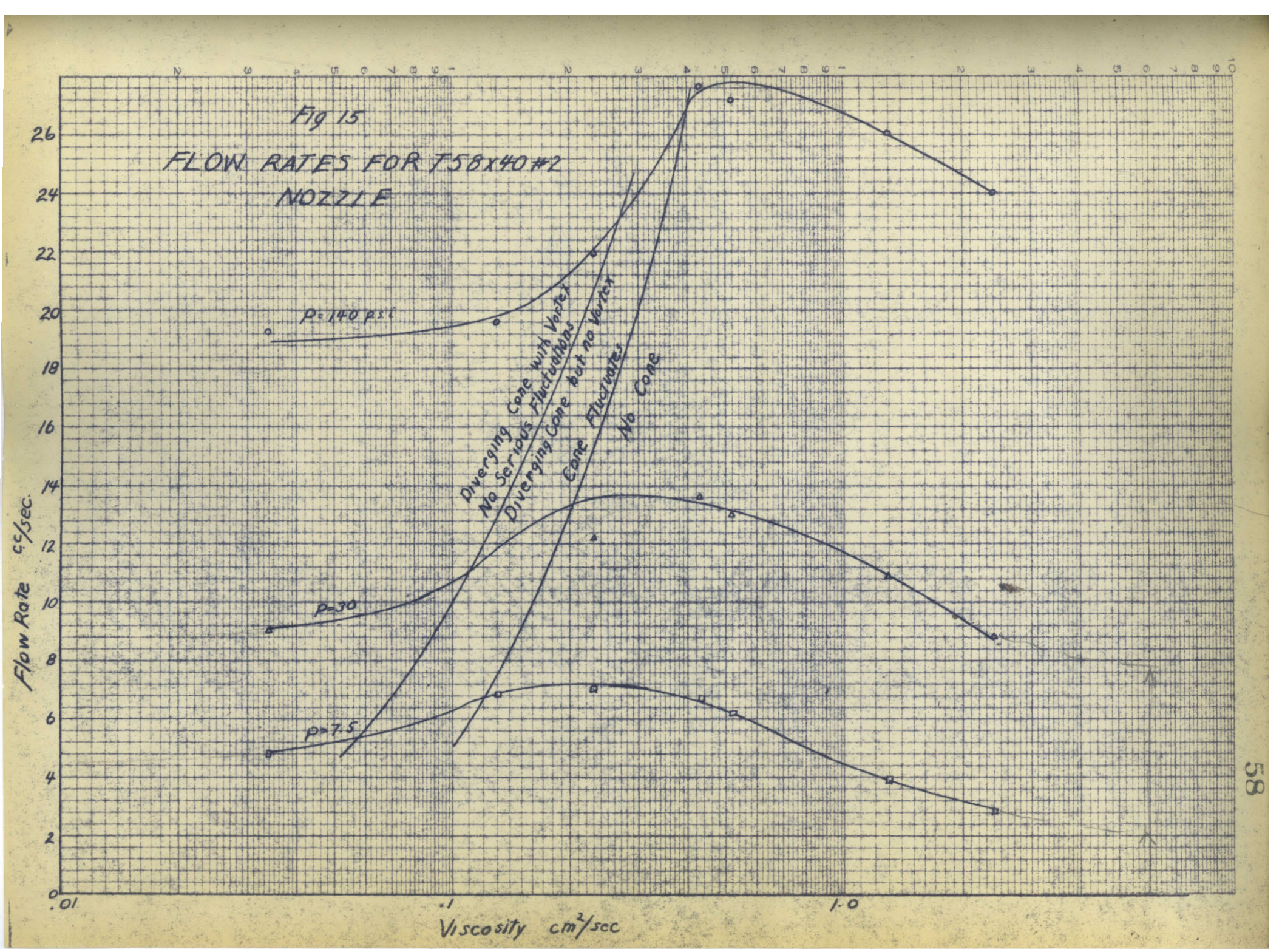
Fig 15
FLOW RATES FOR T58x40 #2 NOZZLE
P=140 p.s.i
P=30
P=7.5
Diverging Cone with Vortex
No Serious Fluctuations
Diverging Cone but no Vortex
Cone Fluctuates
No Cone
Flow Rate cc/sec.
Viscosity cm²/sec
.01
.1
1.0
0
2
4
6
8
10
12
14
16
18
20
22
24
26

is low for two reasons. First a vortex is formed in the orifice which cuts down the effective area for discharge, and second, a considerable portion of the energy which might have been used to increase the discharge rate is consumed in supplying rotation of the jet. As the viscosity increases rotational energy is lost because of the drag of the walls and because of the rubbing of the annuli of fluid at different radii. This rubbing is due to the fact that rotational velocity is a function of radius. Since the increase of rotational energy with decreasing radius depends on the magnitude of the energy, loss of rotational energy in the swirl chamber means that less rotational energy will be added to the fluid. Therefore, it is possible for an increase in viscosity to be accompanied by an increase in the flow rate, since the energy available for increasing the velocity through the orifice can be increased. As the viscosity is increased even more the losses of energy to friction become larger than the gain in translational energy. In this region the discharge rate decreases with increasing viscosity.

Another factor which must be considered is the fact that as the viscosity is increased the size of the vortex in the orifice decreases until at vis-

cosity somewhat before that which corresponds to the maximum of the discharge rate-viscosity curve it disappears entirely. This increases the area for discharge and favors the increase in discharge rate. The above statement is based on the photographs of lucite nozzles which are shown in Figures 34 and 35. A smooth cone forms at a viscosity corresponding to the maximum in the discharge rate-viscosity curve, and although no vortex can be detected at this point the incipient formation of a vortex just at the orifice may be instrumental in causing the discharge rate to drop off with decreasing viscosity at this point.

In the case of nozzles 11X1 and 18X1 the discharge coefficient decreased continuously as the viscosity was increased. This nozzle had small passages for the fluid and it is probable that the increase in loss of energy due to viscous drag prevented any increase in discharge coefficient. It will be noticed that the viscosity at which the maximum of the curve occurs depends on the pressure. The effect of viscosity, pressure, and nozzle design on the formation of the cone is discussed in some detail in the section on that subject.

In the region of low viscosities and high

pressures it was found that the cone angle and the vortex did not change with pressure at any one viscosity. This is taken as an indication that the flow conditions in the nozzle are not a function of pressure at any one viscosity. Under such conditions the flow rate is proportional to the square root of the head. This was found to be the case for the nozzles used.

A discharge coefficient was defined by the equation:

$$Q = \pi r_o^2 c \sqrt{2g \frac{P}{\rho}} \tag{13}$$

where Q is the flow rate

r_o is the radius of the orifice

c is the discharge coefficient

g is the acceleration due to gravity

P is the pressure drop through the nozzle

ρ is the density of the fluid.

Fig. 16 is a plot of this discharge coefficient as a function of viscosity and pressure for two of the nozzles used. Its usefulness for the 10X3 nozzle is indicated by the fact that the same discharge coefficient can be used over a considerable range of pressures and viscosities. The discharge coefficient would have less value for the T58X40 since its design was such that

considerable change in flow conditions took place with viscosity, even at low viscosities. This fact was one of the reasons that nozzles similar to the 10X3 were used in the bulk of the work instead of the T58X40. In either case the discharge coefficient at zero viscosity would be the simplest to generalize although its utility depends on the particular nozzle.

The analysis given in the appendix for the case of frictionless flow indicates that the discharge coefficient could be represented as a function of two dimensionless groups which are defined as follows:

$$b = \frac{\pi^2 r_o^4}{A_s^2}\left(\frac{r_s}{r_o}\right)^2 \quad , \quad a = \frac{r_c}{r_{ip}}$$

where A_s is the area of the tangential slots

r_s is the average radius of a particle of fluid as it enters the swirl chamber from the tangential slots

r_o is the radius of the orifice

r_i is the radius of the vortex at the orifice

r_{ip} is the radius at which all of the energy of a particle would be in the form of rotational energy.

This analysis gave the equation:

$$(14) \quad C_o = \sqrt{1 - bc_o^2} - a\,bc_o^2\sqrt{a^2-1} - bc_o^2 \ln \frac{1+\sqrt{1-bc_o^2}}{\sqrt{bc_o^2}\left(a+\sqrt{a^2-1}\right)}$$

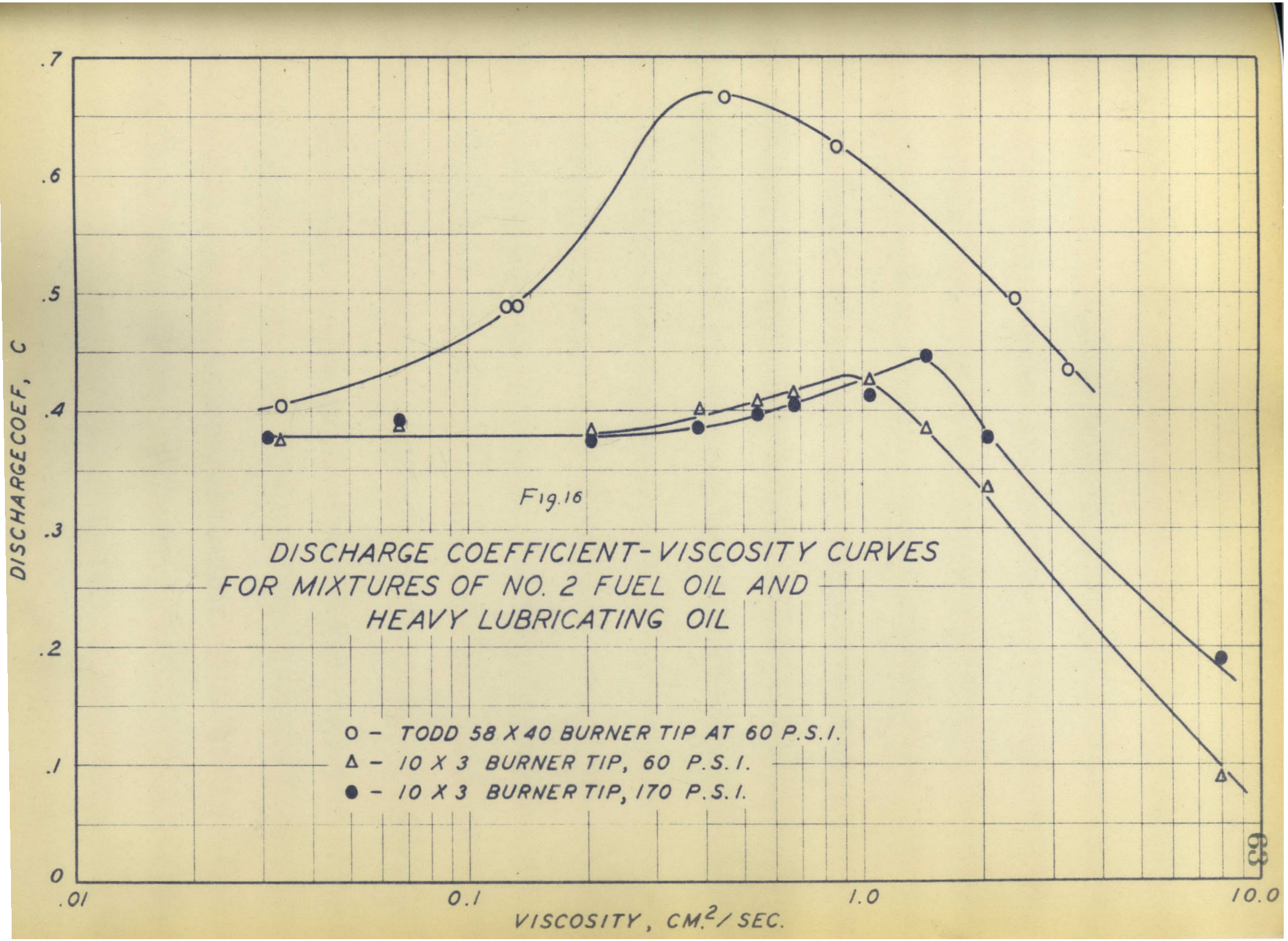

Fig. 16

DISCHARGE COEFFICIENT-VISCOSITY CURVES FOR MIXTURES OF NO. 2 FUEL OIL AND HEAVY LUBRICATING OIL

This equation is plotted in Fig. 17. A check on its validity was available from the study of the transparent models of nozzles T58X40 and 10X3. From measurements of the vortex diameter and the dimensions of the nozzles the value of "a" for the T58X40 nozzle would be predicted to be slightly less than one by Eq. 14, while the measured value was .90. In the case of the 10X3 nozzle the predicted value would be 2.15, while the measured value was 1.97. It was felt that this agreement was sufficiently good to establish the usefulness of this method of representing the discharge coefficient.

Unfortunately this analysis affords no method of predicting the value of "a" to use, so "a" was found using Fig. 17 and the measured values of c and b. Examination of the data indicated that "a" could be correlated by plotting it as a function of the dimensionless group $\frac{r_{sL}}{A_s}$ where L is the length of the nozzle from the back of the swirl chamber to the orifice. This correlation is shown in Fig. 18. The choice of this group was dictated entirely by the data. A number of other combinations were tried but this one proved to be the most successful.

The fact that "a" increases with increasing $\frac{r_{sL}}{A_s}$ seems quite reasonable since it would be ex-

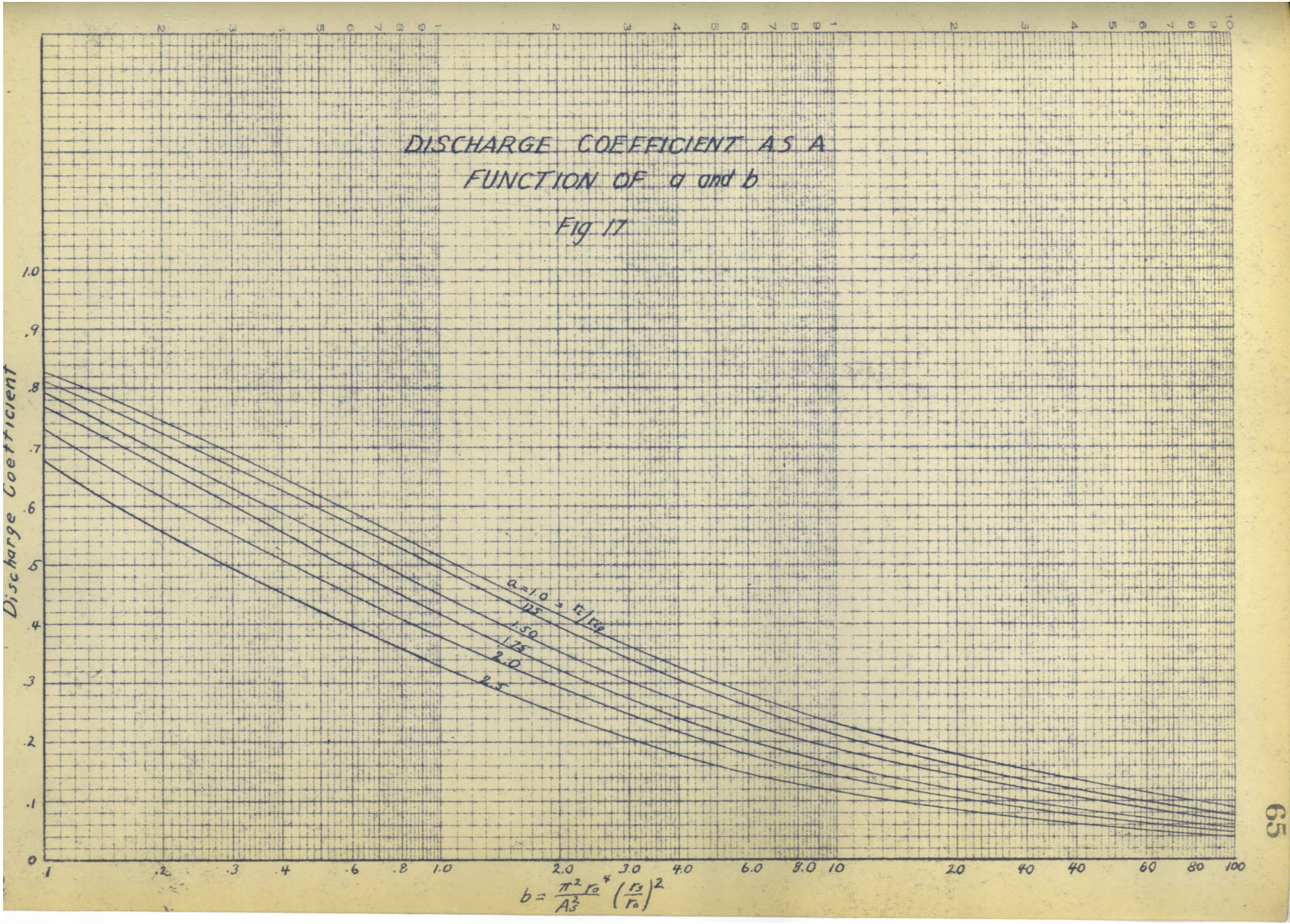
DISCHARGE COEFFICIENT AS A FUNCTION OF a and b
Fig 17
Discharge Coefficient
1.0
.9
.8
.7
.6
.5
.4
.3
.2
.1
0
.1
.2
.3
.4
.6
.8
1.0
2.0
3.0
4.0
6.0
8.0
10
20
40
40
60
80
100
a=1.0 = r1/r0
1.25
1.50
1.75
2.0
2.5
$b = \frac{\pi^2 r_0^4}{A^2_3} \left(\frac{r_3}{r_0}\right)^2$

Fig. 18

a AS A FUNCTION OF $r_s L/A_s$

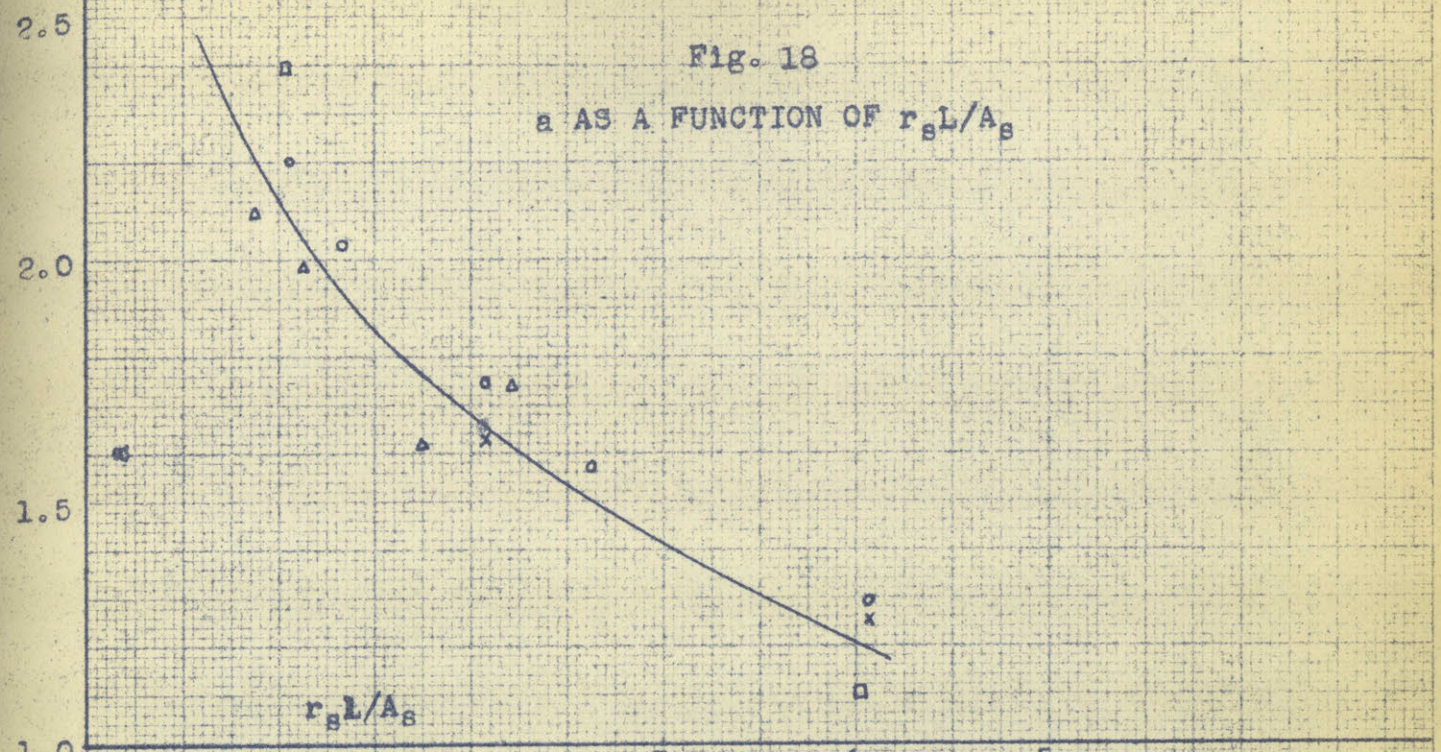

ESTIMATED DISCHARGE COEFFICIENT AT ZERO VISCOSITY
AS A FUNCTION OF THE MEASURED DISCHARGE COEFFICIENT

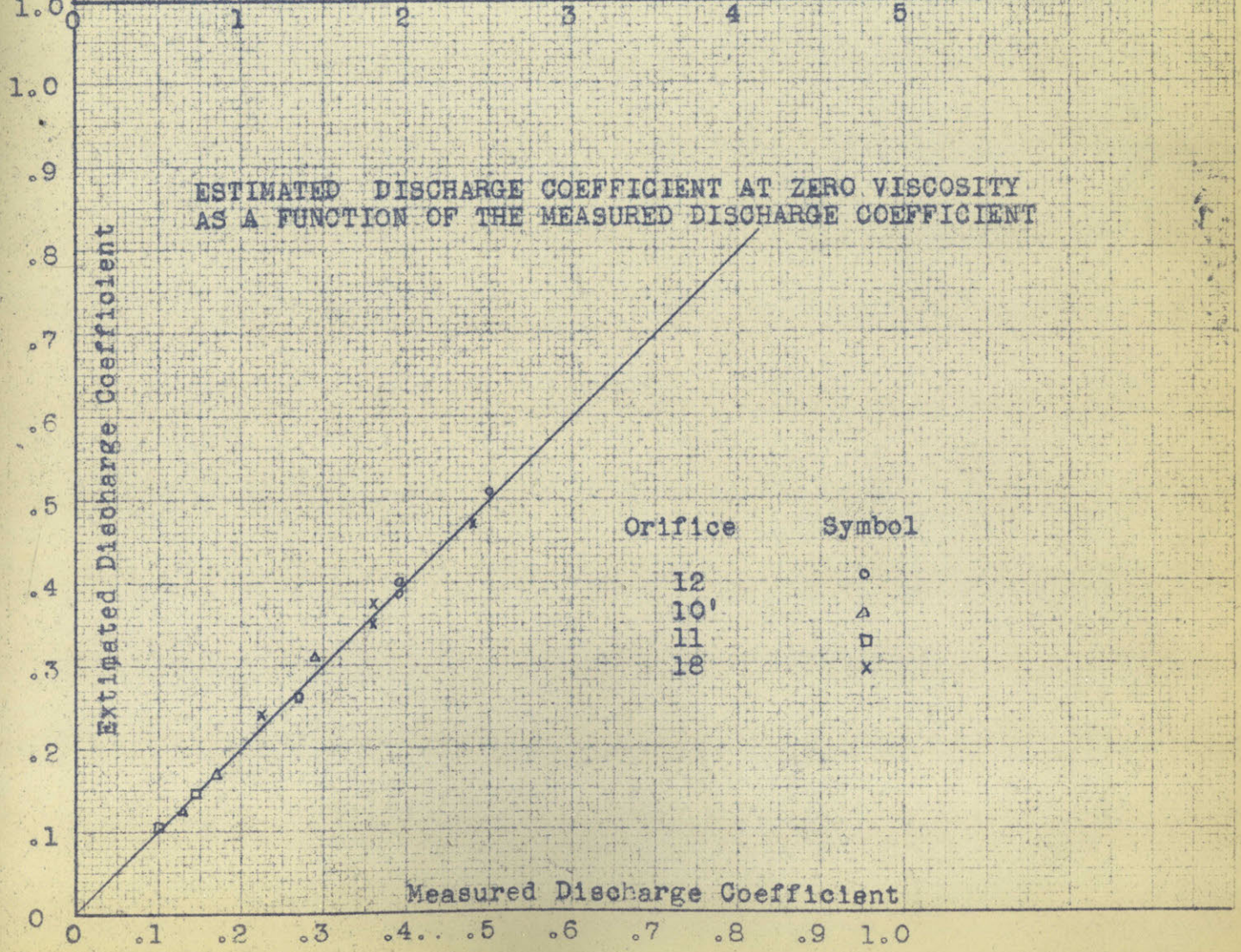

DISCHARGE COEFFICIENT AT ZERO VISCOSITY AS A FUNCTION OF b AND $r_s L/A_s$

The short lines are for the values of $r_s L/A_s$ corresponding to the data points.

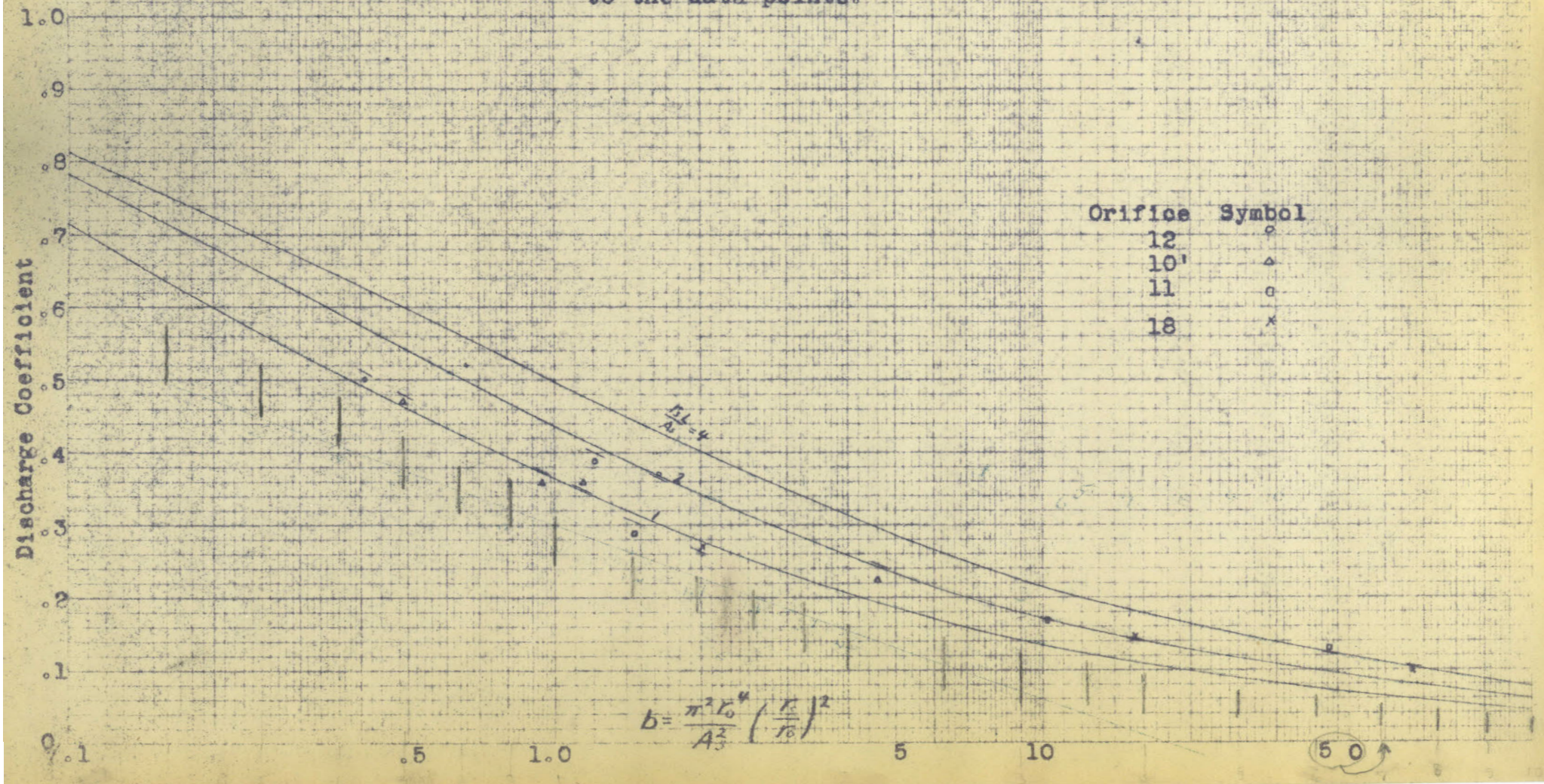

Orifice	Symbol
12	○
10'	△
11	□
18	×

pected that increasing the length of the nozzle and the radius of the swirl chamber would allow more time for the rotational energy to change into translational energy. An analogy to this would be a pipe which contained a rotating slug of fluid. If no restraint was applied to the ends of the slug it would spread out along the surface of the pipe and the rotational energy would change to translational energy. Since a frictionless fluid is being considered the amount of this conversion would depend on the time measured from when the restraint was removed. Or for a continuous feed the conversion would depend on the distance from the entrance. L and r_s would be related to this distance.

Since the discharge coefficient is represented by dimensionless groups involving the dimensions of the nozzle, geometrically similar models of the nozzle would be expected to give the same discharge coefficient at zero viscosity.

The discharge coefficients at the pressure at which a cone was formed, for a given viscosity, was measured. No good method of correlating this information was found but it can be represented roughly by plotting the discharge coefficient at the formation of the cone against the discharge coefficient at the zero

viscosity. Fig. 19 gives this plot. Little faith is placed in this curve since different variables such as the length of the tangential slots enter into the case where the viscous losses are important than enter in the case where viscous losses can be neglected. This discharge coefficient is necessary in estimating the conditions for cone formation and this plot probably has some value for this purpose. The generality of the points at low discharge coefficient are in particular doubt.

With the exception of the 10X3 and the T58X40 nozzles the variation of the discharge coefficient with pressure and viscosity was not fully investigated. However, it is believed that in most of the range of good atomization that use of the discharge coefficient at zero viscosity is good approximation.

The Cone Angle

Since the cone angle effects both the drop size distribution and the mixing characteristics of a flame it is of interest to be able to predict it. In the region of good vortex formation the cone angle decreases as the viscosity is increased. At high viscosities the vortex leaves the back of the swirl chamber and decreases in size. When this occurs the cone angle generally starts to increase until the cone is

DISCHARGE COEFFICIENT AT CONDITION OF CONE FORMATION
AS A FUNCTION OF DISCHARGE COEFFICIENT AT ZERO VISCOSITY

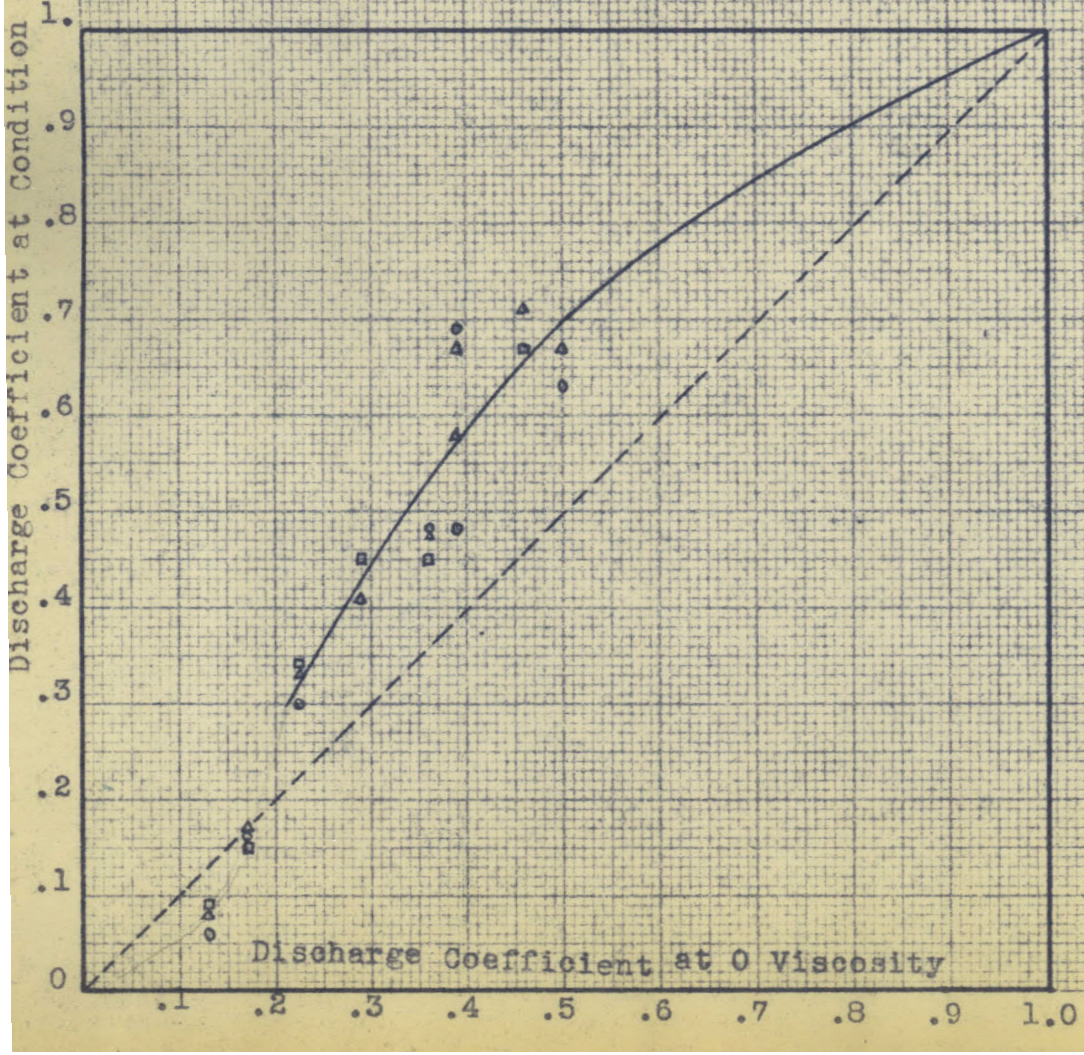

o ν = .375

Δ ν = .52

□ ν = .73

Fig. 19

no longer formed. In the region where the vortex is well formed the cone angle is not a function of pressure, and changes with viscosity only. The higher the pressure the higher a viscosity to which this region will extend.

It was found that if the cone angle divided by the cone angle at zero viscosity was plotted against viscosity that one curve would satisfactorily represent all of the nozzles of the type built in the laboratory. This curve is plotted in Fig. 20. The T58X40 was not well represented, and Fig. 20 can be considered good only for the type of nozzle for which the data was obtained. As would be expected, the T58X40 showed a greater decrease in cone angle with viscosity than the other nozzles. Much of this was probably due to the over-large swirl chamber in which much of the rotation could damp out, and to the fact that the orifice consisted of a tube which would be very effective in dissipating rotational energy.

The values of the cone angle at zero viscosity which would be predicted by the analysis in the Appendix did not agree well with the measured values. This discrepancy was probably due to the actual velocity distribution being different from that predicted. However, it was found that values of an "a" found by using the cone angle and the equation from the analysis

CONE ANGLE AS A FUNCTION OF VISCOSITY

Fig. 20

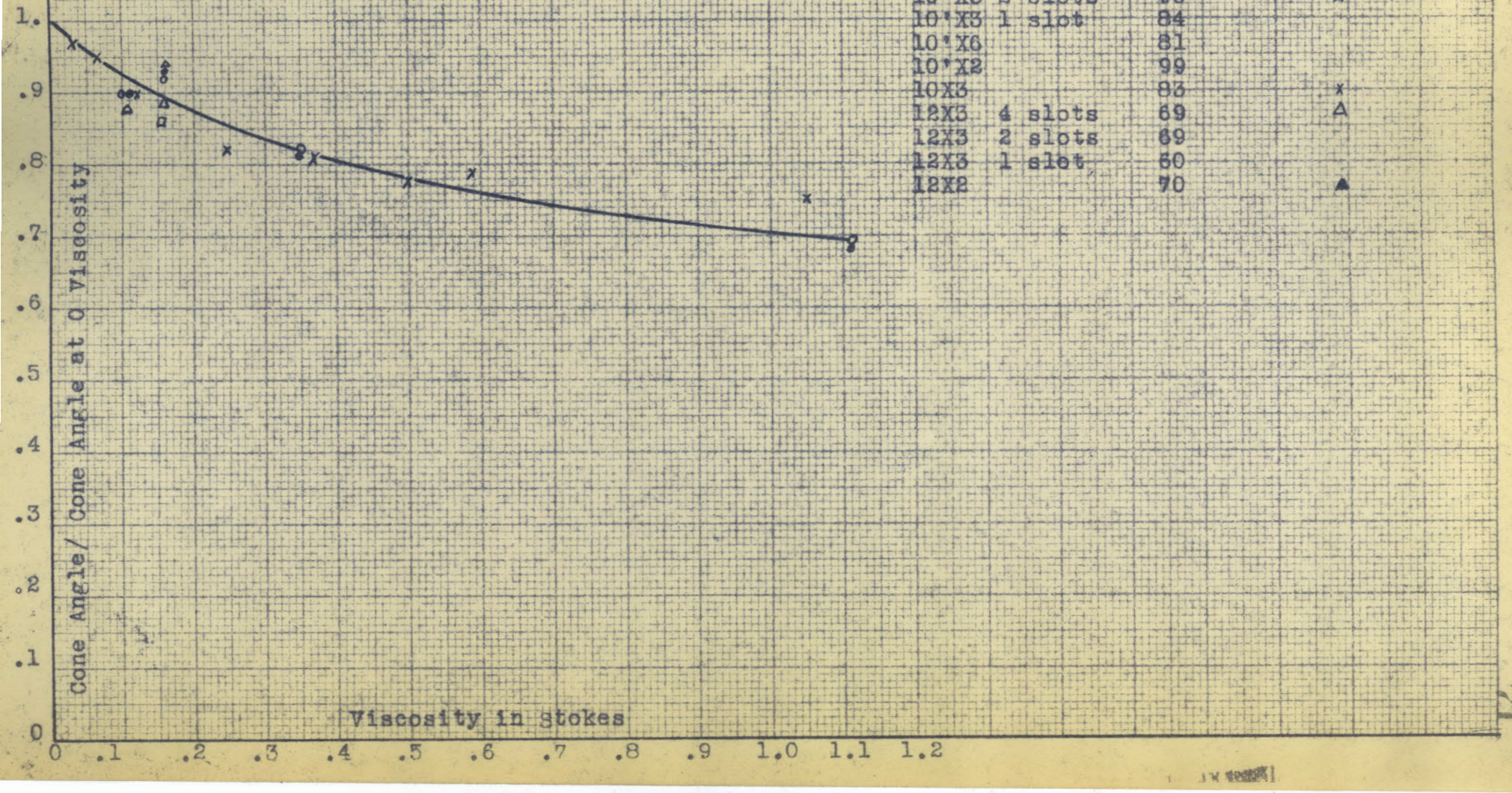

Nozzle		Cone Angle at Zero Viscosity	Symbol
18X6		92	
18X2		106	
18X1		120	
11X6		94	○
11X2		111	●
11X1		118	
10'X3	4 slots	95	
10'X3	2 slots	96	□
10'X3	1 slot	84	
10'X6		81	
10'X2		99	
10X3		83	×
12X3	4 slots	69	△
12X3	2 slots	69	
12X3	1 slot	60	
12X2		70	▲

could be used to correlate the data. The equation for the cone angle which would be expected if the velocity at the orifice was constant was used as a basis for finding a'. This equation is:

$$(15) \qquad \cos \alpha_o/2 = \frac{C_o}{1 - a'^2 C_o^2 b}$$

The method used to find a' was to find c_o from Fig. 18 and b from the dimensions of the nozzle. By using the measured cone angle a' could be found from Eq. (15). a' was plotted against the group $\frac{r_s L}{A_s}$, and it was found that the correlation could be improved by drawing lines of constant L/r_o. Fig. 21 is a graph of a' vs. $\frac{r_s L}{A_s}$ for different values of L/r_o. It will be noted that the values of a' are not very different from those of "a" from Fig. 19. However, this difference is very important since the cone angle is very sensitive to small changes in the value of a' or of c_o. For this reason care should be used in obtaining the value of c_o when it is to be used in estimating the cone angle. The agreement of the estimated cone angle with the predicted cone angle was within eleven degrees for all cases except the case of the T58X40, which was not expected to agree because of the effect of the design of its swirl chamber and orifice which tended to change rotational energy to

Fig. 21

a' AS A FUNCTION OF $r_s L/A_s$ AND L/r_o

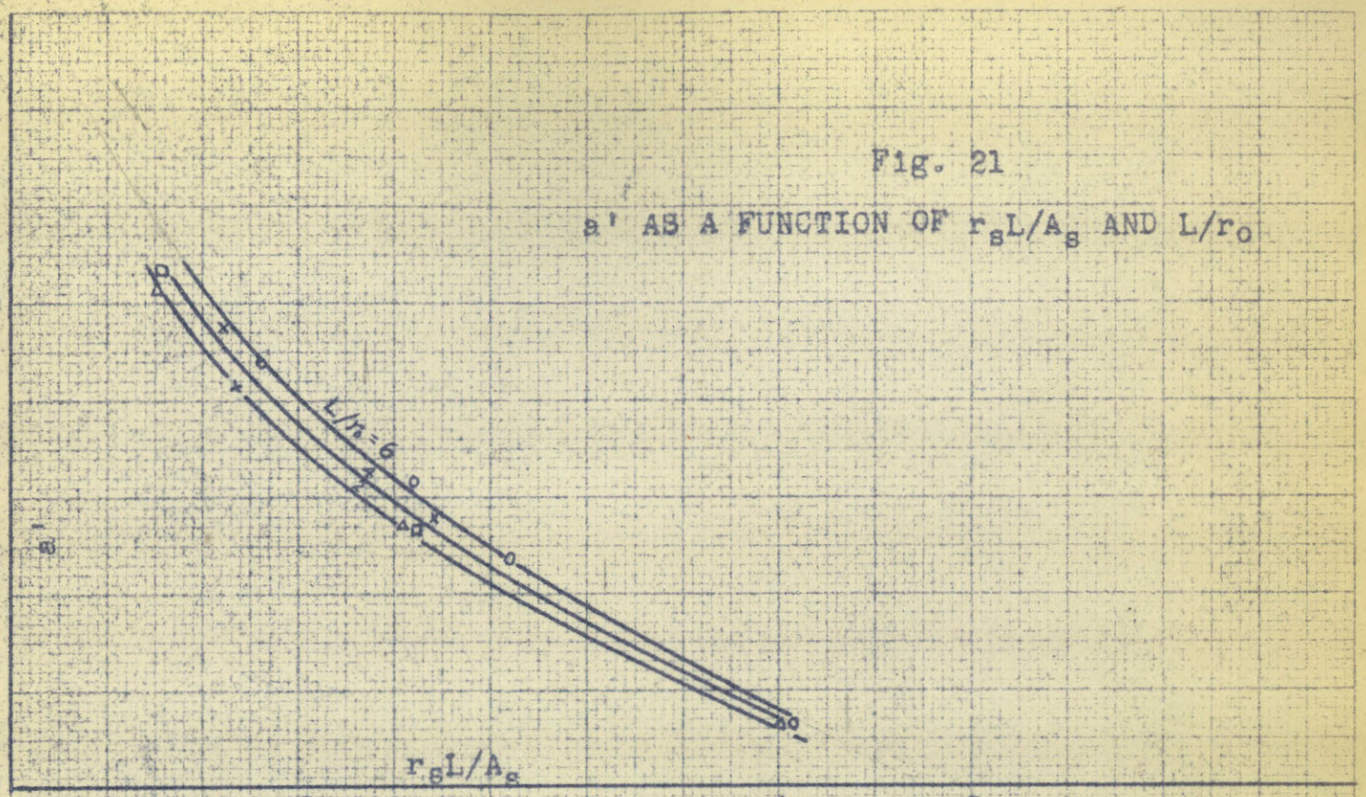

ESTIMATED CONE ANGLE AS A FUNCTION OF MEASURED CONE ANGLE AT ZERO VISCOSITY

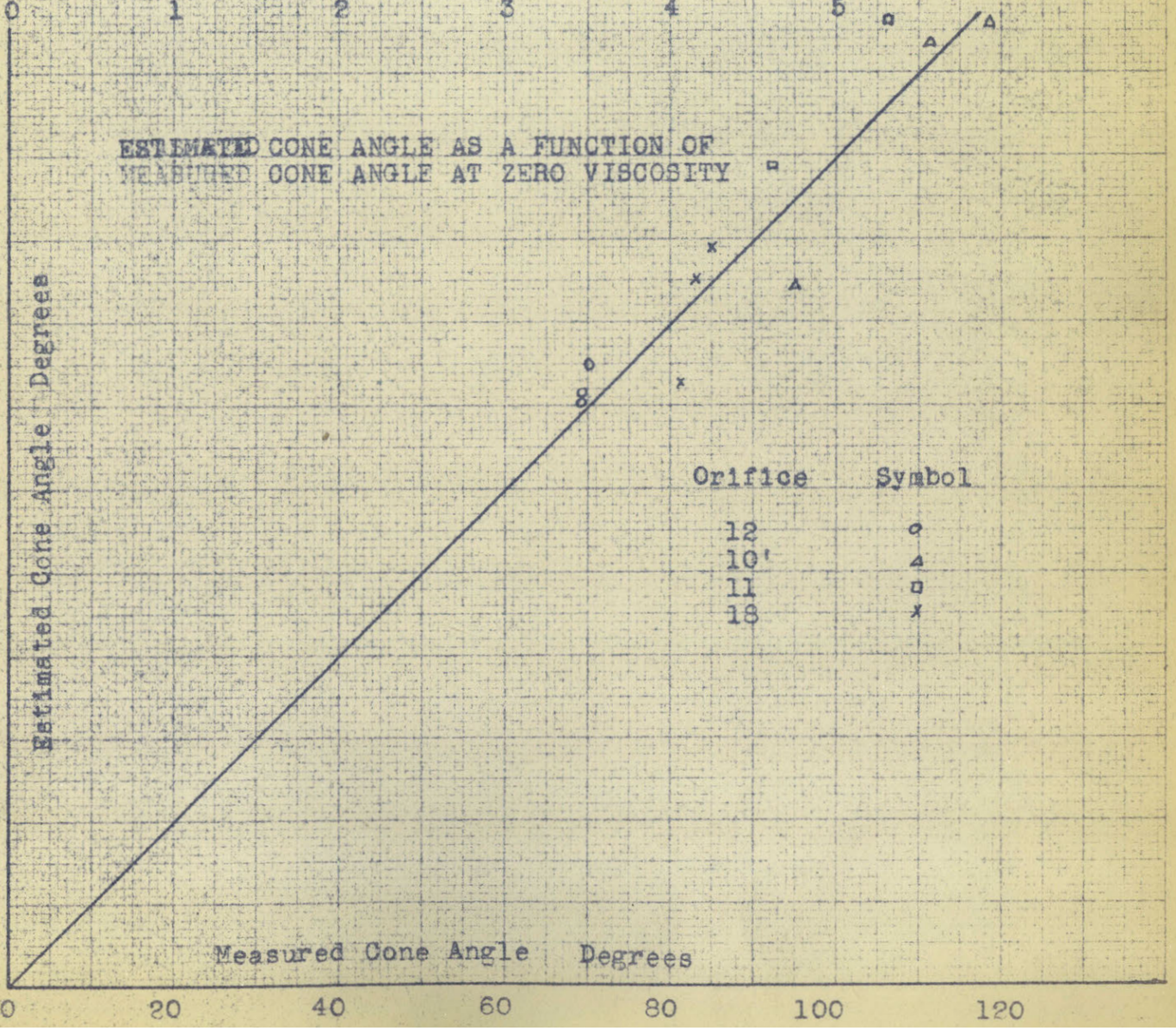

translational energy. As would be expected, the measured cone angle was smaller than the predicted cone angle for this case.

The Formation of a Cone

The pressure and viscosity at which a cone is formed for a particular nozzle design is of interest since good atomization can not be expected unless a cone is formed. Fig. 32 of the Appendix illustrates this statement by showing the large change in Do which occurs when a cone is not formed. The pictures in Fig. 7 illustrate the difference in appearance between the jet which merely breaks up and one which forms a cone. The pressures at which a cone was formed were found for different nozzles and viscosities. The data are given in Table 7.

It was found that the pressure required to obtain a cone at one viscosity and orifice diameter goes through a minimum if plotted against discharge coefficient. This fact can be explained by the following reasoning. Probably a jet of a certain diameter must have a definite amount of rotational energy before it will form a cone. A nozzle of very high discharge coefficient obtains that high discharge coefficient by not adding much rotation to the jet, so a decrease in the discharge coefficient with a corresponding increase in the amount of rotational energy in the jet

would be expected to reduce the pressure necessary to get the fluid through the nozzle quickly enough to allow a sufficient amount of rotational energy to reach the jet so that a cone will be formed.

If a nozzle of very high discharge coefficient is considered the slots control the flow rate since they must be made small to reduce the discharge coefficient based on the orifice radius. When the flow rate is very low through a nozzle the fluid must make so many revolutions before getting out of the nozzle that most of the rotation is damped out. In this case increasing the discharge coefficient increases the amount of rotation that gets through since the fluid flows through more quickly. An increase in the discharge coefficient therefore would be expected to decrease the pressure required to get the fluid through the nozzle quickly enough. The combination of these two causes of loss of rotational energy would give a curve in which the necessary pressure went through a minimum with change in discharge coefficient.

The fact that the pressure for the formation of a cone increased when r_o was decreased, and that the pressure increased as L was increased suggested the use of the ratio L/r_o to correlate the data at constant viscosity. It was found that if ln P_c was plotted

against the ratio L/r_o at one discharge coefficient that a line of slope .67 would represent the data points fairly well. Also, if $\ln P_c - .67L/r_o$ was plotted against the viscosity for constant discharge coefficient lines of slope 3.25 would represent the data. This means that if $\ln P_c - .67L/r_o - 3.25$ is plotted against the discharge coefficient that a single line should be obtained.

Fig. 22 gives this curve and the data points. This correlation should not be used for nozzles which are not similar to those for which it was obtained. For example, the T58x40 nozzle needs a pressure of 105 p.s.i. at a viscosity of .3 poises to form a cone. The pressure that would have been predicted from this curve is 300 p.s.i. Any extrapolation beyond the range of variables actually studied in a correlation of this kind is probably dangerous. However, it does afford a convenient means of interpolating between the data points for use in design calculations on the type of nozzle tested.

Formation of a Diverging Cone

Under certain conditions when a cone is formed the surface tension causes it to converge. Good atomization cannot be expected if the cone pulls together, so it is of interest to determine the conditions under

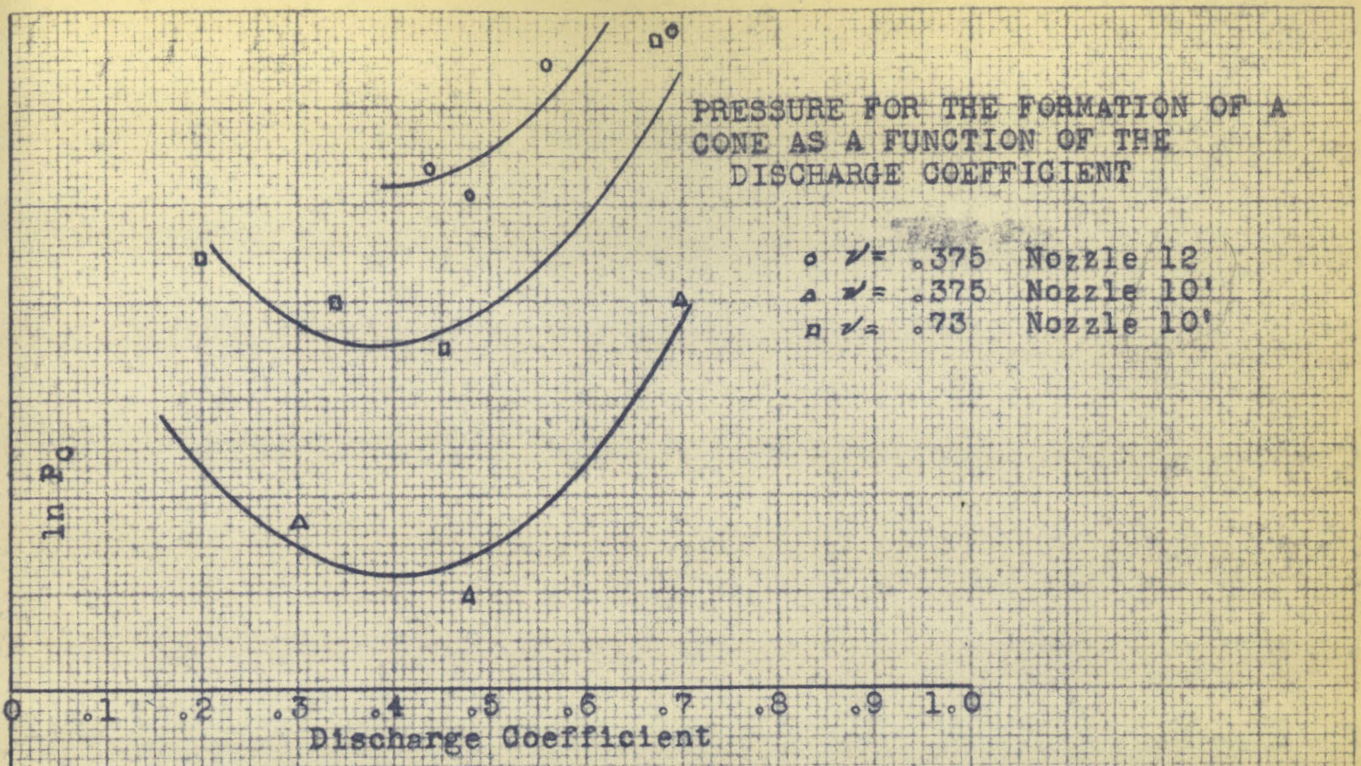

Fig. 22

$\ln P_o - .67\ L/r_o - 3.25\nu$ AS A FUNCTION OF THE DISCHARGE COEFFICIENT

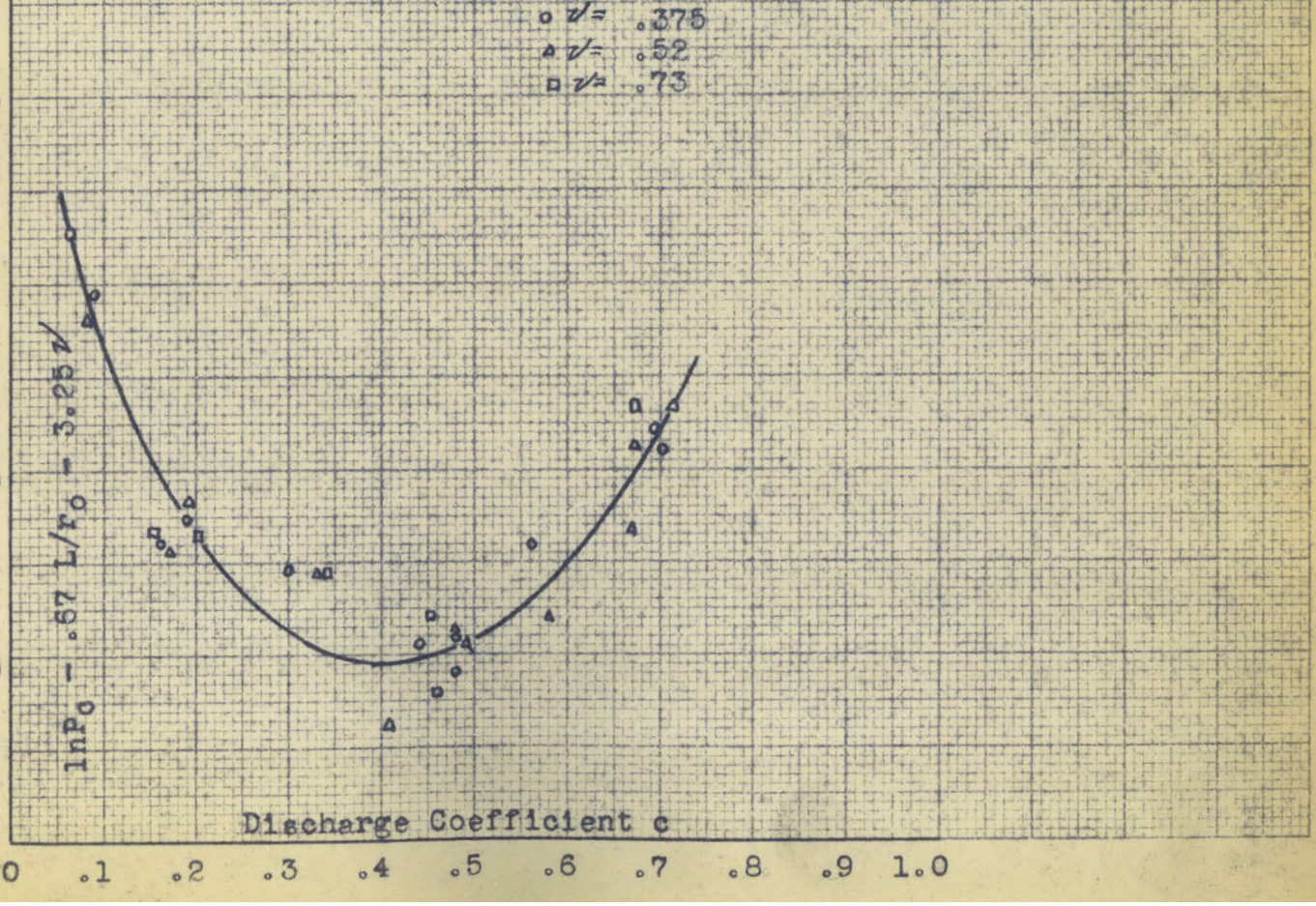

which a diverging cone is obtained. The viscosity and the pressure were measured for the point where drops formed no longer seemed to converge. Fig. 8 illustrates the appearance of a cone which was considered converging and one which was considered barely satisfactory.

Whether or not a cone will converge depends on the distance to the point of breakup where the surface forces no longer act to cause convergence and on the rate of convergence. Whether or not the drops formed will converge depends on the manner of breakup; however an analysis based on the behavior of the cone alone would probably indicate the variables of interest in correlating the data.

The force acting to pull the cone together is:

$4\mathcal{J}dl$

where $\mathcal{J}$ is the surface tension

dl is a differential length of the surface of the cone.

The force which must counteract this is:

$2\ rF \cos \alpha/2\ dl$

where F is the force acting on a unit area of the cone perpendicular to its surface

$$2\ rF \cos \alpha/2\ dl = 4\mathcal{J}dl$$

$$F = \frac{2\mathcal{J}}{r \cos \alpha/2}$$

This force is caused by the acceleration of the fluid in a direction at perpendicular to the surface.

Since F = ma

where m = mass of oil in a unit area. Which is equivalent to $\frac{t\rho}{g}$ where t is the thickness of the sheet and ρ is the density

a_s = the acceleration of the fluid

g = acceleration due to gravity

since the velocity of the sheet will be approximately

$$\sqrt{2g\,p/\rho}$$

and the flow rate is Q

for a thin sheet:

$$Q = 2\pi r\, t \sqrt{2g\,p/\rho}$$

$$t = \frac{Q}{\sqrt{2g\,p/\rho}} \frac{1}{2\pi r}$$

Since

$$F = \frac{t\rho}{g} a_s \;,\quad t = \frac{Fg}{\rho a_s} = \frac{Q}{\sqrt{2g\,p/\rho}} \frac{1}{2\pi r}$$

so

$$F = \frac{\rho a_s Q}{g\sqrt{2g\,p/\rho}\,(2\pi r)} = \frac{2J}{r\cos\alpha/2}$$

$$a_s = \frac{2gJ/\rho \sqrt{2g\,p/\rho}\,(2\pi r)}{Q\, r \cos\alpha/2}$$

since

$$C = \frac{Q}{\pi r_o^2 \sqrt{2g P/\rho}}$$

$$a_s = \frac{4g\, T/\rho}{r_o^2 \cos \alpha/2}\, C \tag{16}$$

No effort was made to integrate this equation to obtain the shape of the sheet since the equations became rather complicated and a method of evaluating the length of the sheet was lacking. If this integration was attempted the contraction of the sheet in a lengthwise direction should also be taken into account.

In hopes that the acceleration of the sheet at the orifice would prove to be significant, the pressure at which a diverging cone was formed was plotted against $cr_o^2 \cos \alpha/2$ for constant viscosity. The surface tension was not included since its effect was not studied. It was found that different curves were obtained for different viscosities, and that the curve was a straight line with a slope of -.78 when the data was plotted on log log paper, and that the lines were parallel. When the pressure was plotted against the viscosity at constant $cr_o^2 \cos \alpha/2$ on log log paper, straight lines with a slope of .78 were obtained. The combination of these

two effects gave the dimensional empirical equation:

$$(17) \qquad P_d = .39 \left(\frac{\nu}{c r_o^2 \cos \alpha/2} \right)^{.78}$$

where P_d = pressure in p.s.i. at which a diverging cone is formed

c = discharge coefficient at viscosity

ν $cm^2/sec.$

$\alpha/2$ = cone angle at that condition.

Fig. 22½ shows the pressure at which a diverging cone is formed as a function of the ratio $\frac{c\, r_o^2 \cos \alpha/2}{\nu}$. The solid line corresponds to Eq. 17. The data for this correlation are shown in Table 7.

Design of Nozzles

The data presented make it possible to find the operating characteristics for a given nozzle of design comparable to those tested. If a certain flow rate at a given pressure is specified the problem would be to find the nozzle which would give the smallest drop size, the widest range of operating viscosities, and the most stable cone. No method of predicting the cone stability is available, but the first two characteristics can be studied.

The drop size is probably the most important

Fig 22.5

PRESSURE NECESSARY TO FORM A DIVERGING CONE
AS A FUNCTION OF $cr_0^2 \cos \alpha/2 / \nu$

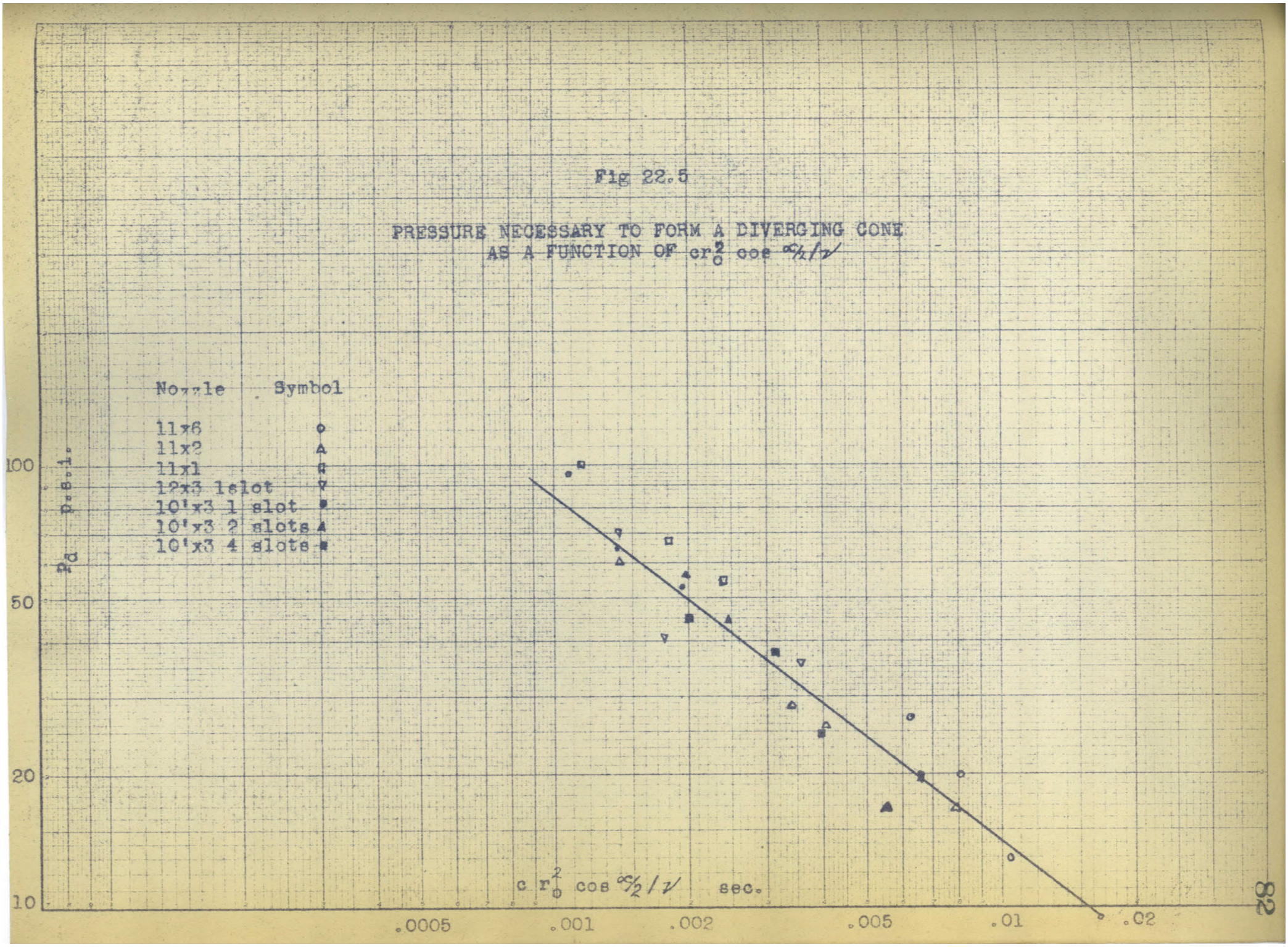

characteristic of the nozzle since the viscosity of fuel oils can, in general, be adjusted to such a value that the nozzles of the sizes studied would operate satisfactorily. The work on drop size indicates that the value of Do at zero viscosity is a satisfactory criterion of the performance of the nozzle in regard to drop size distribution. It was found that for this case the radio Do sin $\alpha/2/r_o$ is constant for a given pressure. Making $r_o/\sin \alpha/2$ as small as possible would give the smallest drop size. Since at one discharge rate the radius depends on the square root of the discharge coefficient sin $\alpha/2\sqrt{c_o}$ can be used instead. The discharge coefficient and the cone angle at zero viscosity are the same for nozzles that are dimensionally similar, so the magnitude of sin $\alpha_o/2\sqrt{c_o}$ does not depend on the size of the nozzle, and therefore nozzles of different sizes can be judged as to design by this criterion, which will be called the atomization criterion. It should be noted that no information as to the absolute value Do is given by the atomization criterion, but for a given radius or discharge rate the nozzle which has the largest value of sin $\alpha_o/2\sqrt{c_o}$ will give the smallest drop size. Table 7 gives the discharge coefficient at zero viscosity, the cone angle at zero viscosity, and the value of the atomization cri-

terion. From this table it can be seen that the 10'x3 and the 10'x6 gave the best performance by this criteria.

The variables which must be used to find the performance of a nozzle are the radius of the orifice, the distance from the back of the swirl chamber to the orifice, the average radius of the point where a particle of fluid enters the swirl chamber, and the area of the tangential slots. From these variables the discharge coefficient, the cone angle, the conditions for the formation of a cone, and the conditions for the formation of a diverging cone can be found. Only the last of these depends on the scale of the nozzle; so the following variables will be used: L/r_o , r_s/r_o, and A_s/r_o^2 . r_o must be used separately when determining the conditions for the formation of a diverging cone. A_s/r_o^2 will be recognized as being directly related to the ratio of ten times the area of the slots over the area of the orifice which is known as the nozzle ratio. This ratio is commonly used in commercial nozzles as a criterion of their characteristics. For example, the 40 in the T58X40 nozzle refers to the nozzle ratio. The other number refers to the size drill used to make the orifice. A nozzle ratio of 40 corresponds to a value of A_s/r_o^2 of 12.7.

An example of the type of calculation which could be made is shown below.

The object is to find the operating characteristics at zero viscosity for the following nozzle design: $A_s/r_o^2 = 10$, $L/r_o = 3$, $r_s/r_o = 3$, $r_o = .03$ cm, and an operating pressure of 150 p.s.i.

From these dimensions $\frac{r_{sL}}{A_s} = .9$

with this value "a" is found to equal 2.18 from Fig. 18, and a' = 1.99 from Fig. 21.

$$b = \left(\frac{\pi r_o^2}{A_s}\ \frac{r_s}{r_o}\right)^2 = (3.14 \times .1 \times 3)^2 = .89$$

Using a and b and Fig. 17

$$\frac{c_o = .375}{\cos \alpha_o/2} = \frac{c_o}{1 - a'^2 b c_o^2} = \frac{.375}{1-(.375 \times 1.99)^2 .89} = .74$$

$$\alpha_o/2 = 42° \qquad \alpha_o = 84°$$

$$\sqrt{c_o} \sin \alpha_o/2 = \sqrt{.375} \times .675 = .413$$

From Fig. 19 the value of the discharge coefficient at the condition where the cone is formed is .54. From Fig. 22 the value of $\ln P_c - .67\ L/r_o - .325\nu$ is -1.8.

Substituting the given values:

$$3.25\nu = +1.8 + \ln 150 - .67 \times 3$$

$$= 4.8$$

$$\nu = 1.48 \text{ cm}^2/\text{sec.}$$

Eq. 17 can be written:

$$(18) \qquad \nu = \frac{c\, r_o^2 \cos \alpha/2\, P_d^{1.28}}{.30}$$

The value of c and cos α /2 depends on the viscosity so a trial and error solution will be necessary. It was found that the viscosity was such that c_o could be used for the discharge coefficient. Fig.20 is used to find the cone angle which was 64°.

$$\nu = \frac{.375 \times .0009 \times .85 \times 610}{3.0} = .58$$

This value of viscosity is smaller than the value for the cone formation so as viscosity is decreased the cone will form and when a viscosity of .58 is reached the cone will diverge. It would be expected that very poor atomization would occur at viscosities higher than .54 cm^2/sec.

A number of calculations similar to the above example were made. Figures 23, 24, 25, and 26 show the effect of changing some of the variables. The results of the calculations can be summarized as follows:

Increase of	Discharge Coefficient	Cone Angle	Value of A_s/r_o^2 for maximum $\sin \alpha/2\sqrt{C_o}$	Viscosity for cone formation	Viscosity for formation of diverging cone
A_s/r_o^2	increases	decrease over range of interest		goes thru maximum	increases
L/r_o	increases	decreases	decreases	decreases	increases slightly
r_s/r_o	decreases	increases	increases	small effect	decreases

The effect of these variables on the value of the atomization criterion is probably of greatest interest. This value goes through a maximum with decreasing A_s/r_o^2. The magnitude and position of the maximum point are of particular interest since it is desirable to have as large a value of the atomization criterion as is concordant with ease of construction and range of viscosity of fluid which can be atomized. The general effects are summarized in the preceding table but it might be noted that the advantage of going to a very large A_s/r_o^2 to obtain a high value of the atomization criterion is offset by a decreased viscosity for cone formation without a large increase in the atomization criterion. If range of atomization is of primary interest, for

Fig. 23

ESTIMATED DISCHARGE COEFFICIENT AT ZERO VISCOSITY
AS A FUNCTION OF A_s/r_o^2

r_s/r_o 3
E/r_o 3
L/r_o 6

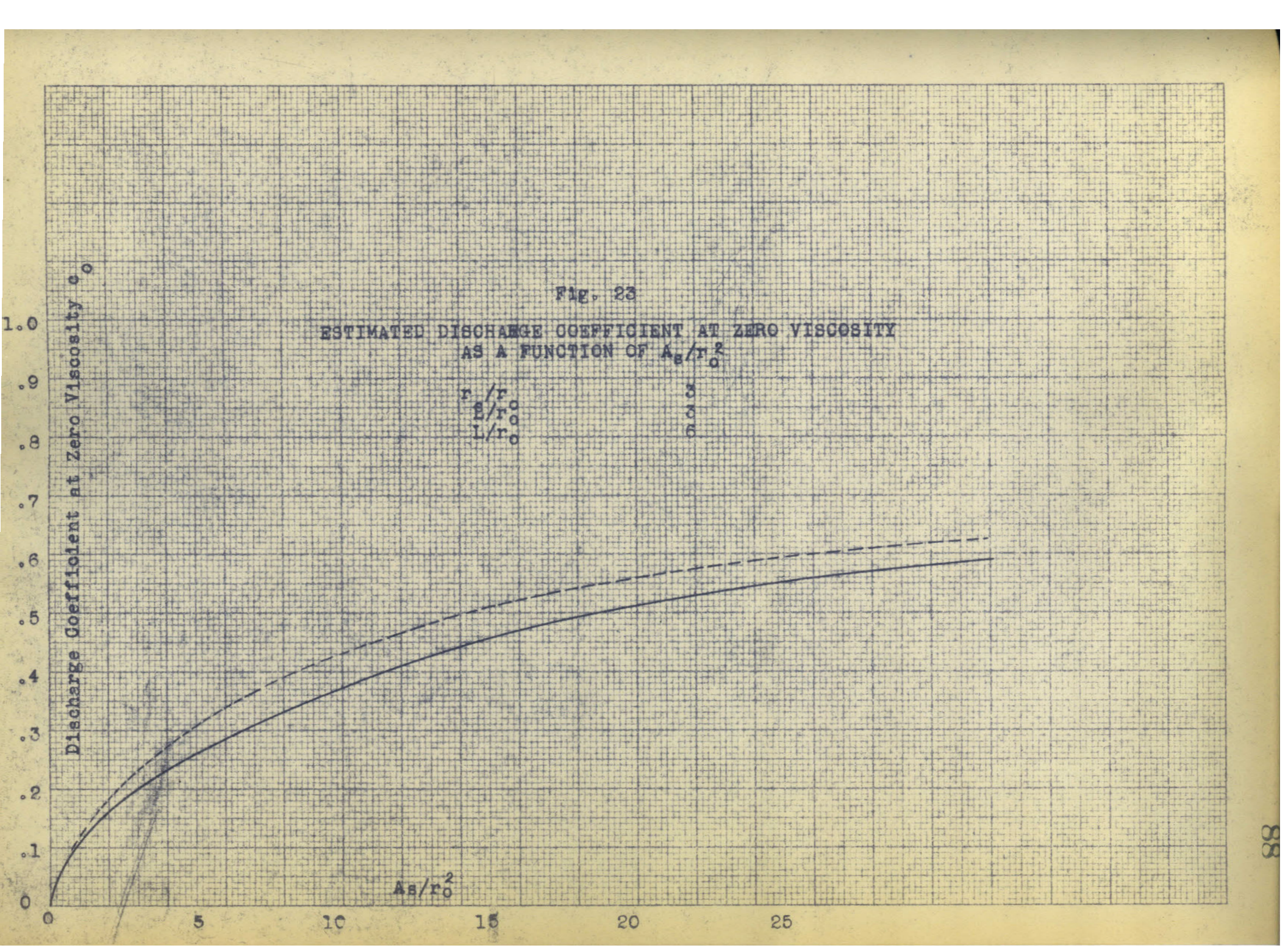

Fig. 24

ESTIMATED CONE ANGLE AT ZERO VISCOSITY
A S A FUNCTION OF A_s/r_o^2

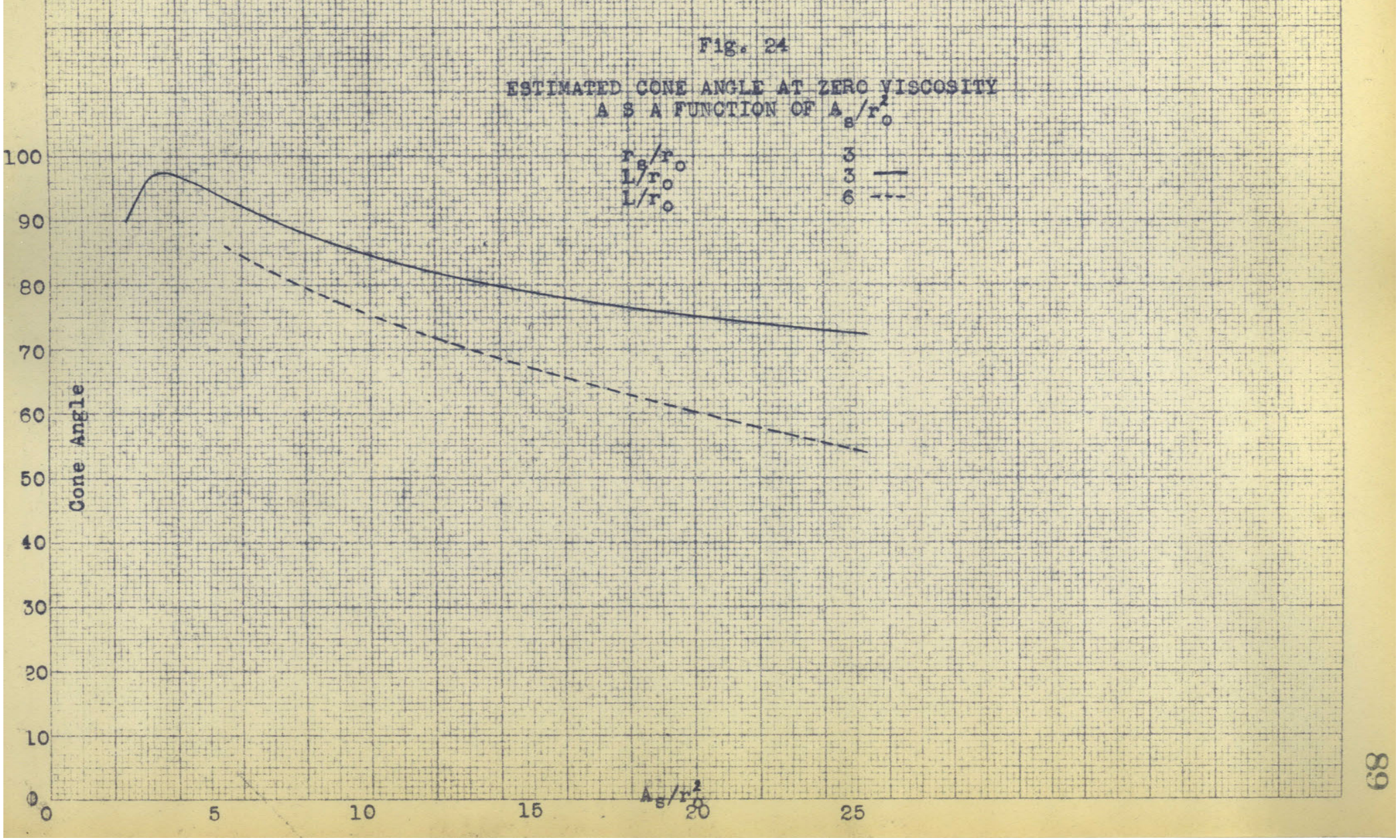

Fig. 25

FORMATION OF A CONE AND THE FORMATION OF A DIVERGING CONE AS A FUNCTION OF A_s/r_o^2

Pressure 150 p.s.i.
r_s/r_o 3
L/r_o 3 —
L/r_o 6 ---

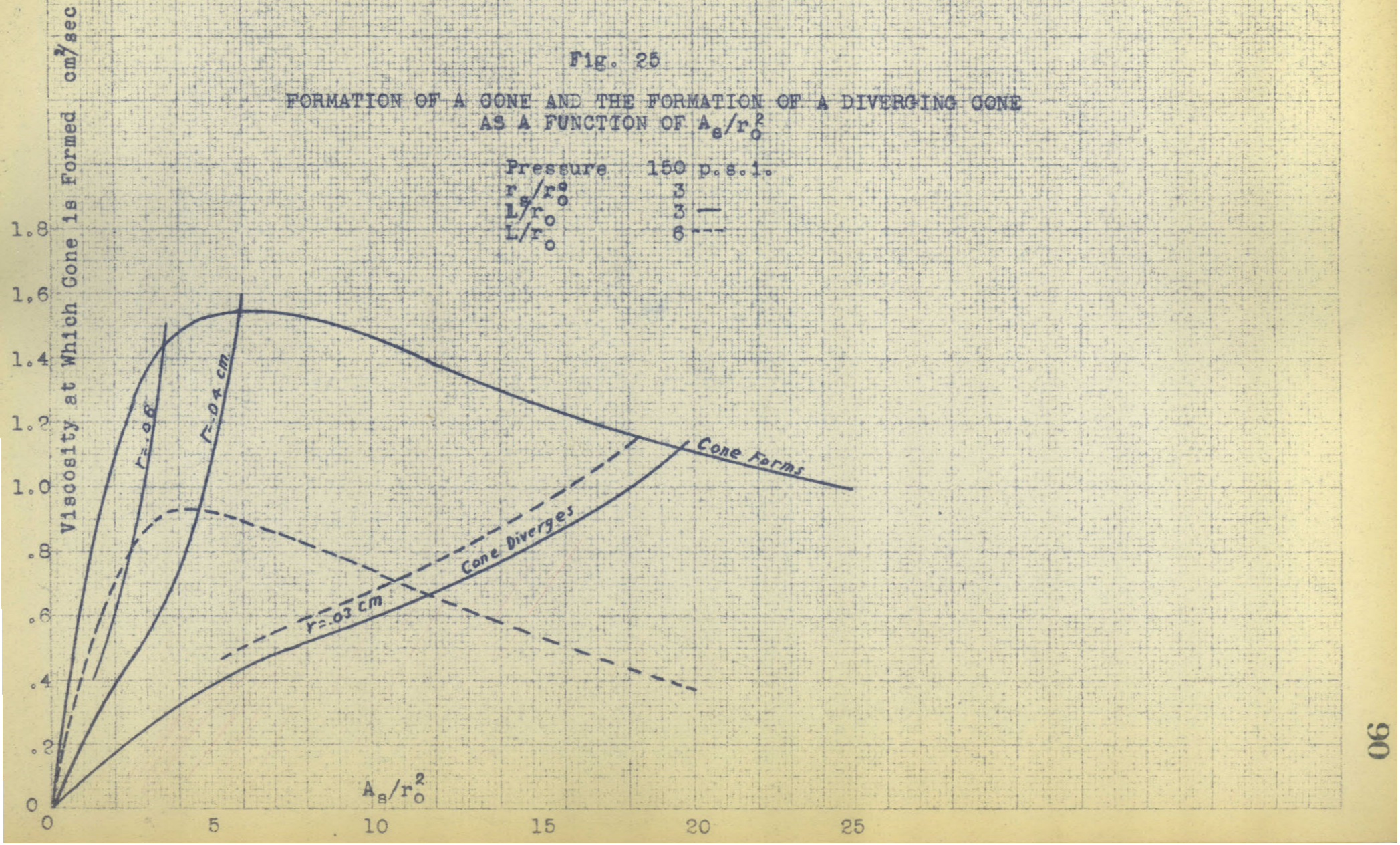

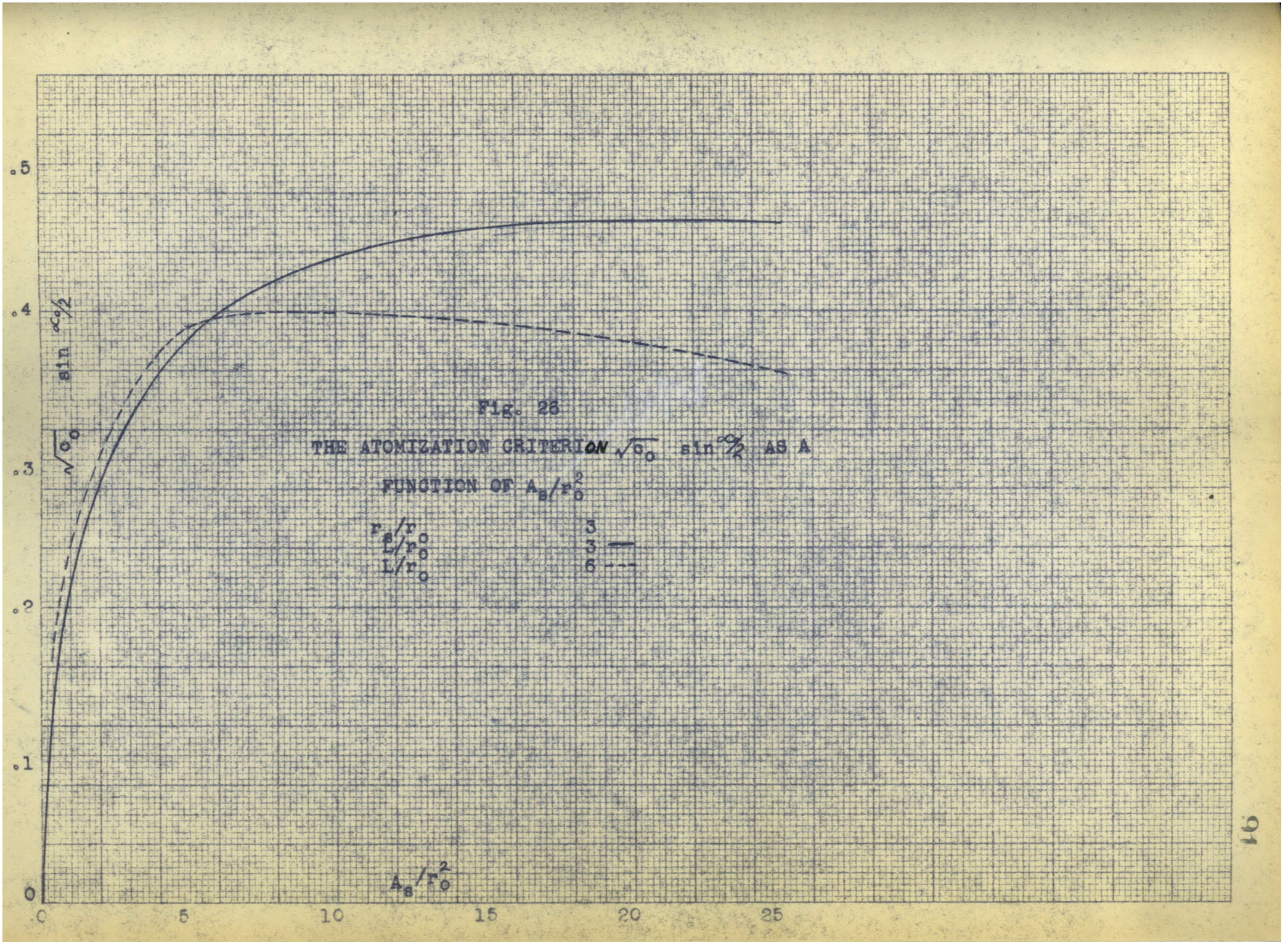

Fig. 26

THE ATOMIZATION CRITERION $\sqrt{c_o}$ sin $\alpha_o/2$ AS A FUNCTION OF A_s/r_o^2

nozzles with r_o greater than .03 cm, value of A_s/r_o^2 of 10 will give the best results with L/r_o and r_s/r_o set at 3.

The disadvantage of a large L/r_o is obvious from the preceding figures and the indication is that the smaller L/r_o is the better the performance will be. The type of construction used in these nozzles is limited to a lower value of L/r_o of about 3 in the region of high A_s/r_o^2 and r_s/r_o .

Increasing the value of r_s/r_o increases the value of A_s/r_o^2 necessary to obtain as low a value of the atomization criterion / as was obtained before r_s/r_o was increased. Since the viscosity for cone formation is not changed much by increasing r_s/r_o either poorer atomization will be obtained or the range of viscosities at which successful atomization can be obtained will be reduced, since in the region of best performance increasing A_s/r_o results in a decrease at allowable atomizing viscosity. When A_s/r_o^2 is large it is difficult to make a nozzle with a value of r_s/r_o much less than three and still keep L/r_o small.

Examination of the calculations made indicated that a nozzle which would be a good compromise between range of atomization and quality of atomization would have the following dimensions:

A_s/r_o^2	20
L/r_o	3
r_s/r_o	3

This nozzle would have a cone angle at zero viscosity of about 77° and a discharge coefficient of about .53. If r_o was less than .03 cm, the viscosity at which a diverging cone would form would seriously limit the type of fluid which could be atomized by the nozzle. This limitation as well as the difficulty of maintenance of small nozzles will tend to set a lower limit on the diameter of nozzle orifice which is practical to use with an oil of a given viscosity.

A nozzle which is similar to number 15, which is merely a sharp-edged orifice, will give the minimum L/r_o, and is probably the easiest to make. This nozzle performed satisfactorily at high pressures, but it was noticed that at low pressures, as when starting or stopping the flow, that the fluid tended to spread out over the face of the nozzle. The tests noted were done with water, but if oil did this the result might be quite serious since this oil would tend to carbonize on the surface of the nozzle and could ruin the atomization by making the edge of the orifice rough. This effect should be more extensively studied before

it is used as a limitation on nozzle construction, however, it does appear that it would be well to have some rounding of the entrance of the orifice.

Some general remarks on the design of the tangential slots might be made. It is desirable to make the length of the slots as small as possible in order to reduce viscous losses through the slots. Only enough length to give the proper direction to the flow of the fluid is necessary. It is also very important that there be more than one slot and that the slots be symmetrically placed so that a symmetrical cone will be obtained. Experiment showed that if only one slot or an unsymmetrical arrangement of slots was used that a poorly shaped cone results.

CONCLUSIONS

The following conclusions can be drawn from the experimental work on a series of nozzles constructed in the laboratory using a hydrocarbon oil as the fluid:

(1) The Rosin equation is satisfactory for describing the drop size distribution obtained in this work.

(2) Rapid fluctuations of the cone which originate in the nozzle are likely to occur. These fluctuations increase the drop size over what it would have been if they had not been present, but their effect becomes much less serious as the pressure is increased and viscosity is decreased.

(3) When fluctuations do not occur and the vortex is well formed in the nozzle, it was found that $\frac{Do \sin \alpha/2}{r_o}$ is substantially constant for a given pressure and viscosity, and that the effect of viscosity and pressure could be summarized by the equation

$$\frac{Do \sin \alpha/2}{r_o} = .72\, p^{-.375}\, e^{.705}$$

, and that n was a function of Do. This relation was found to hold for all nozzles tested including the T58x40 #2.

(4) The fact that Do is directly proportional

to the orifice radius indicates the desirability of using nozzles with small orifices.

(5) It was found that a discharge coefficient at zero viscosity would be useful in characterizing most of the nozzles, and that the discharge coefficient could be predicted by the equation:

$$C_o = \sqrt{1-bc_o^2} - abc_o^2\sqrt{a^2-1} - bc_o^2 \ln \frac{1+\sqrt{1-bc_o^2}}{\sqrt{bc_o^2}\left(a+\sqrt{a^2-1}\right)}$$

Since the constant "a" is difficult to determine experimentally it was correlated in terms of $\frac{r_s L}{A_s}$. Use of this correlation and the equation make it possible to predict the discharge coefficient by knowing the nozzle dimensions.

(6) The cone angle was found to decrease with viscosity and this data is represented by a plot of cone angle divided by cone angle at zero viscosity against viscosity. All the nozzles except the T58X40 fall on the curve.

(7) The cone angle at zero viscosity is correlated in terms of dimensionless groups involving the nozzle dimensions.

(8) For the nozzles built in the laboratory

the pressure at which a cone is formed can be predicted from a correlation in which $\ln P_c - .67\ L/r_o - 3.25\sqrt{}$ is plotted against the discharge coefficient.

(9) The pressure at which a diverging cone is formed can be represented by the empirical equation:

$$P_d = .34 \left(\frac{\sqrt{}}{r_o^2\ c\ \cos\ \alpha/2}\right)^{+.78}$$

This indicates that nozzles of small r_o will be unable to atomize viscous oil. This effect becomes serious at $r_o = .03$ cm.

(10) $\sin \alpha_o/2\sqrt{c_o}$ can be used as a criterion of quality of atomization for a given size of nozzle. Good nozzles were found to have a value of $\sin \alpha_o/2\sqrt{c_o}$ of around .45.

(11) Extrapolation of the correlations indicates that $\sin \alpha_o/2\sqrt{c_o}$ greater than .45 could be obtained, but at the expense of range of oil viscosity which could be successfully atomized.

(12) It was found that the smaller L/r_o was the better performance was obtained from the nozzle in all respects. Commercial nozzles usually have too large a value of L/r_o.

(13) The following dimensions are recommended for a nozzle which will have good atomizing characteristics and a good range of viscosities:

$$A_s/r_o^2 = 20$$

$$L/r_o = 3$$

$$\frac{r_s}{r_o} = 3$$

APPENDIX

NOMENCLATURE

a r_i/r_{ip}

a_s acceleration of the cone sheet in a direction perpendicular to its surface

A_s combined area of the tangential slots which lead into the swirl chamber of the nozzle

b a constant in the Rosin equation

$b = \frac{\pi^2 r_o^4}{A_s^2} (r_s/r_o)^2$

c discharge coefficient based on the area of the orifice

c_o discharge coefficient for a fluid of zero viscosity

D drop diameter

D_o weight median drop diameter

D_m weight mean drop diameter

e logarithmic base

E energy of a unit mass of fluid

E_r rotational energy

E_{rs} rotational energy of the fluid at the tangential slots

E_{ro} rotational energy at the radius of the orifice

E_t translational energy

E_p energy equivalent to the original pressure head

$F = ma_s$

g	acceleration due to gravity
G	amount of oil collected in the sampler in time θ
I	amount of oil in a spray that passes a unit area in unit time
l	length of the surface of the conical sheet of fluid
L	distance from the back of the swirl chamber to the orifice of the nozzle
m	mass of oil in a unit area of cone sheet
n	a constant in the Rosin Equation
P	pressure drop through the nozzle in p.s.i.
P_c	the minimum pressure at which a cone will be formed
P_d	the minimum pressure at which a diverging cone will be formed
Q	the discharge rate of a nozzle
r_s	distance of a particle of fluid from the center line of the nozzle
r_o	radius of the orifice of the nozzle
r_i	radius of the vortex core
r_{ip}	radius at which all of the energy of a particle of fluid in the nozzle is in the form of rotational energy
R	fraction of a sample of drops which is above a given size
t	thickness of the cone sheet

t_o thickness of the cone sheet at the orifice

v velocity of a particle of fluid

V velocity of the drop sampler

w width of the sampler opening

x distance of sampler from the center of the spray

α the spray cone angle

α_o the spray cone angle for zero viscosity

ϵ $= E_{ro}/E_p$

ρ fluid density

ω rotational velocity

θ sampling time

J surface tension

ν kinematic viscosity

EXPANSION OF PROCEDURE

An important part of the work of this thesis consisted of the development of a technique of determining the drop size distribution quickly and easily enough so that the operating variables could be studied in the time available. The technique decided upon consists of collecting the drops, freezing, sieving, and determining the relative weights of the various fractions on the sieves. Since none of these operations are performed by standard techniques they will be discussed in more detail than was given in the section on apparatus and procedure.

The collection of a representative sample of a spray of this type is one of the first problems to be considered. Since the collecting aperture of the apparatus was limited it was necessary to collect drops by moving the collector across the spray. If it is assumed that the spray is symmetrical around the axis of the cone it will be possible to obtain a sample along any radius. This assumption is believed to be of sufficient accuracy for the nozzles used and for the required accuracy of the results. Care was taken to insure that the orifice of the nozzle was round and that there were no notches on the edge of the orifice. The

swirl chamber was fed by symmetrically arranged tangential slots, which is important in attaining a symmetrical cone. For most of the distance of sampling the width of the sampler is small as compared to the circumference of the circle.

If G is the amount of oil collected in time Θ,
w is the dimension of the sampler along the circumference,
dx is the width of the sampler along a radius,
I is the amount of oil crossing a unit area in unit time Θ,
Then: $G = I\ \Theta\ w\ dx$.

The amount of oil in unit time that could be collected in an annulus of width dx is $2\pi x\ w\ dx$. To obtain a representative sample it is necessary that these two amounts have a constant ratio at any radius.

$$\frac{w\ \Theta}{2\ \pi\ x} = \text{const. or } \frac{\Theta}{x} = \text{const.}$$

Since the time necessary to cross a certain distance is inversely proportional to the velocity of travel

$$x\ V = \text{const. or } V \propto \frac{1}{x}$$

where V is the velocity of the collector.

The collector was drawn from the center of the spray toward the outside at a velocity inversely proportional to the distance from the center by means of a string which was wound up on a rectangular hyperbola of revolution. Of course the sample taken very near the center did not follow this law since the equation would call for a very high velocity. However, since this constituted a relatively small proportion of the total sample it is believed that this source of error can be neglected. To check this method of sampling, samples were taken at various radii along the spray and two were taken by the above method. An integration of the point data gave a value of Dm of 170 microns, while the automatic integration gave values of 170 microns and 178 microns, which constituted a satisfactory check. Runs 98 - 102 are the size data which were used for this purpose and Fig. 27 shows change of spray intensity and drop size along a radius. Table I gives the spray intensity data.

TABLE I

SPRAY DISTRIBUTION CORRESPONDING TO RUNS 98-102

Dist. from center line in.	Gms. of oil in 10 sec.
.5	1.053
2.75	.678
5.35	.322
7.75	.123
10.25	.028

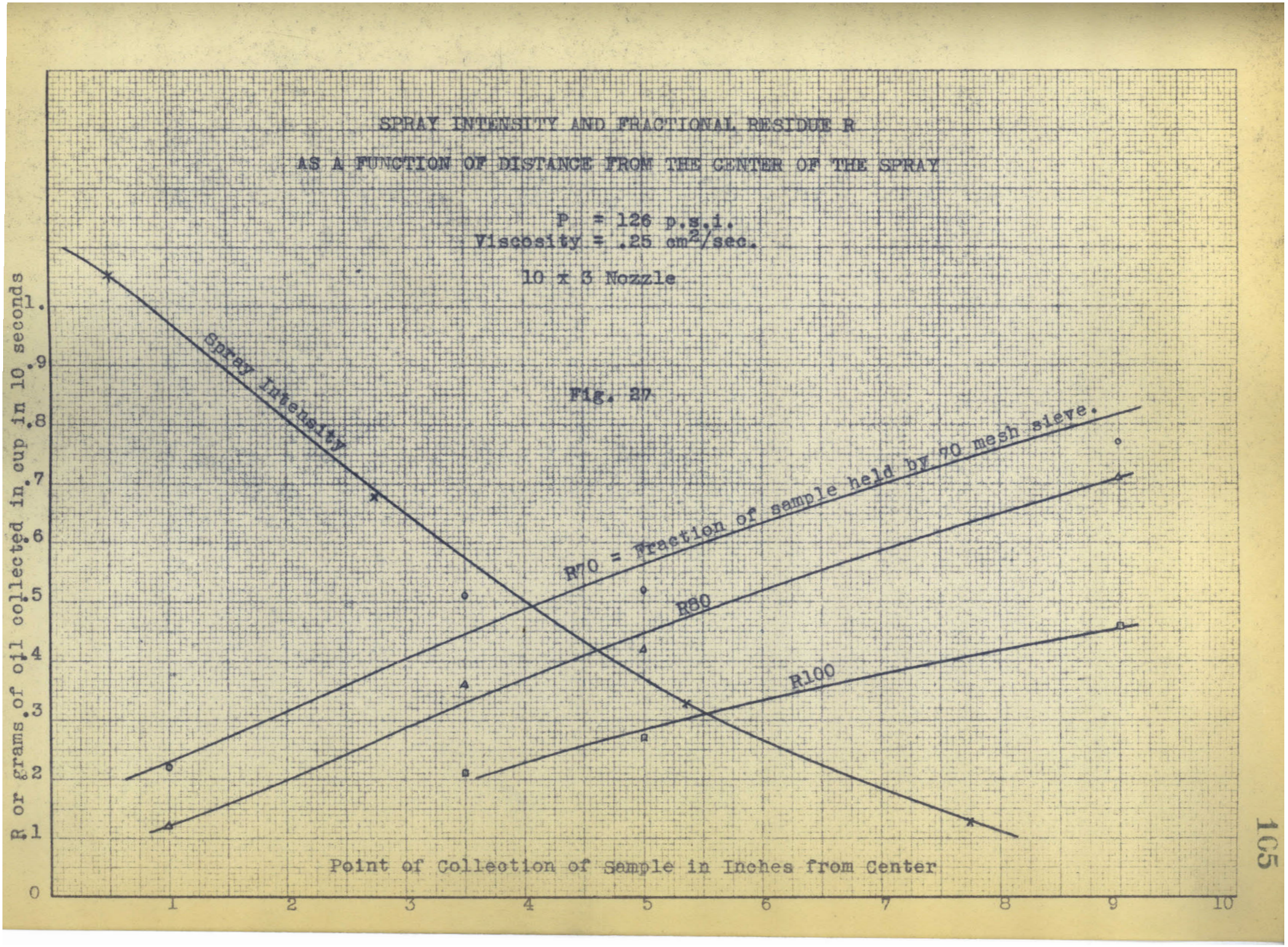
SPRAY INTENSITY AND FRACTIONAL RESIDUE R
AS A FUNCTION OF DISTANCE FROM THE CENTER OF THE SPRAY
P = 126 p.s.i.
Viscosity = .25 cm²/sec.
10 x 3 Nozzle
Fig. 27
Spray Intensity
R70 = Fraction of sample held by 70 mesh sieve.
R80
R100
R or grams of oil collected in cup in 10 seconds
Point of Collection of Sample in Inches from Center
0
1
2
3
4
5
6
7
8
9
10

Since the big drops fall more quickly than the small ones it is necessary to let the spray run for a while before a sample is taken in order that it be representative of what is leaving the nozzle. Air was drawn through the chamber by a vacuum cleaner blower in order to hasten the fall of the small drops. Runs were taken to study the effect of time of run of spray on the mean drop size and on n. No effect on n was found but the drop size for a five-second run was about five percent smaller than for a run at a time of twenty seconds.* The twenty-second run was essentially the same as some runs at thirty-five and forty seconds. Although the difference was small the procedure used was to let the spray run about thirty seconds before the sample was taken.

Even if the spray has run long enough it is not certain that a representative sample will fall into a hole such as the opening on the collector. Particularly near the center of the spray the air velocity is quite appreciable due to the drag of the drops, and small drops are more likely to follow changes in direction of the air stream than big ones. For this reason the collector was designed to disrupt the flow as little as possible and it was made possible for air which

---

* See runs 1 and 2 in Tabulation of Drop Distribution Data.

enters the opening to escape out another opening so that there would not be a stagnation point above the collector. After entering the collector the air made a sudden ninety-degree change in direction and was slowed down considerably due to the larger cross section on the interior of the collector. Although some trouble was experienced with drops being deposited on the sides and back of collector, it is believed that this source of error was not large since the amount thus deposited was small compared with the total amount collected. This loss would be most serious for small drops and the distribution curve when plotted on lnln 1/R vs ln Dm increased in slope at high values of R in many cases, while the work of Koulpaev and Houghton indicated that such a change was not to be expected. This could be taken as an indication at loss of small drops.

Solid carbon dioxide offered itself as the most convenient means of attaining a low temperature and several different methods of using it were tried. An attempt was made to spray liquid carbon dioxide into the chamber with the drops, and to collect the drops with the carbon dioxide snow formed, but in order to obtain any snow it was necessary to use quite high gas velocities which resulted in the drops being thrown vi-

olently against the chamber wall. This technique was abandoned since other methods seemed to offer fewer difficulties. The collection of the drops on a smooth bed of solid carbon dioxide was successful but some of the larger drops were flat on the bottom where they rested on the carbon dioxide, and moisture from the air condensed on the surface of the drops, thus increasing their size. This film of ice was difficult to remove without softening the drops so that there was danger of their sticking together. Another difficulty with this apparatus was that it was more bulky than the one finally adopted, and it was felt that it would disturb the flow of air in the spray chamber enough to make the sample less representative than one taken with the other apparatus. Gas phase freezing offered some possibilities but it was not tried.

The method which was adopted was to freeze the drops in the liquid phase. It was found that if the drops were collected directly in a cold liquid that they flattened when they hit the surface and froze before they regained their spherical shape. To prevent this they were collected in liquid warm enough to permit their regaining their spherical shape, after which they were frozen. The oil spray was dense enough to make it necessary to remove the collected drops from under the

collector opening continuously so that the drops would not land on each other and stick together , or two drops form a larger drop. This was accomplished by having a stream of warm liquid flowing over a glass plate under the collector opening at a velocity such that a negligibly small number of drops stuck together.

The requisites of the fluid to be used for the freezing and sieving medium are that it does not dissolve the oil, that it does not freeze at dry ice temperatures, and that it has a fairly low viscosity at these low temperatures so that sieving will not be too slow and will be effective. Ethyl alcohol was found to be quite satisfactory for this purpose. The oil will dissolve in it to a limited extent at room temperature but does not seem to dissolve appreciatly at dry ice temperature in the time ordinarily allowed for contact. It was found that a drop of the oil used in this work will remain in cold alcohol for over an hour without changing its diameter as measured under a microscope.

The size of drop that can be collected by this method is definitely limited since too large a drop will break when it strikes the liquid surface. A brief study of the factors involved in the breakage of drops

striking a liquid surface was made in order to determine whether or not the method could be used in the range of drop sizes of interest in this work. The following variables were found to be of importance.

Drop diameter

Drop velocity

Drop viscosity

Surface tension between the drop and collecting fluid

Viscosity of collecting fluid

Velocity of collecting fluid

Depth of collecting fluid

The maximum drop diameter is controlled by the other variables. The drop velocity was not measured but the drops were collected at a distance of two and one-half feet from the Chang (5) dropper which was used to form the drops. Although the drop velocity varies with the drop size it is believed that the conditions were representative of those in the spray chamber.

For some cases there was an optimum depth of collecting fluid. If the fluid was deep the drop would be deformed as it hit the surface and the drag of the fluid on the drop as it was slowed down would tear off satellites. If the depth of the fluid was reduced

the drop would not be broken. Evidently the distance of travel was not enough to tear off the satellite which was being formed. If the collecting fluid was too thin the drop was shattered when it struck the bottom of the container. It was found that if some water was mixed with the alcohol that the drops could be much larger before they broke. This is probably due to the fact that the interfacial surface tension between the oil and the water-alcohol mixture is greater than the interfacial surface tension between the oil and pure alcohol. No direct measurements were taken, but it was observed that if a drop of oil in the water-alcohol mixture was deformed it would come back to spherical shape much more quickly than if it was in pure alcohol. Since the resistance to being restored to spherical shape is about the same in both cases this phenomena was taken as qualitative evidence that the surface forces were greater in the case of the water-alcohol mixture. However, if too much water is added the oil will spread out on the surface of the liquid.

For the case of drops falling into a container of still fluid it was found that if the viscosity of the fluid was increased by mixing glycerine with the alcohol that the breaking diameter of the drop increased. This

effect was not due to the increase of surface tension alone since just mixing water in amounts which would be expected to give the same surface tension did not give such good results. This effect of increase in viscosity was believed to be similar to the effect of decreasing the depth of the fluid film. It is not desirable to mix too much glycerine with the alcohol since the viscosity gets too great when it is cold and since the mixture will foam when dry ice is placed in it. Also there is a limit to the amount of water which can be used since it will precipitate at low temperatures and form a sludge which clogs the screens and the filter. After a number of qualitative tests with static fluids, a mixture of 80% commercial denatured ethyl alcohol, 10% water, and 10% glycerine was chosen.

The limiting drop size was then determined for various operating conditions with the collector and a two and a half foot fall of the drops. Fig. 28 shows that replacing some of the water with glycerine has little effect. However, the 10% glycerine, 10% water, and 80% ~~glycerine~~ eth. alc. mixture was used.

When the alcohol is flowing down the glass plate the drops are broken at a smaller diameter than would be the case if the fluid were static. The effect of alcohol flow rate is shown in Fig. 30 where the

TABLE 2

DATA ON DROP BREAKAGE

Height of Fall - 2.5 feet Fluid - Static
Drop Viscosity = .05 Poise

Maximum Diameter of Drop which will not Break. - Microns	Composition of Collecting Liquid
800	Ethyl Alcohol (commercial denatured)
880	15% H_2O 85% Alcohol
1,170	30% H_2O 70% Alcohol
920	10% H_2O 10% Glycerine 80% Alcohol
1,130	15% H_2O 15% Glycerine 70% Alcohol

Height of Fall - 2.5 feet Flow Rate - 5.5 cc./sec.

10% H_2O 10% Glycerine 80% Alcohol

Maximum Diameter of Drop which will not Break. -Microns	Viscosity of Drop
520	.11
550	.22
640	.6

Height of Fall - 2.5 feet Drop Viscosity .37 Poise

10% H_2O 10% Glycerine 80% Alcohol

Maximum Diameter of Drop which will not Break. -Microns	Alcohol Flow Rate cc./sec.
1,020	0
580	5.5
460	10

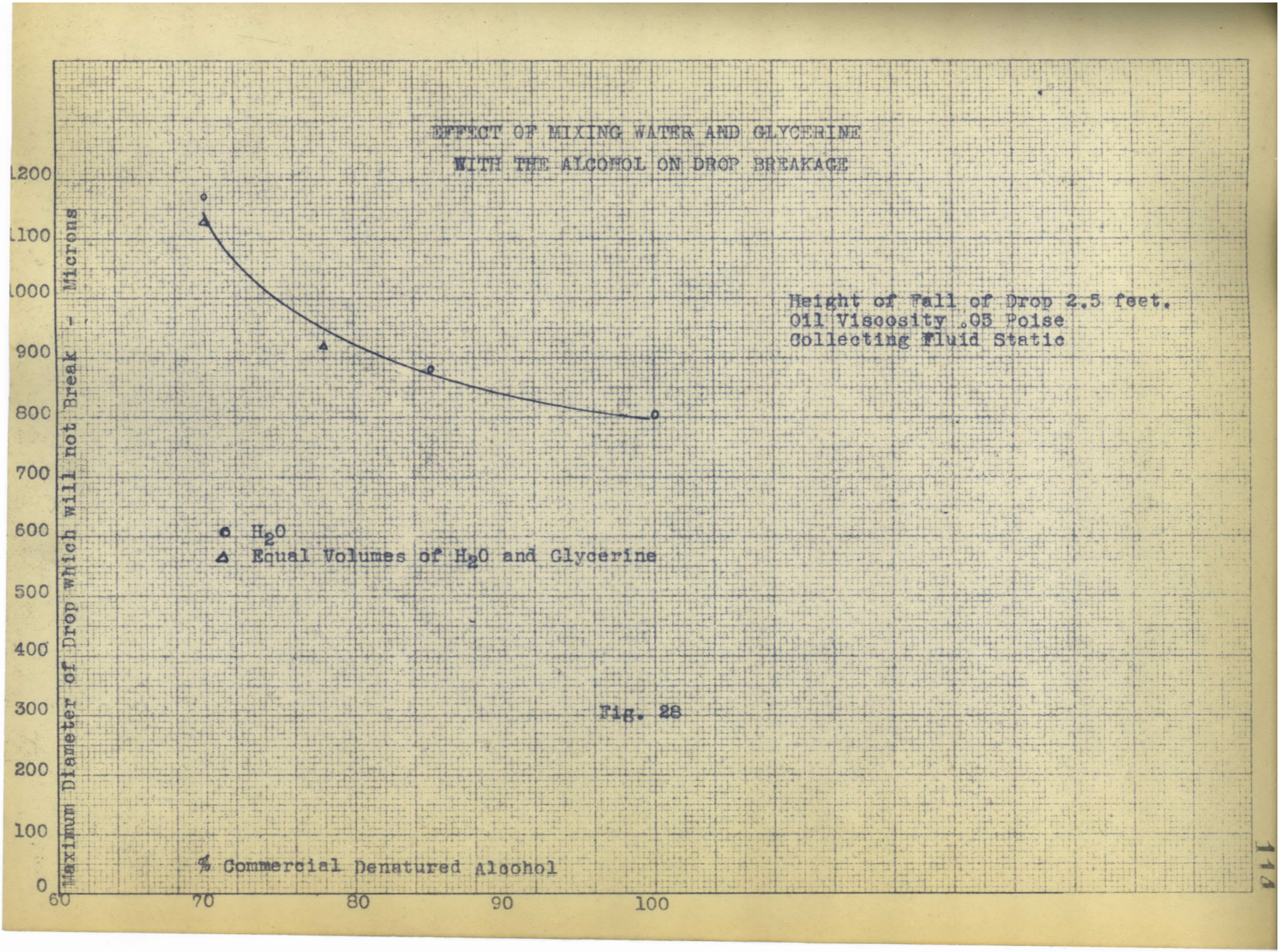
EFFECT OF MIXING WATER AND GLYCERINE
WITH THE ALCOHOL ON DROP BREAKAGE
Maximum Diameter of Drop which will not Break - Microns
1200
1100
1000
900
800
700
600
500
400
300
200
100
0
60
70
80
90
100
% Commercial Denatured Alcohol
Height of Fall of Drop 2.5 feet.
Oil Viscosity .05 Poise
Collecting Fluid Static
o H_2O
Δ Equal Volumes of H_2O and Glycerine

Fig. 28

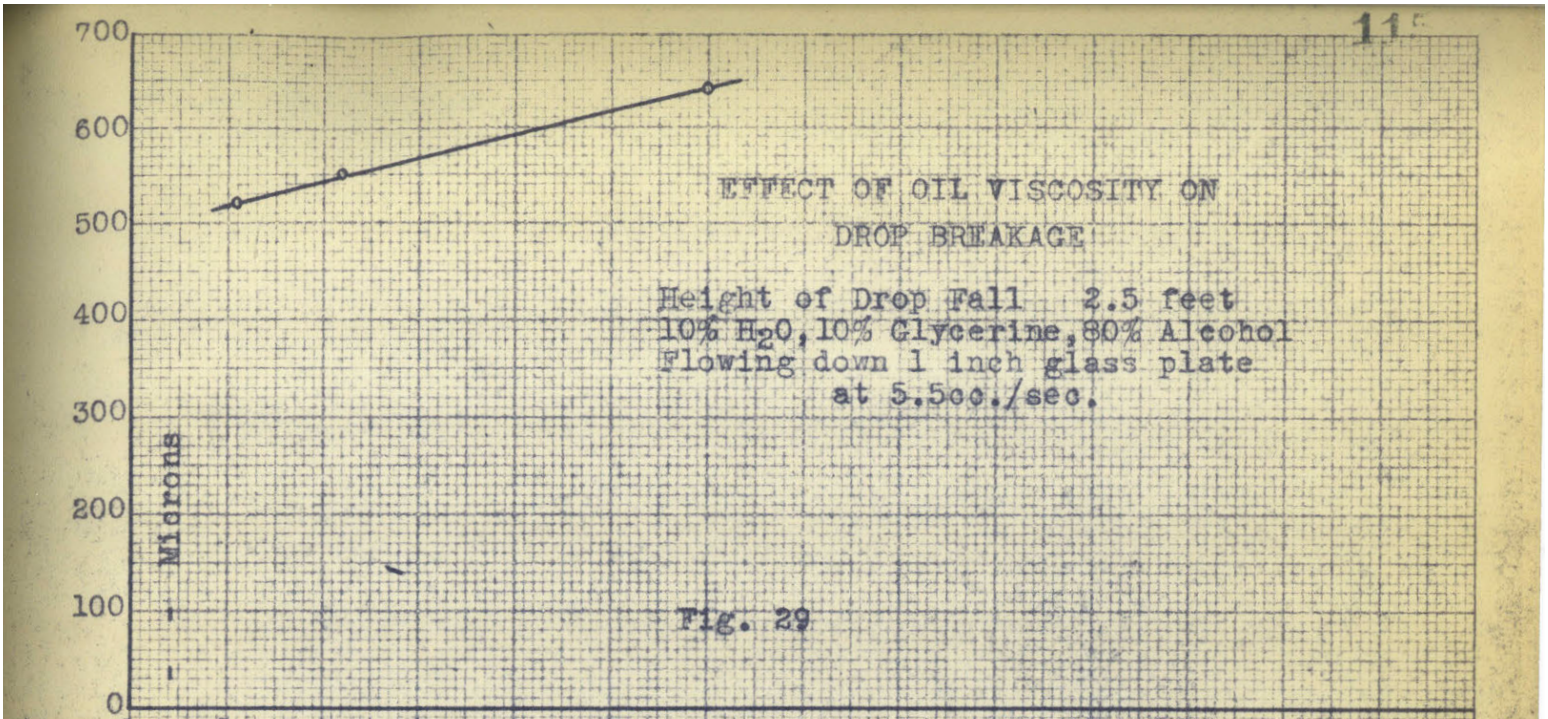
EFFECT OF OIL VISCOSITY ON
DROP BREAKAGE
Height of Drop Fall 2.5 feet
10% H_2O, 10% Glycerine, 80% Alcohol
Flowing down 1 inch glass plate
at 5.5cc./sec.
Maximum Diameter of Drop which will not Break - Microns
Viscosity of Oil Poises
0
100
200
300
400
500
600
700
.1
.2
.3
.4
.5
.6
.7

Fig. 29

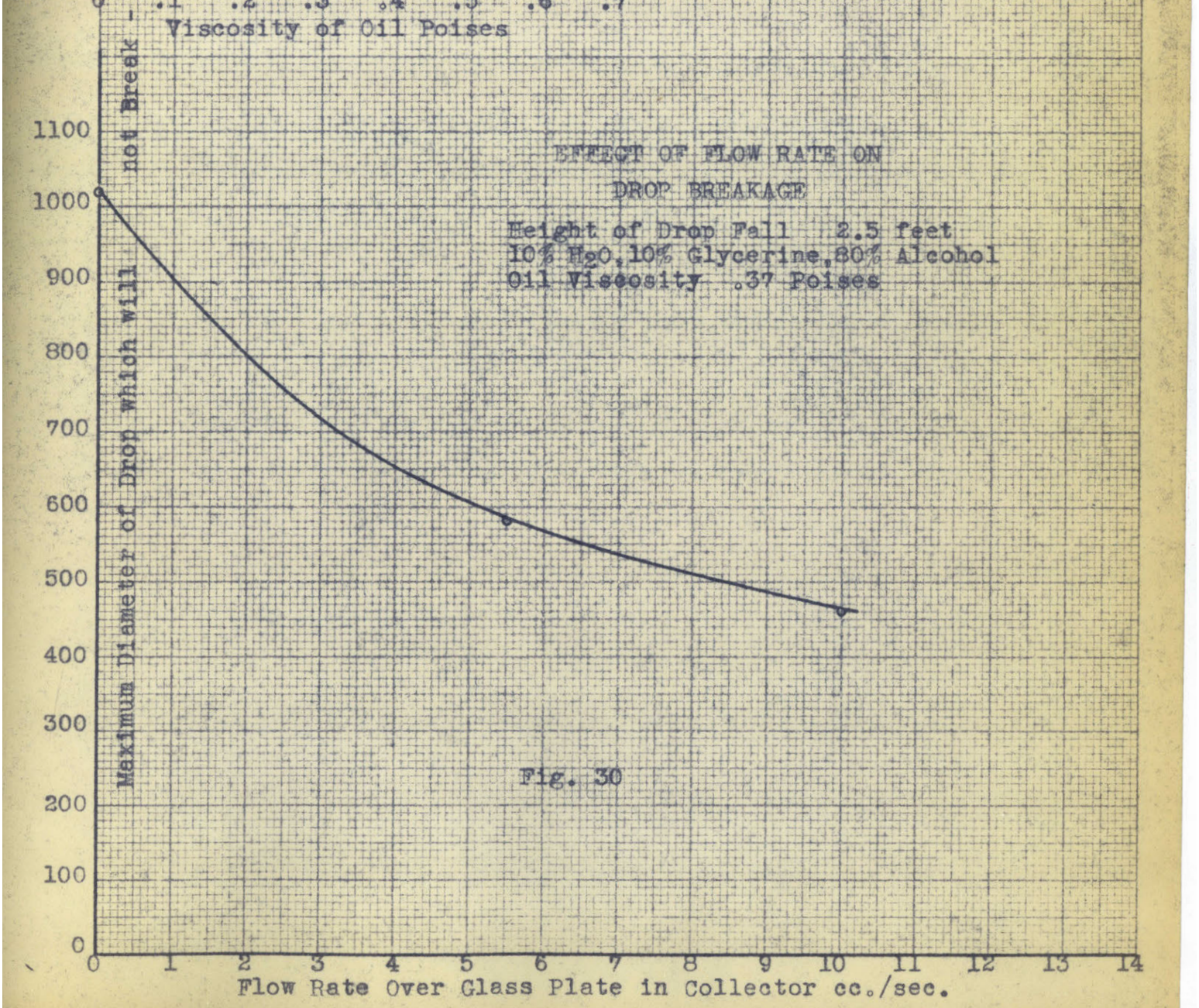
EFFECT OF FLOW RATE ON
DROP BREAKAGE
Height of Drop Fall 2.5 feet
10% H_2O, 10% Glycerine, 80% Alcohol
Oil Viscosity .37 Poises
Maximum Diameter of Drop which will not Break - Microns
Flow Rate Over Glass Plate in Collector cc./sec.
0
100
200
300
400
500
600
700
800
900
1000
1100
1
2
3
4
5
6
7
8
9
10
11
12
13
14

Fig. 30

flow rate of the fluid is plotted against the maximum diameter at which a drop of oil of viscosity of .17 cm/sec will break. The alcohol flow rate which was adopted for use was about five cc. per sec. Since this was the minimum rate which would give certain coverage of the glass plate and little agglomeration. The viscosity of the oil in the drop has considerable effect, as is shown in Fig. 29 where the maximum drop size is plotted against the viscosity of the oil in the drop. If a heated oil like Bunker C is used the maximum drop size is considerably greater since the drops cool when falling and after striking the fluid surface which increases their viscosity. Using a cold fluid would give a similar effect with the room temperature oil, but it was not necessary to do this since the effect of drop breakage on the results was considered to be small. It is possible to detect breakage since if the drop is torn apart it does not have time to return to its spherical shape before it freezes. Therefore, when breakage does occur drops with tails and dumb-bell shaped drops which did not quite break are found. From this work it was concluded that this method would be satisfactory for the study of drops sizes encountered with the particular nozzles used.

It was found that the best method of freezing the drops was to let them fall into a container of alcohol which was cooled by a jacket of dry ice. If dry ice was put into the alcohol foaming was caused and the drops would be carried to the edge of the container where they would stick to the wall or to each other. This tendency caused some difficulty since some of the drops contained air bubbles and would float on the surface of the alcohol. When the dry ice jacket was used the lighter drops still had a tendency to collect at the container walls, but the effect was much less serious, and if a small enough number of drops was taken it could be neglected. It also helps if the warm alcohol-water-glycerine mixture has a specific gravity greater than or about equal to that of the cold fluid so that the warm fluid will sink to the bottom of the container or will mix well with the cold liquid. If the warm fluid was lighter it would float on top and the light drops would have more opportunity to stick to the walls and to each other since freezing would take longer. After the mixture has cooled off it can be poured into a beaker with some lumps of dry ice to keep it cold until sieved.

The sieves were made of Tyler U.S. standard wire mesh mounted on the end of a pyrex tube of the di-

mensions shown in Fig. 6. The screens were soldered to a layer of platinum which was deposited on the pyrex tube by dipping in a solution of chloroplatinic acid and heating the tube to red heat, which left a deposit of platinum on the surface. This procedure was repeated until a sufficiently thick deposit was formed over the desired portion of the surface.

Measurement of the sieve openings showed that there was considerable variation in size. The measurements made are given in Table 3. The size given is the diameter of the largest circle that would fit in the hole. If sieving was perfect every drop would try to pass through the largest opening and this size could be taken as the sieve size. However, in practice this is far from being the case; so measurements of the drop diameters of sieved portions were made to help in estimating the sieve opening to use. These measurements are tabulated in Table 4, and Fig. 31 illustrates the results obtained.

The drops used in these measurements were formed from Bunker C oil, and contained a considerable number of air bubbles. Measurements were made at random with no effort to obtain an average diameter, and since some of the drops were misshapen by air bubbles near the surface, some of the drop measurements are ap-

TABLE 3

MEASUREMENT OF OPENINGS IN SIEVES
GIVEN IN MICROSCOPE EYEPIECE DIVISIONS

40 m.		45 m.		50 m.		60 m.	
Microns 14.6	No.	Microns 14.6	No.	Microns 14.6	No.	Microns 6.93	No.
30.0	5	26.0	1	21.3	1	37.5	2
29.5	5	25.75	1	21.0	2	37.0	1
29.0	8	25.25	3	20.6	5	36.5	2
28.5	4	25.0	5	20.3	6	36.0	1
28.0	3	24.75	6	20.0	6	35.5	2
		24.25	2			35.0	5
		24.0	3			34.5	5
						34.0	3

70 m.		80 m.		100 m.		120 m.	
Microns 6.93	No.	Microns 6.93	No.	Microns 14.6	No.	Microns 6.93	No.
32.0	1	27.5	4	10.0	4	17.6	1
31.5	3	27.0	8	10.3	10	18.0	5
31.0	3	26.5	1	10.6	14	18.3	15
30.5	16	26.0	2	11.0	11	18.6	3
30.0	18	25.5	4	11.3	1	19.0	14
29.5	8	25.0	9				
29.0	5	24.5	1			19.3	2
		24.0	1				
		23.5	3				
		23.0	3				

TABLE 4

Multiply Miscroscope Division by 14.6 to get Microns. 100m - 70m refers to the fraction of a sieved sample which was found on a 100 mesh sieve and which passed through a 70 mesh sieve.

100m - 70m*		70m - 50m*	
Divisions on Microscope	No. of Drops	Divisions on Microscope	No. of Drops
11.0	2		
11.0 - 11.5	3	14.5 - 15.0	1
11.5 - 12.0	7	15.0 - 15.5	2
12.0 - 12.5	11	15.5 - 16.0	5
12.5 - 13.0	13	16.0 - 16.5	9
13.0 - 13.5	11	16.5 - 17.0	16
13.5 - 14.0	17	17.0 - 17.5	10
14.0 - 14.5	16	17.5 - 18.0	8
14.5 - 15.0	17	18.0 - 18.5	10
15.0 - 15.5	9	18.5 - 19.0	6
15.5 - 16.0	7	19.0 - 19.5	7
16.0 - 16.5	3	19.5 - 20.0	5
16.5 - 17.0	5	20.0 - 20.5	5
17.0 - 17.5	2	20.5 - 21.0	5
		21.0 - 21.5	4
		21.5 - 22.0	3

*100m - 70m 176 drops weigh .43 m.g.
70m - 50m 150 drops weigh .95 m.g.

Drops Greater Than 80 m.			
Microscope Div.	No.	100 m. - 80 m.	No.
13.0 - 13.5	2		
13.5 - 14.0	8	9.0 - 9.5	1
14.0 - 14.5	19	9.5 - 10.0	1
14.5 - 15.0	21	10.0 - 10.5	2
15.0 - 15.5	14	10.5 - 11.0	8
15.5 - 16.0	11	11.0 - 11.5	14
16.0 - 16.5	11	11.5 - 12.0	23
16.5 - 17.0	11	12.0 - 12.5	31
		12.5 - 13.0	28
		13.0 - 13.5	19
		13.5 - 14.0	8
		14.0 - 14.5	6
		14.5 - 15.0	4
		15.0 - 15.5	1

50 m - 45 m		Greater than 45 m	
Divisions	No. of Drops	Divisions	No. of Drops
19.0-19.5	1		
19.5-20.0	2	22.5-23.5	1
20.0-20.5	2	23.5-24.5	2
20.5-21.0	2	24.5-25.5	2
21.0-21.5	6	25.5-26.5	5
21.5-22.0	9	26.5-27.5	9
22.0-22.5	12	27.5-28.5	5
22.5-23.0	7	28.5-29.5	6
23.0-23.5	20	29.5-30.5	3
23.5-24.0	10	30.5-31.5	6
24.0-24.5	11	31.5-32.5	4
24.5-25.0	2		
25.0-25.5	8		
25.5-26.0	4		
26-26.5	2		

100 m - 70 m*		70 m - 60 m*	
Size	Number	Size	Number
11.5 - 12.0	6	15.0	3
12.0 - 12.5	5	15.0 - 15.5	5
12.5 - 13.0	18	15.5 - 16.0	9
13.0 - 13.5	9	16.0 - 16.5	14
13.5 - 14.0	17	16.5 - 17.0	17
14.0 - 14.5	5	17.0 - 17.5	10
14.5 - 15.0	16	17.5 - 18.0	4
15.0 - 15.5	7	18.0 - 18.5	6
15.5 - 16.0	4	18.5 - 19.0	2
16.0 - 16.5	1		
16.5 - 17.0	3		

* 100 m - 70 m 164 drops weigh .592 m.g.
70 m - 60 m 110 drops weigh .430 m.g.

Microscope Div.	8-8.5	8.5-9	9-9.5	9.5-10	10-10.5	10.5-11	11-11.5	11.5-12
120m - 100m	1	7	16	28	22	13	11	3
100m - 80m					1	9	20	18

Microscope Div.	12-12.5	12.5-13	13-13.5	13.5-14	14-14.5	14.5-15	15-15.5
120m - 100m	3						
100m - 80m	19	13	17	10	4	1	
80m - 70m	2	10	18	16	12	18	16
70m - 50m				2	3	8	10

Microscope Div.	15.5-16	16-16.5	16.5-17	17-17.5	17.5-18	18-18.5	18.5-19
80m - 70m	5	4					
70m - 50m	10	15	19	14	10	7	9

Microscope Div.	19-19.5	19.5-20	20-20.5	20.5-21	21-21.5	21.5-22	22-22.5
70m - 50m	5	3	4	2	4	2	1
50m	1	2	4	10	12	20	16

Microscope Div.	22.5-23	23-23.5	23.5-24
50m	28	15	15

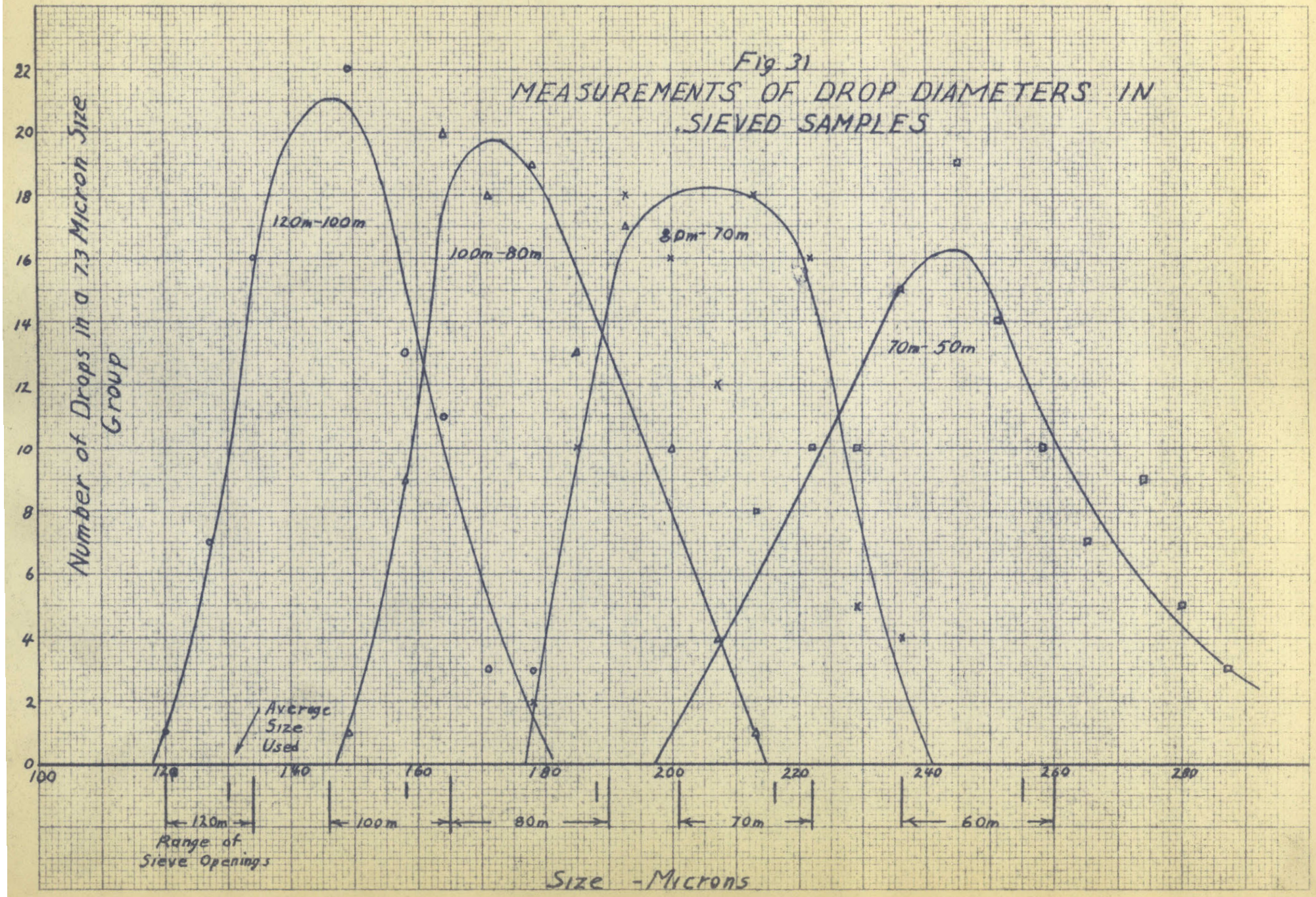
Fig. 31
MEASUREMENTS OF DROP DIAMETERS IN SIEVED SAMPLES
Number of Drops in a 7.3 Micron Size Group
120m-100m
100m-80m
80m-70m
70m-50m
Average Size Used
120m
Range of Sieve Openings
100m
80m
70m
60m
Size - Microns

parently larger than the maximum opening in the sieve. Drops which were not spherical could slip through the square opening diagonally.

On examination of the data thus obtained it was decided to use the sieve opening which was larger than 75% of the openings. A rigorous selection of a sieve opening which would give the correct distribution curve for the drops would involve perfectly reproducible sieving and very detailed study of the shapes of the drops. It was not felt that such a study was justified in view of the small increase in accuracy which would result. Probably the selected sizes are within 5% of the correct size.

The dimensions which were adopted for use in this work are given in the table below.

TABLE 5a

Sieve Mesh	Size of Opening Microns
40	435
45	369
50	302
60	255
70	216
80	188
100	158
120	130
140	109

An effort was made to sieve the drops in the same way for each run so that the results would be consistent even if the absolute size was slightly incorrect.

The original suspension of oil drops in cold alcohol was poured through the sieves as rapidly as possible. Then the sieves were each washed with 50 cc. of cold alcohol, which was poured from a height of about one foot at such a rate that the bottom of the sieve was not flooded. An effort was made to hit the bottom of the sieve with the falling stream so that the impact of the stream on the drops would tend to force them through the openings. When one sieve was washed it was removed from the sieve holder illustrated in Fig. 6, and the same process was repeated on the next below. It was found that when the washing was carried this far that more washing would force drops through at a very low rate so from the point of view of time involved in the sieving this was a good time to stop since more washing would produce relatively little effect. This fact probably also helped the reproducibility of the results considerably.

As was pointed out in the section on atomization, there is advantage for a study of this sort in

using an oil which is at the same temperature as the atmosphere into which it is sprayed. In order to use the technique which was described on the preceding pages it was necessary to make a special blend of oil to give it the proper physical properties. The base of the oil used was #2 fuel oil of a viscosity of approximately .03 cm^2/sec. This oil did not freeze at a high enough temperature so about three hundred grams of paraffin wax was dissolved in each gallon of the oil. This raised the freezing point enough to make freezing at dry ice temperature quite satisfactory. The colorimetric method of comparing the weights of the various fractions of the spray offered such great advantages that it was found to be desirable to color the oil. Since the viscosity of the oil was to be varied, mixing Bunker C oil for the purpose of both coloring the oil and changing its viscosity was found to be quite satisfactory. Occasionally a little trouble was met with from the asphaltenes settling out of the oil, but if the oil was occasionally heated until a homogeneous fluid was obtained, trouble from this source could be avoided.

DERIVATION OF EQUATIONS FOR THE DISCHARGE COEFFICIENT AND THE CONE ANGLE

Equations can be derived for the cone angle and the discharge coefficient in terms of nozzle dimensions if the following assumptions are made:

1. No losses to friction
2. Each particle leaves with the total energy equal to the pressure head
3. The velocity of a particle of fluid in the radial direction is small as compared to the rotational velocity

A particle of fluid enters the swirl chamber with a tangential velocity v_s. This particle of fluid is then forced to rotate around the axis of the nozzle, and at the radius rs at which it entered the swirl chamber it will have an energy of rotation Ers = $\frac{v_s^2}{2}$ if the particle is of unit mass. The fluid is then forced toward the center of the nozzle, and in order to do this, work must be done against the centrifugal force $\omega^2 r$, ω is the rotational velocity at radius r. The work dE to move a particle a distance dr is expressed by the equation

$$dE_r = -\omega^2 r\, dr$$

This equation can bd divided by the equation for the rotational energy which is $Er = \frac{\omega^2 r^2}{2}$ to give:

$$\frac{dEr}{Er} = -\frac{2\,dr}{r}$$

integration of this equation gives

$$\ln Er = -2 \ln r + \text{const.}$$

By substituting the condition that Er = Ers at r=rs the following equation is obtained:

$$(19) \qquad \frac{Er}{Ers} = \left(\frac{rs}{r}\right)^2$$

In other words, the rotational kinetic energy in a system of this sort is inversely proportional to the square of the radius of rotation. If Q is the flow rate through the nozzle and As is the area of the tangential slots then the velocity v_s is Q/As and Ers = $\frac{Q^2}{2A_s^2}$
The rotational energy at the radius of the orifice Ero is then:

$$(20) \qquad Ero = \frac{Q^2}{2A_s^2}\left(\frac{rs}{ro}\right)^2$$

If a particle of fluid keeps the rotational energy obtained by the above mechanism, then the energy left for conversion into translational velocity is Ep - Er

where Ep is the original total energy of a particle which corresponds to its original pressure head. The velocity at which a particle leaves the orifice is then:

$$(21) \qquad v = \sqrt{2(E_p - E_r)}$$

If this velocity is in a direction parallel to the axis of the orifice then the flow rate is:

$$(22) \qquad Q = \int_{r_i}^{r_o} 2\pi r v \, dr$$

where ri is the radius of the vortex. Eq. 21 can be substituted in Eq. 22 to give

$$(23) \qquad Q = \int_{r_i}^{r_o} 2\pi r \sqrt{2(E_p - E_r)} \, dr$$

$$(24) \qquad \text{since} \quad \frac{E_r}{E_{ro}} = \left(\frac{r_o}{r}\right)^2$$

$$Q = \int_{r_i}^{r_o} 2\pi r \sqrt{2\left(E_p - E_o\left(\frac{r_o}{r}\right)^2\right)} \, dr$$

If ε is defined as Eo/Ep then Eq. 24 becomes:

$$(25) \qquad Q = \int_{r_i}^{r_o} 2\pi \sqrt{2E_p} \sqrt{r^2 - \varepsilon r_o^2} \, dr$$

The integral of this equation is:

$$(26)\quad Q = \pi\sqrt{2E_p}\left(r_o^2\sqrt{1-\varepsilon} - r_i\sqrt{r_i^2-\varepsilon r_o^2} - \varepsilon r_o^2 \ln\frac{r_o + r_o\sqrt{1-\varepsilon}}{r_i + \sqrt{r_i^2-\varepsilon r_o^2}}\right)$$

The discharge coefficient is defined by the equation:

$$(27)\quad Q = \pi r_o^2 C_o\sqrt{2E_p}$$

Combining this equation with Eq. 26 gives:

$$C_o = \frac{1}{r_o^2}\left(r_o^2\sqrt{1-\varepsilon} - r_i\sqrt{r_i^2-\varepsilon r_o^2} - \varepsilon r_o^2 \ln\frac{r_o + r_o\sqrt{1-\varepsilon}}{r_i + \sqrt{r_i^2-\varepsilon r_o^2}}\right)$$

$$(28)\quad C_o = \sqrt{1-\varepsilon} - \sqrt{\left(\frac{r_i}{r_o}\right)^4 - \varepsilon\left(\frac{r_i}{r_o}\right)^2} - \varepsilon \ln\frac{r_o + r_o\sqrt{1-\varepsilon}}{r_i + \sqrt{r_i^2-\varepsilon r_o^2}}$$

The value of ri/ro depends on the shape of the nozzle, and since this equation does not take the shape of the nozzle into account, information on the value of ri/ro must come from another source. The smallest value of ri, which would be possible for a nozzle of this type, would correspond to that radius at which all of the

energy was used in rotation. For this case $\frac{r_{ip}}{r_o} = \sqrt{\varepsilon}$ where r_{ip} is this smallest value. If "a" is defined as the ratio $\frac{r_i}{r_{ip}}$ then ri/ro is $a\sqrt{\varepsilon}$. If this definition is substituted into Eq. 28 it becomes:

$$(29)\quad C_o = \sqrt{1-\varepsilon} - \sqrt{a^4\varepsilon^2 - a^2\varepsilon^2} - \varepsilon \ln \frac{1+\sqrt{1-\varepsilon}}{a\sqrt{\varepsilon} + \sqrt{a^2\varepsilon - \varepsilon}}$$

ε can be written in terms of the dimensions of the nozzle. Substituting Eq. 27 in Eq. 20, one obtains:

$$(30)\quad E_{r_o} = \frac{\pi^2 r_o^4 c_o^2 E_p}{A_s^2} \left(\frac{r_s}{r_o}\right)^2$$

$$(31)\quad \varepsilon = \frac{E_o}{E_p} = \frac{\pi^2 r_o^4}{A_s^2} \left(\frac{r_s}{r_o}\right)^2 C_o^2 = b C_o^2$$

$$(32)\quad \text{where} \qquad b = \frac{\pi^2 r_o^4}{A_s^2} \left(\frac{r_s}{r_o}\right)^2$$

Substitution of Eq. 31 in Eq. 29 gives: Eq. 14, which is:

$$(14)\quad C_o = \sqrt{1-bc_o^2} - abc_o^2\sqrt{a^2-1} - bc_o^2 \ln \frac{1+\sqrt{1-bc_o^2}}{\sqrt{bc_o^2}\left(a+\sqrt{a^2-1}\right)}$$

Fig. 17 is a solution of this equation in which the discharge coefficient is plotted against b for different values of "a." As is explained in the section on results, the agreement of this equation with results is quite good.

It was hoped that this analysis could be used to predict the cone angle as well as the discharge coefficient. An expression for the cone angle can be derived if it is assumed that when the fluid leaves the orifice that all particles assume an average velocity such that the kinetic energy of the fluid traveling in the axial direction is the same as the translational energy of the fluid in the orifice, and that the kinetic energy in the direction at right angles to the axis of the cone is the same as the kinetic energy of rotation of the fluid in the nozzle. In this case the sine of the cone angle is the square root of the ratio of the kinetic energy of rotation of the fluid to the energy equivalent to the pressure drop through the nozzle.

The average rotational energy of the fluid leaving the nozzle is:

$$(33)\quad E_{r_{ave}} = \frac{\int_{r_i}^{r_o} E_r v 2\pi r dr}{\int_{r_i}^{r_o} v 2\pi r dr} = \frac{1}{Q}\int_{r_i}^{r_o} E_r v 2\pi r dr$$

Equations 21 amd 24 are then substituted in Eq. 33 to give:

$$(34)\quad E_{r_{ave}} = \frac{2\pi r_o^2 E_{r_o}\sqrt{2E_p}}{Q}\int_{r_i}^{r_o}\sqrt{1-\varepsilon\left(\frac{r_o^2}{r^2}\right)}\;\frac{dr}{r}$$

Integration and the substitution of the definition of "a" and c_o gives:

$$E_{r_{ave}} = \frac{2E_{r_o}}{c_o}\left(\frac{\sqrt{a^2-1}}{a} - \sqrt{1-\varepsilon} + \ln\frac{1+\sqrt{1-\varepsilon}}{\sqrt{\varepsilon}\,(a+\sqrt{a^2-1})}\right)$$

since $\varepsilon = bc_o^2$

$$E_{r_{ave}} = \frac{2E_{r_o}}{c_o}\left(\frac{\sqrt{a^2-1}}{a} - \sqrt{1-bc_o^2} + \ln\frac{1+\sqrt{1-bc_o^2}}{\sqrt{bc_o^2}\,(a+\sqrt{a^2-1})}\right)$$

$$(35)\quad \sin\alpha/2 = \sqrt{\frac{E_{r_{ave}}}{E_p}} = \left[2bc_o\left(\frac{\sqrt{a^2-1}}{a} - \sqrt{1-bc_o^2} + \ln\frac{1+\sqrt{1-bc_o^2}}{\sqrt{bc_o^2}\,(a+\sqrt{a^2-1})}\right)\right]^{1/2}$$

Although this equation checked well for those nozzles in which "a" was about one, it was found that for most of the nozzles which had an "a" of about two that the predicted cone angles were considerably lower than the measured ones. An explanation is that the velocity distribution is actually not as predicted by this

analysis. The equation for the cone angle is very sensitive to small changes in "a" or in the discharge coefficient. The problem of correlating the cone angles was solved by using a different value of "a" for calculating the cone angles than was used to calculate the discharge coefficient. Since Eq. 35 was quite inconvenient to use an equation for the cone angle which was derived from the assumption of constant translational velocity at the orifice was used in connection with this correlation. If Et is the average translational kinetic energy of a particle of fluid leaving the nozzle, the cone angle can be expressed by the equation:

$$(36) \quad \cos \alpha_0/2 = \sqrt{\frac{Et}{E_p}}$$

Since for this case

$$Et = \frac{1}{2}\left(\frac{Q}{\pi(r_0^2 - r_c^2)}\right)^2 = \frac{1}{2}\left(\frac{\pi r_0^2 C_0 \sqrt{2E_p}}{\pi r_0^2 (1-(\frac{r_c}{r_0})^2}\right)^2$$

$$(37) \quad Et = \left(\frac{C_0}{1-(\frac{r_c}{r_0})^2}\right)^2 E_p$$

$$(38) \quad \cos \alpha_0/2 = \frac{C_0}{1-(\frac{r_c}{r_0})^2}$$

It has been previously shown that

$$\left(\frac{r_i}{r_o}\right)^2 = a^2 c_o^2 b$$

so

$$(39) \qquad \cos \alpha_{o/2} = \frac{c_o}{1 - a^2 c^2 b}$$

This equation gave cone angles which were very nearly the same as those given by Eq. 35 when "a" was the order of two, and gave slightly larger values when "a" was about one.

It was found that an equation derived from the assumption of constant linear velocity in the orifice gave discharge coefficients which were practically identical with those given by Eq. 14. Also it was found that equations for the cone angle based on the assumption of constant momentum as the jet left the nozzle gave results which differed negligibly from those given by the equations which used the assumption of constant energy.

STUDY OF THE T58X40 NOZZLE

The T58X40 nozzle was the first to be studied in this work and considerably more detail was obtained on its performance than on the other nozzles.

After the freezing technique for studying the drop size distribution was developed, an effort was made to obtain a curve of mean drop size as a function of viscosity at constant pressure. This data is included in runs 1 to 34. The fact that the points obtained scattered badly causes considerable concern and when it was noticed that T58X40 #1 had a rough orifice, the T58X40 #2 nozzle was obtained and a similar set of runs was made. These runs, 35 to 59, seemed to also give badly scattered points, but on close examination it was seen that the points could be divided up into four groups which gave four different curves. This indicated that perhaps a different mechanism of atomization occurred in the different regions of pressure and viscosity. Fig. 32 shows the four curves drawn through the data of runs 35 to 59.

Since high speed photographic apparatus was available it was used to study the cone formed under different conditions. Fig. 33 shows typical photographs of the sprays which correspond to the four curves

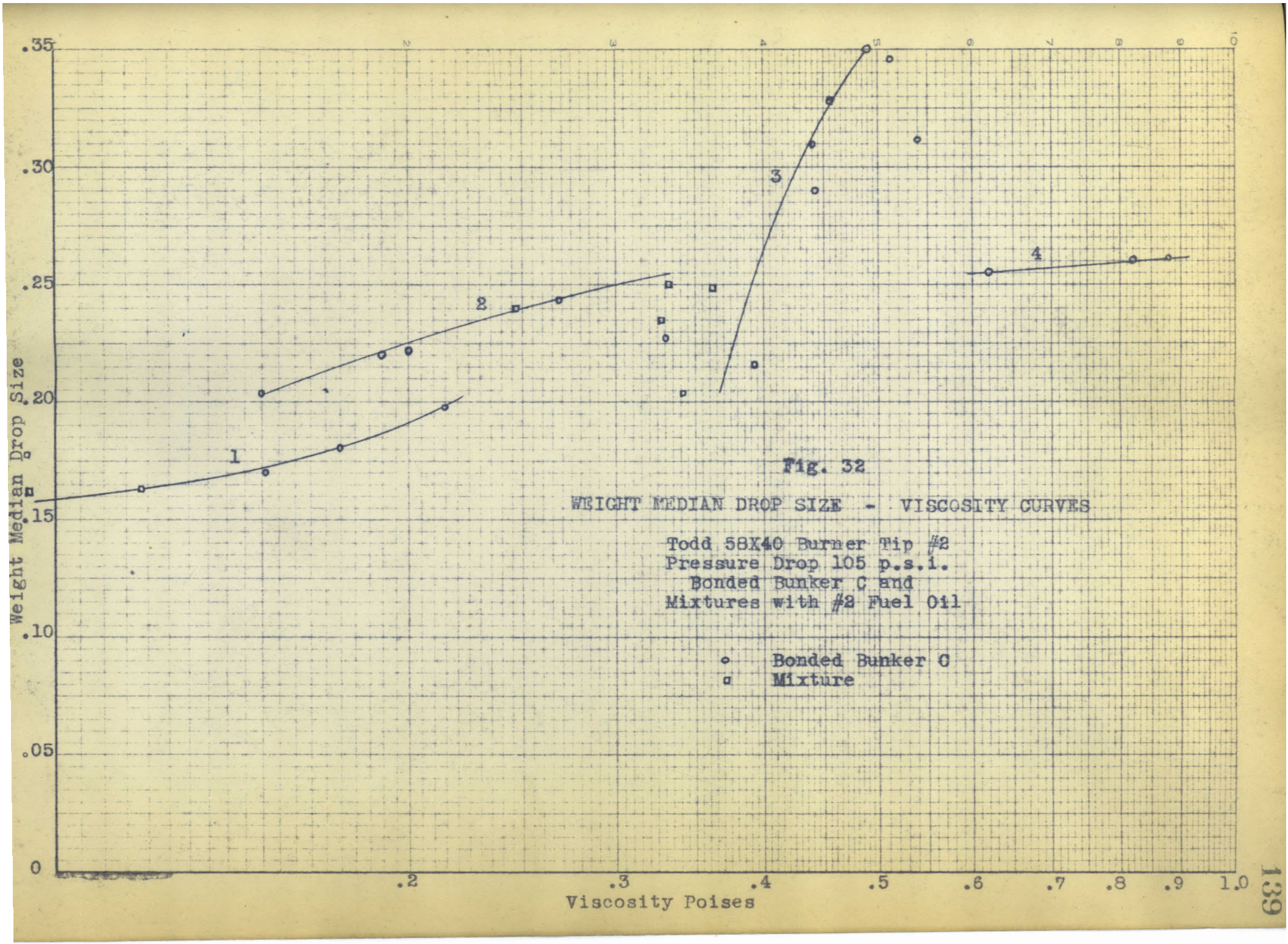

Fig. 32

WEIGHT MEDIAN DROP SIZE - VISCOSITY CURVES

Todd 58X40 Burner Tip #2
Pressure Drop 105 p.s.i.
Bonded Bunker C and
Mixtures with #2 Fuel Oil

○ Bonded Bunker C
□ Mixture

CURVE 1
VISCOSITY .08 STOKES D_o 160 MICRONS

CURVE 2

VISCOSITY .21 STOKES
D_o 220 MICRONS

VISCOSITY .31 STOKES
D_o 245 MICRONS

CURVE 3

VISCOSITY .50 STOKES
D_o 305 MICRONS

VISCOSITY .52 STOKES
D_o 325 MICRONS

VISCOSITY 1.0 STOKES D_o UNKNOWN
CURVE 4

HIGH SPEED PHOTOGRAPHS OF TODD 58x40 #2 NOZZLE

Fig 33

drawn in Fig. 32. It was suspected that the formation of a vortex in the swirl chamber was related to these discontinuities in the drop size vs. viscosity curve, so a model of this nozzle was constructed of transparent lucite and photographs were taken of the spray and of the inside of the swirl chamber. Fig. 34 and 35 show a series of the pictures for one atomizing viscosity, and a variety of pressures. The uneven appearance of the vortex in these photographs is due to drops of oil being on the outside of the nozzle.

The interpretation of the photographs of the spray corresponding to curve 4 of Fig. 32 was in doubt since the pictures appeared as though two concentric cones were formed. To check this a cross section of the spray was taken by quickly passing an opening over a piece of blotting paper which was placed a few inches under the spray. Fig. 36 shows these cross sections and the corresponding photographs. The spray was "S" shaped in cross section and this "S" was always oriented the same way with respect to the nozzle. The assumption that a sample taken along any radius will be representative of the whole spray could not be valid for this case, and the fact that a relatively low drop size was obtained for curve 4 of Fig. 32 indicates that the

HIGH SPEED PHOTOGRAPHS OF T58x40 LUCITE NOZZLE - VISCOSITY .11 POISE

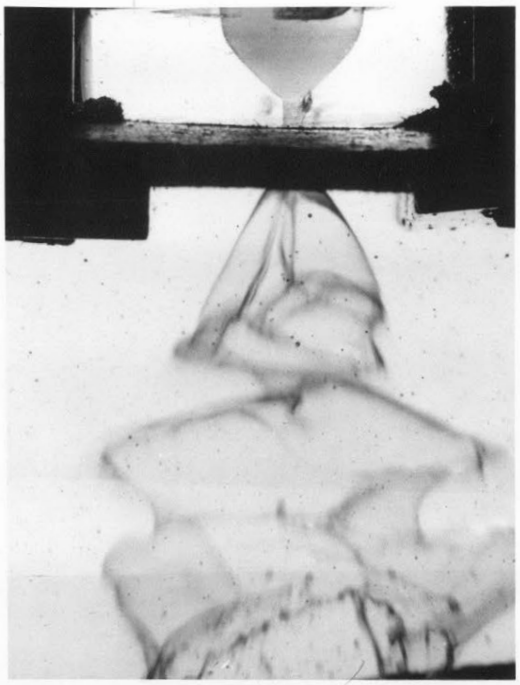

Pressure 7.5 p.s.i.
Cone not formed

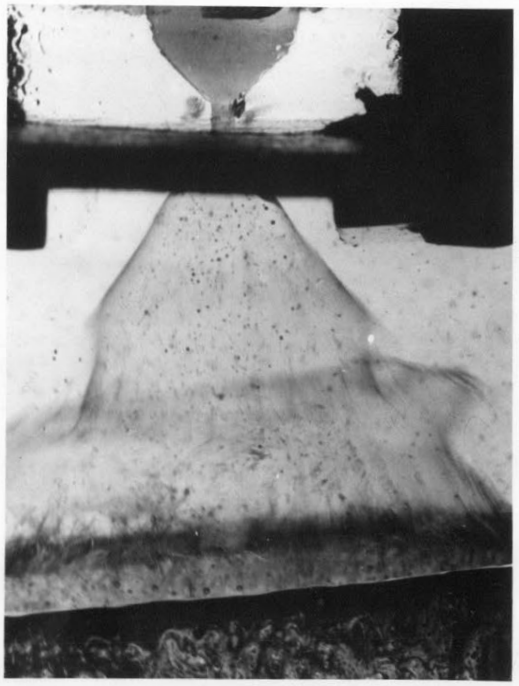

Pressure 11 p.s.i.
Cone formed

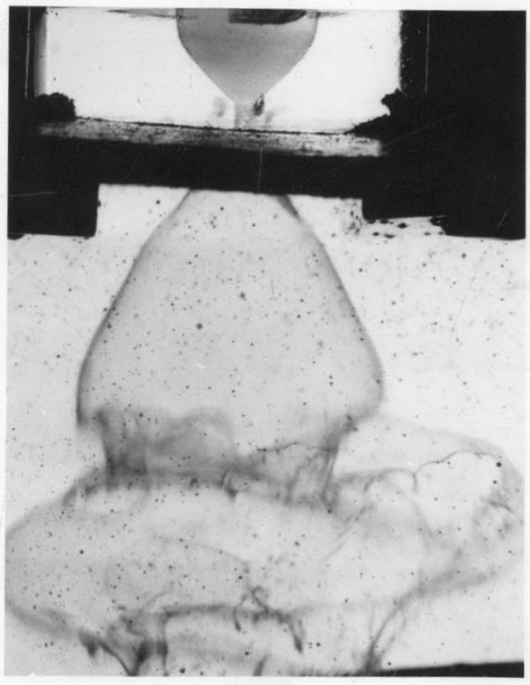

Pressure 15 p.s.i.
No vortex core yet visible

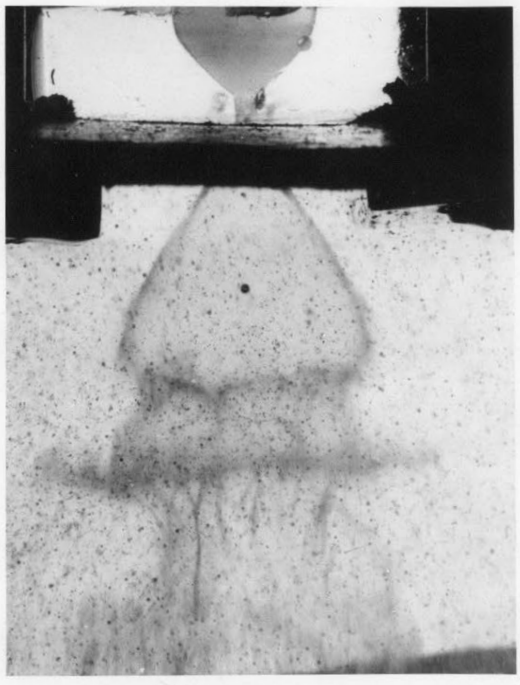

Pressure 22.5 p.s.i.
Note beginning of vortex core.

FIG. 34

HIGH SPEED PHOTOGRAPHS OF T58x40 LUCITE NOZZLE - VISCOSITY .11 POISE

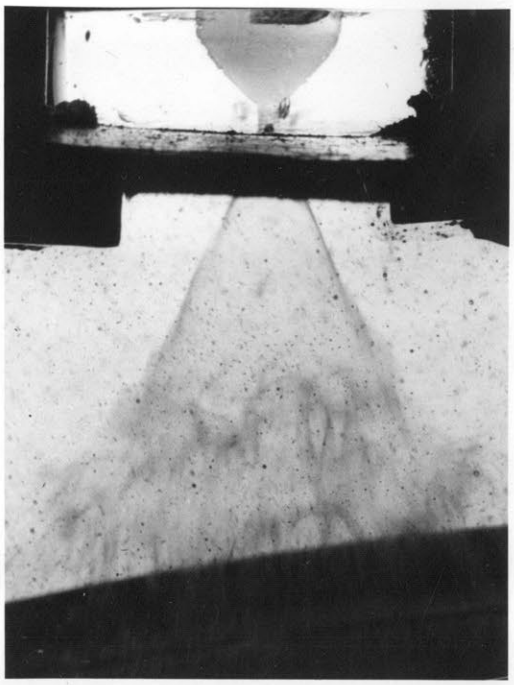

Pressure 30 p.s.i.
Vortex core appears and cone angle decreases.

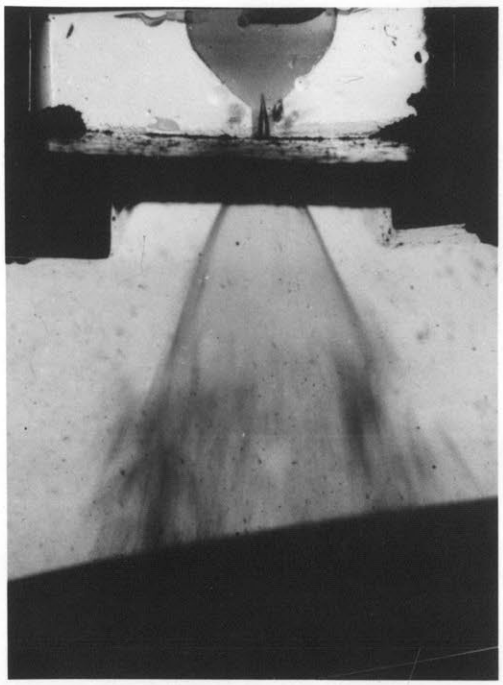

Pressure 60 p.s.i.

Pressure 105 p.s.i.
Cone angle no longer changes with pressure.

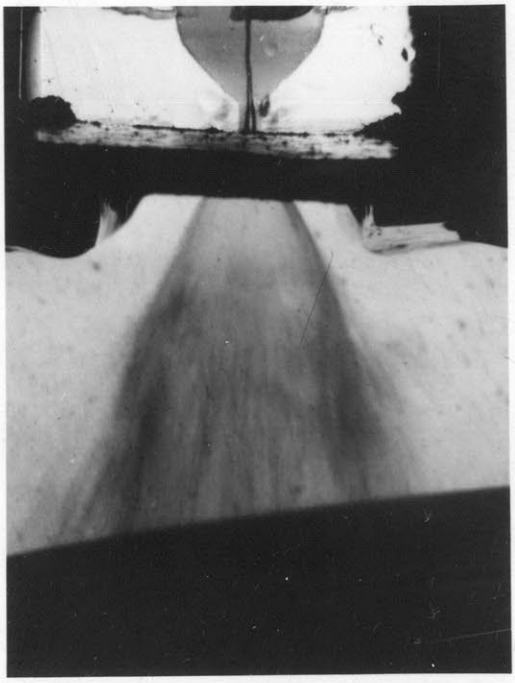

Pressure 140 p.s.i.

FIG. 35

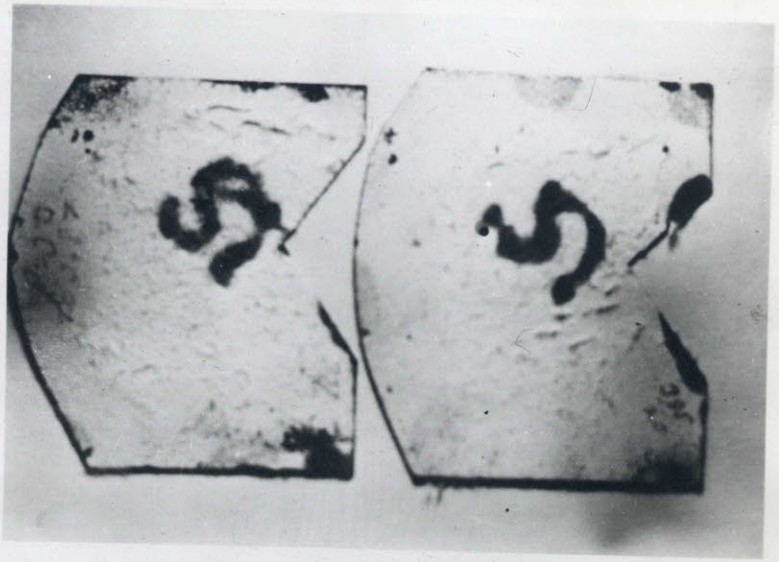

BOTTOM VIEWS

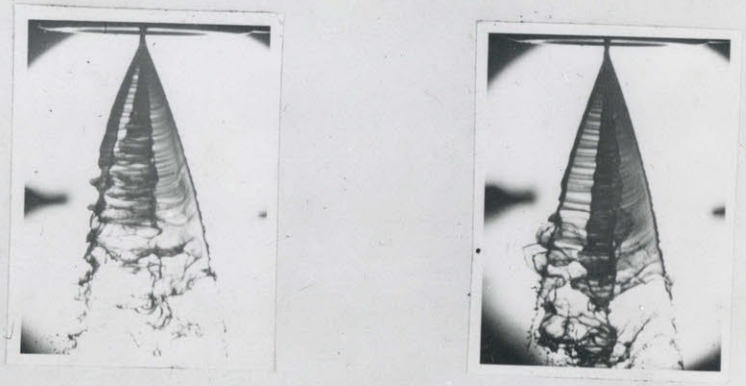

SIDE VIEWS

CROSS SECTIONS AND HIGH SPEED SHADOW PHOTOGRAPHS
CORRESPONDING TO CURVE 4

Fig. 36

samples were taken where there were no drops from the edges of the sheets since visual observation and combustion experience indicates that these drops are quite large. It is of interest to note that the drop sizes obtained in curve 4 were roughly what might be expected from an extrapolation of curve 1, which indicates that good atomization can be expected as long as a smooth continuous sheet of oil is obtained.

The studies of the transparent nozzle showed that curves 3 and 4 of Fig. 32 corresponded to conditions where no vortex was formed in the swirl chamber. Under these conditions the spray often breaks up into a more complex group of sheets than correspond to Fig. 36. Curve 3 of Fig. 32 has a vibration superimposed on the sheets coming out which breaks them up and gives quite a different appearance to the cone. Vibrations of the jet when the cone was not formed were not observed for any of the other nozzles.

Curves 1 and 2 of Fig. 32 correspond to the region where a smooth cone is formed and good atomization can be expected. As can be seen by examination of Figures 34 and 35, the vortex does not become visible until the pressure is considerably increased over the minimum required for the formation of a cone. Fig. 15 shows roughly the conditions under which a cone is formed,

and those under which a vortex is formed in the swirl chamber.

Fluctuations of the cone are indicated by these photographs in the region where a vortex is not formed. These fluctuations disappear in the region where a vortex is well formed and the change corresponds to the shift from curve 2 to curve 1. The drops become smaller when the fluctuations disappear. For other nozzles the fluctuations do not always disappear when the vortex is formed.

It can also be noted that the cone angle decreases until the vortex is well formed, at which time it becomes independent of pressure. This characteristic was observed in all of the nozzles used. The general curves for drop size are for the region of operation where the cone angle and the vortex core diameter are not a function of pressure.

STUDY OF 10x3 NOZZLE

A rather complete study of the 10x3 nozzle was also made. Runs 67 to 91 were taken to find the general effect of pressure and viscosity on one nozzle. These runs were made following those with the T 58x40 #2 nozzle and the distance of travel of the collector was not changed. The 10x3 nozzle gave a distribution of drop sizes in the spray such that the drops that were far from the center of the spray were much larger than those at the center. This fact is illustrated by Fig. 27, which gives drop size distributions for different points in the spray. After the runs had been made it was found that, although the collector traveled far enough for the T58x40 nozzle, under some conditions it did not travel far enough to collect a sample of the whole spray for the 10x3 nozzle. Therefore, the magnitude of the drop size in some of these runs is probably in error so they were not used in the general correlation. Some of the runs are plotted in Figure 37.

A sudden change in the shape of the drop size vs pressure curve at constant viscosity was found at the point where high speed photographs showed that the cone suddenly shortened and some vibrations set in. Fig.14 shows roughly the conditions under which this takes place for this nozzle.

A lucite model of this nozzle was constructed and photographs were taken of the cone and of the vortex under various pressures and viscosities. In this case the fluctuations of the cone did not occur at the same conditions as for the formation of a vortex. After the vortex was well formed it did not change in size as the pressure was changed. The size of vortex for this condition is plotted as a function of viscosity for both the 10X3 and the T58X40 lucite nozzles in Fig. 38.

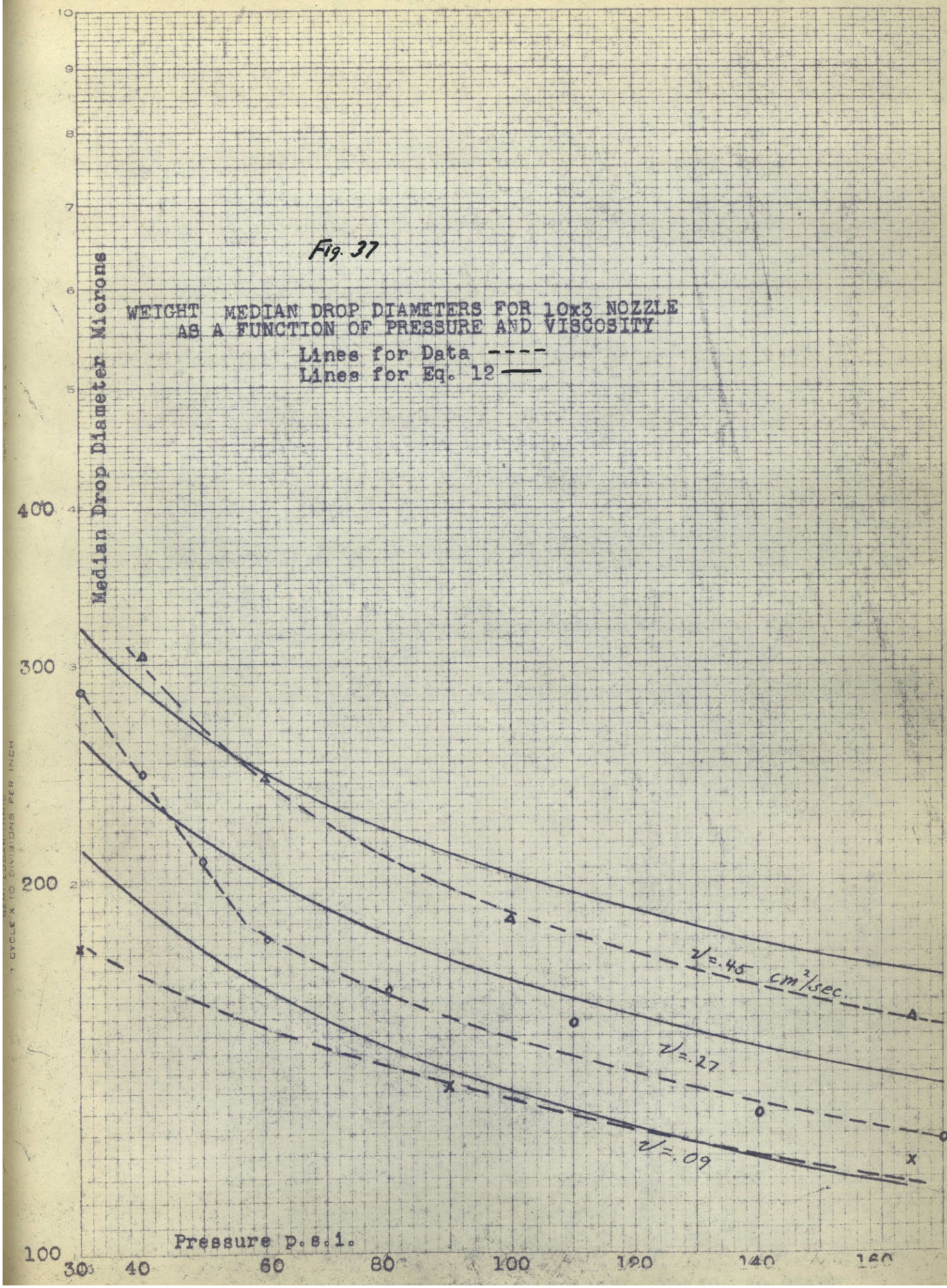
Fig. 37
WEIGHT MEDIAN DROP DIAMETERS FOR 10x3 NOZZLE
AS A FUNCTION OF PRESSURE AND VISCOSITY
Lines for Data ----
Lines for Eq. 12 ——
Median Drop Diameter Microns
400
300
200
100
ν=.45 cm²/sec.
ν=.27
ν=.09
Pressure p.s.i.
30
40
60
80
100
120
140
160

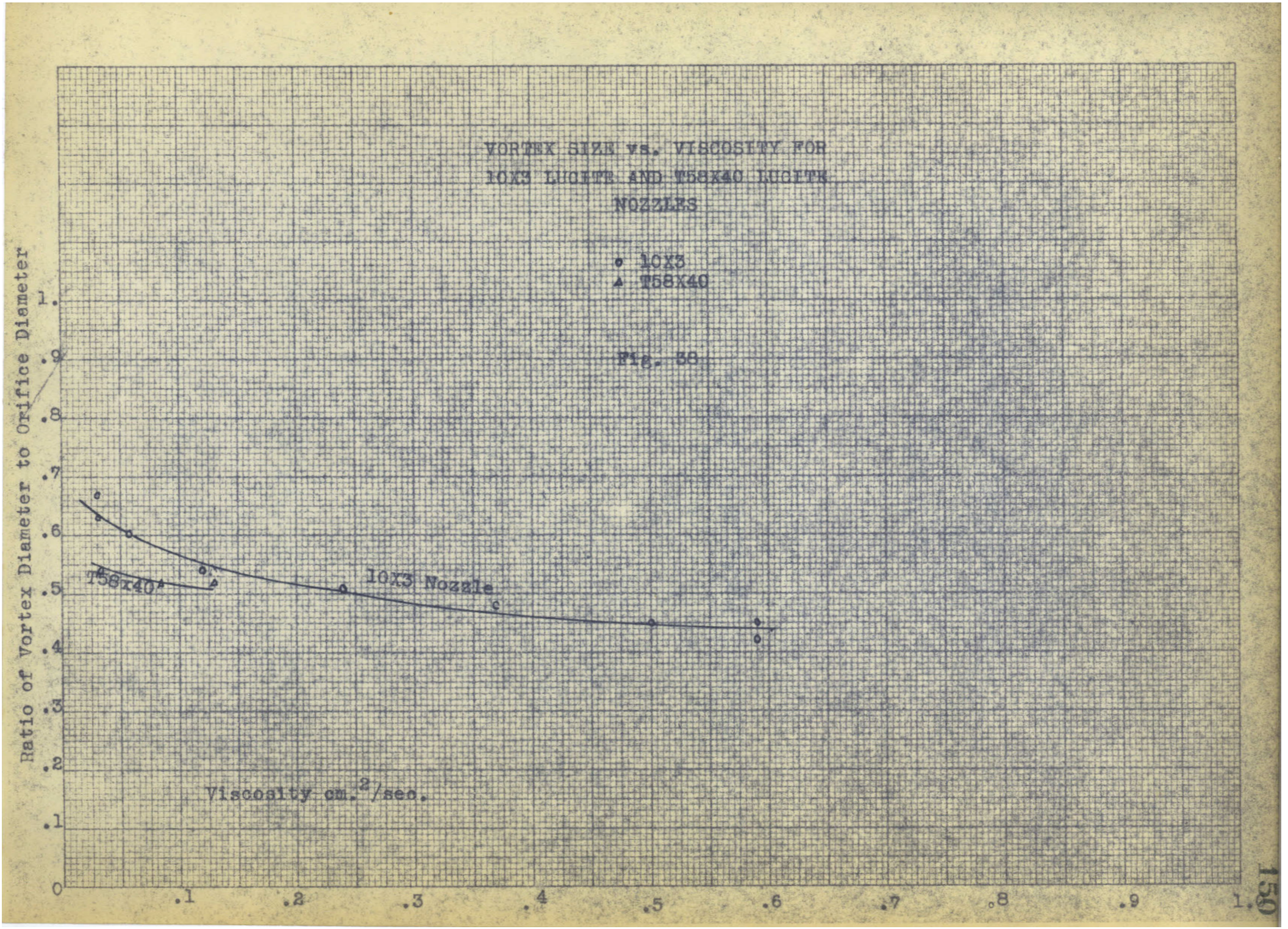
VORTEX SIZE vs. VISCOSITY FOR
10X3 LUCITE AND T58X40 LUCITE
NOZZLES
10X3
T58X40
Fig. 38
Ratio of Vortex Diameter to Orifice Diameter
Viscosity cm.²/sec.
10X3 Nozzle
T58x40
0
.1
.2
.3
.4
.5
.6
.7
.8
.9
1.

TABLE V

SIZE DISTRIBUTION DATA

	T 58x40 #1 Nozzle					Bunker C Oil Used						
No.	Temp. °C.	Press. p.s.i.	Viscosity $cm^2/sec.$	n	Do microns	R45	R50	R60	R70	R80	R100	R120
1	112	98	.15	4.0	208			.22	.45			
2	112	93	.15	4.0	201			.18	.40			
3	106	122	.19	3.4	200		.08	.24	.36	.52	.74	
4	109	122	.18	3.1	180		.046	.15	.31	.448	.645	
5	111	118	.17	3.1	194		.081	.18	.37	.51	.70	
6	107	120	.185		225				.54		.85	
7	107	120	.185		220				.52		.88	
8	110	120	.175		243			.41	.67		.92	
9	110	120	.175		235			.35	.62		.86	
10	112	85	.15		230			.39	.55			
11	112	120	.15		217			.31	.50			
12	112	145	.15		185			.20	.31			
13	85.5	114	.42	3.4	242		.21	.41	.63	.74	.85	
14	98.5	132	.25	3.4	212		.05	.01	.46	.63	.77	
15	83.5	80	.46	2.7	283		.44		.70		.87	
16	88	85	.38	2.7	243		.28		.60		.87	
17	98	105	.175	3.6	217		.33	.33	.50		.81	
18	112	113	.16	3.5	185		.06		.31		.66	
19	104	105	.21		150		.06			.22		.51
20	84	105	.42	2.3	198		.16	.	.44	.53	.66	
21	79	106	.56	3.2	253	.14	.30	.50	.72			
22	80	105	.53	3.6	186			.13		.49	.68	.85
23	80	105	.53	3.0	172		.04	.12	.25	.41		
24	80	105	.53	2.8	168			.12		.38	.55	.72
25	91	105	.34	3.0	187			.17		.48	.65	.75
26	80	105	.53	3.8	260			.53	.71	.85	.95	
27	82	105	.49	3.6	265	.15	.33	.58	.72			
28	106	105	.19	3.6	202			.18	.41	.575	.75	

Table V - continued

No.	Temp. °C.	Press. p.s.i.	Viscosity $cm^2/sec.$	n	D_o microns	R40	R45	R50	R60	R70	R80	R100	R120
29	80	105	.54		310				.73	.87	.92	.95	
30	83	105	.46	3.6	310	.11	.28	.54	.76				
31	117	105	.135	2.6	178				.16	.30	.45	.59	
32	92	105	.31	3.0	200		.018	.08	.23	.41			
33	93	105	.30	4.0	228		.	.10	.36	.55	.72		
34	82	105	.48		245		.13	.28	.44	.65			
		T 58 x 40 #2 Nozzle					Bunker C Oil Used						
35	128	105	.10	3.6	177				.10	.25	.42	.63	
36	127	105	.10	3.2	163				.08	.19	.35	.52	
37	120	105	.13	2.8	162				.09	.21	.35	.52	
38	112	105	.16	2.6	170				.14	.28	.42	.56	
39	107	105	.19	2.8	181			.06	.25	.44	.65		
40	110	105	.17	3.2	204			.09	.25	.43	.59		
41	111	105	.23	2.9	197			.09	.40	.56	.68		
42	115	105	.20	3.6	220			.12		.52	.67	.77	
43*	80	105	.27	3.2	240			.25	.42	.60	.72		
44	95	105	.29	3.9	240		.05	.18	.40	.68			
45*	80	105	.35	4.7	250		.06	.19	.46	.71			
46	90	105	.34	3.4	235		.06	.18	.38	.61			
47	89	105	.35	4.3	228			.12	.31	.58	.74		
48*	82	105	.36	2.9	203			.12	.27	.44	.56		
49*	80	105	.38	3.7	248		.07	.21	.44	.68			
50	85	105	.41	3.1	217		.05	.15	.32	.49			
51	83	105	.47	4.2	290		.16	.44	.67	.82			
52	83	105	.47	3.8	310		.29	.52	.73	.86			
53	82	105	.49	3.4	328		.35	.59	.75	.84			
54	80.5	105	.52	4.8	350		.43	.70	.89	.96			
55	79.5	105	.54	3.8	347	.21	.41	.65	.80				
56	78.5	105	.57	4.3	312	.08	.25	.57	.74				
57	75.5	105	.66	2.8	257	.05	.16	.33	.51				
58	71	105	.87	3.2	260		.14	.34	.54	.70			
59	70	105	.92	2.5	262	.08	.15	.32	.54				

*Mixtures of #2 Fuel Oil and Bonded Bunker C

Table V - continued

10 x 3 Nozzle

No.	Temp. °C.	Press. p.s.i.	Viscosity $cm^2/sec.$	n	D_o microns	Oil Used	R45	R50	R60	R70	R80	R100	R120
60	112	105	.16	3.0	152	BBC			.04	.13	.27	.44	
61	100	110	.16	2.4	140	2-247			.06	.13	.25	.38	
62	101	100	.26	2.7	175	2-150			.13	.29	.44	.57	
63	102	103	.23	3.1	167	2-207			.10	.21	.36	.55	
64	94	105	.28	3.1	187	BBC			.16	.30	.49	.65	
65	106	105	.19	2.6	152	BBC			.07	.16	.28	.46	
66	104	110	.14	2.6	152	2-247				.16	.31	.45	

10 x 3 Nozzle Oil used was a mixture of #2 fuel oil, BBC, and paraffin at room temperature.

No.	Press. p.s.i.	Viscosity $cm^2/sec.$	n	D_o microns	R40	R45	R50	R60	R70	R80	R100	R120	R140
67	60	.27	3.2	180				.14	.27	.44	.58		
68	170	.27	2.4	123					.05	.14	.25		
69	130	.27	2.5	140					.11	.25	.40	.56	
70	110	.28	2.0	153					.24	.36	.48	.60	
71	80	.28	2.5	163					.19	.39	.53	.70	
72	30	.28	2.7	280				.58	.68	.78	.83		
73	40	.28	2.9	245				.47	.62	.72	.76		
74	50	.28	2.6	208				.27	.46	.60	.70		
75	90	.09	2.5	137						.21	.37	.54	.69
76	30	.09	2.6	177					.26	.45	.57	.70	
77	165	.09	2.6	118						.15	.25	.43	.62
78	165	.45	2.9	155				.07	.18	.34	.47		
79	100	.45	2.7	188				.22	.35	.50	.61		
80	60	.45	2.4	243				.47	.58	.69	.77		
81	40	.45	4.2	305			.52	.75	.84				
82	100	.73	2.7	260			.33	.52	.64	.74			
83	167	.73	2.3	160				.12	.22	.35	.47		
84	143	.51	2.4	170				.16	.29	.42	.57		
85	165	.74	2.3	160				.19	.27	.39	.50		
86	110	.76	2.5	235				.37	.50	.61	.70		
87	167	.32	2.3	132					.10	.22	.34	.52	

Table V - continued

No.	Press. p.s.i.	Vis. $cm^2/sec.$	n	D_o microns	R45	R50	R60	R70	R80	R100	R120	R140	
88	162	.38	2.4	148				.15	.29	.43	.60		
89	40	.16	2.6	178				.30	.44	.58	.70		
90	168	.49	2.6	150				.18	.30	.43	.61		
91	70	.60	3.1	252	.14	.29	.50	.65					
92	126	.25		170			.13	.27	.42	.53			5" *
93	126	.25		210			.21	.46	.71	.77			9" *
94	126	.25		107					.12	.22	.35		1" *
95	126	.25		160				.21	.36	.51	.65		3.5" *
96	126	.25		179				.34	.47	.58			
97	126	.25		100					.42	.58	.67	.38	
98	95	.175		147					.12	.26	.42		

*Distance of sampling point from center of spray.

No.	Nozzle	Press. p.s.i.	Vis. $cm^2/sec.$	n	D_o microns	R40	R45	R50	R60	R70	R80	R100	R120	R140
99	8x5	126	.29	2.5	172					.29	.43	.57	.71	
100	11x2	121	.088	2.4	195						.52	.65	.76	
101	8x5	125	.11	2.0	125					.20	.30		.46	
102	11x2	121	.12		207					.46		.80		
103	T58x40	121	.14	2.2	138						.25	.38	.59	.66
104	12x3	121	.082	2.0	96							.21	.30	.43
105	12x3-2 slots	121	.082	2.0	87							.09	.19	.32
106	11x6	121	.105	2.9	206				.12	.32	.44	.58		
107	11x6	121	.095	3.0	225					.36	.55	.66		
108	18x6	121	.14		255					.60				
109	18x6	121	.105	4.0	290			.16	.32	.66	.81			
110	18x1	121	.102	3.6	235				.20	.39	.61			
111	11x1	50	.098	3.2	255		.11	.30	.49					
112	10x3	50	.26	2.8	220		.07	.18	.37	.48				
113	11x1	50	.175	2.6	247		.14	.26	.47					
114	18x1	126	.175	3.4	260			.30	.54	.67				
115	18x6	126	.23	4.5	300		.20	.48	.76	.89				

Table V - continued

No.	Nozzle	Press. p.s.i.	Vis. $cm^2/sec.$	n	D_o microns	R40	R45	R50	R60	R70	R80	R100	R120	R140
116	18x6	130	.50	4.5	370		.49	.77	.86					
117	18x6	55	.41	4.5	400		.61	.82	.90	.93				
118	10'x6	300	.26		126						.26	.34	.47	.62
119	11x2	55	.40	4.8	420	.45	.69	.87						
120	11x2	300	.83	3.4	260			.30	.56	.77				
121	11x2	300	.81	3.4	260			.28	.52	.68				
122	10'x6	300	.49	2.0	155					.27	.39	.48	.60	
123	11x1	120	.25	3.2	280									
124	10'x3	290	.11	2.0	90							.14	.25	.40
125	10'x3	300	.225	2.7	132							.34	.52	.66)
126	10'x3	300	.245	2.7	145							.40	.60	.72)
127	12x3	126	.27	3.0	183					.30	.50	.64	.77	
128	12x3	126	.22	2.8	160					.22	.36	.50	.69	
129	12x3-2slots	50	.22	2.8	225					.54	.67	.77		
130	10x3	121	.088		120								.44	
131	10x3	121	.122		120					.18			.44	

TABLE VI

VALUES OF DISCHARGE COEFFICIENTS AND CONE ANGLES FOR FRICTIONLESS FLOW

(Extrapolation to zero viscosity)

Nozzle		c_o	α_o	$\sqrt{c_o} \sin \alpha_o/2$
T 58x40 #2		.42	63°	.34
12x3	1 slot		60°	
	2 slot	.39	69°	.36
	4 slot	.50	69°	.40
12x1		.34		
12x2		.39	70°	.36
12x6		.61		
10x3		.36	83°	.40
10'x3	1 slot		84°	
	2 slot	.225	96°	.35
	4 slot	.36	95°	.44
10'x6		.47	81°	.45
11x1		.13	110°	.31
11x2		.170	111°	.34
11x6		.29	94°	.39
18x1		.10	120°	.28
18x2		.145	106°	.30
18x6		.27	92°	.37
15x3		.47	75°	.42

TABLE VII

DISCHARGE RATE DATA

T58 x 40 #2 Nozzle

P	p.s.i.	105	105	105	105	105	105	105		7.5	15	30	60	105	140
ν	$cm^2/sec.$	.20	.37	.40	.45	.52	.85	.99		.52	.52	.52	.52		
ρ	cms/cc	.94	.95	.95	.95	.96	.96	.96		.865					
c		.45	.57	.59	.63	.62	.60	.60		.57	.61	.61	.635	.615	.59
Q	cc/sec.	17.3	21.7	22.6	24.1	23.4	22.7	22.8		6.1	9.2	13.0	19.2	24.5	27.1

P	7.5	15	30	60	105	140		7.5	15	30	60	105	140	
ν	.43							.23						
ρ	.865							.86						
c	.61	.59	.64	.65	.63	.60		.65	.65	.57	.56	.525	.47	
Q	6.5	8.9	13.6	19.5	25.0	27.7		7.0	9.9	12.2	17.0	21.0	21.9	

P	7.5	15	30	60	105	140		7.5	15	30	60	105	140	
ν	.13							.034						
ρ	.86							.855						
c	.63	.64	.56	.48	.46	.42		.45	.43	.42	.40	.43	.42	
Q	6.7	9.6	11.9	14.5	18.3	19.6		4.8	6.5	9.0	12.1	17.1	19.3	

P	7.5	15	30	60	105	140		7.5	15	30	60	105	140	
ν	1.3							2.4						
ρ	.88							.88						
c	..37	.45	.50	.57	.57	.57		.25	.35	.41	.49	.51	.51	
Q	3.95	6.8	10.7	17.0	22.4	26.2		2.65	5.2	8.8	14.6	20.	24.0	

Lucite Model of T 58x40 #2 Nozzle

P	7.5	15	30	60	105	140					7.5	15	30	60	105	140
ν	.58	----------									.22	----------				
ρ	.865	----------									.86	----------				
c	.52	.55	.62	.64	.57	.59					.62	.66	.66	.60	.53	..47
Q	5.75	8.5	13.6	19.9	23.6	28.2					6.8	10.3	14.6	18.8	21.7	22.2

P	7.5	15	30	60							7.5	15	30	60	105	140
ν	.12	----------									.034	----------				
ρ	.86	----------									.855	----------				
c	.73	.63	.55	.50							.51	.40	.47	.44	.45	.43
Q	8.1	9,8	12.0	15.5							5.5	7.4	10.2	13.4	18.3	20.2

P	5.0	7.5	10	11	15	22.5	30	45	60	80	90	105	115	120			
ν	.14	----------															
ρ	.865	----------															
c	.61	.63	.65	.63	. 57	.53	.52	.48	.48	.46	.46	.47	.46	.47			
Q	5.5	6.9	8.3	8.5	8.9	10.0	11.2	12.9	15.1	16.4	17.8	19.3	19.5	20.7			

P	130	140	140	150		7.5	11	15	20	25	30		40	50			
ν	.14	----------				.07	----------										
ρ	.865	----------				.855	----------										
c	.47	.45	.44	.45		.55	.51	.51	.50	.46	.46		.45	.46			
Q	21.7	21.7	21.1	22.2		6.0	6.9	7.9	9.0	9.3	10.0		11.6	13.1			

P	60	80	137
ν	.07	---------	
ρ	.855	---------	
c	.46	.44	.44
Q	14.4	15.9	20.6

10x3 Nozzle

P		10	20	30	45	60	90	120	162		10	20	30	45	60
√	.032	----------									.079	----------			
ρ	.85	----------									.85	----------			
c		.39	.365	.37	.38	.38	.39	.37	.37		.37	.37	.37	.38	.39
Q		6.05	8.03	10.0	12.5	14.2	18.0	20.0	23.3		5.8	8.1	9.9	12.5	14.6

P	90	120	165		10	20	30	45	60	90	120	120	165	165
√	.079				.242	----------								
ρ	.85				.86	----------								
c	.38	.37	.38		.42	.41	.40	.39	.38	.37	.37	.37	.38	.37
Q	17.9	20.2	23.9		6.52	8.9	10.7	12.8	14.1	17.2	19.6	19.9	24.0	23.4

P	10	25	20	25	30	45	60	90	120	165		10	20	30	45
√	.58	----------										1.15	----------		
ρ	.885	----------										.895	----------		
c	.41	.40	.39	.43	.43	.41	.42	.41	.40	.40		.27	.34	.38	.42
Q	6.3	7.4	8.4	10.4	11.3	13.2	15.4	18.7	20.9	24.5		4.1	7.2	10.1	13.4

P	60	90	120	165	75		30	60	120	170		10	20	30	45
√	1.15	----------					8.65	----------				2.3	----------		
ρ	.895	----------					.91	----------				.86	----------		
c	.43	.46	.44	.41	.43		.044	.085	.16	.185		.185	.23	.27	.27
Q	15.8	21.0	23.2	25.2	18.0		1.55	3.1	8.3	11.5		2.87	4.70	7.20	8.75

P	60	90	120	165		10	20	45	60	90	120	165
√	2.3	----------				.43	----------					
ρ	.86	----------				.885	----------					
c	.33	.37	.39	.42		.43	.42	.40	.41	.40	.40	.38
Q	12.3	17.0	21.0	26.0		7.2	9.1	12.8	14.7	18.1	21.2	23.6

10x3 Nozzle

P	10	20	30	60	90	120	165
v	.76	----------					
ρ	.9	----------					
c	.32	.37	.41	.42	.40	.40	.37
Q	4.8	7.9	10.7	15.3	18.1	21.2	24.4

P	10	20	30	45	60	90	120
v	1.61	----------					
ρ	.9	----------					
c	.19	.25	.30	.33	.40	.40	.42
Q	2.9	5.35	7.8	10.7	14.5	18.1	22.0

P	165	20	40	60	70	120	160
v	1.61	.01	----------				
ρ	.9	1.0	----------				
c	.44	.36	.36	.36	.36	.36	.37
Q	27.2	7.4	10.2	12.7	13.8	17.9	21.1

	40	80	160
v	.08	----------	
ρ	1.135	----------	
c	.35	.35	.36
Q	9.5	13.4	19.5

	40	80	167
v	.15	----------	
ρ	1.183	----------	
c	.35	.35	.35
Q	9.1	13.1	19.1

11x6

P	3	7
v	.52	.73
ρ	.88	.88
c	.41	.46
Q	11.6	20.0

The following pressure on the maximum pressures for which a converging cone is obtained

12x3 1-s

P	36	41	70
v	.16	.37	52
ρ	.86	87	88
c	.40	.44	.49
Q	4.8	5.6	8. 2

10'x3 1s

P	53	65	95
v	37	52	.73
ρ	.87	88	89
c	.195	.195	.205
Q	7.9	8.6	11.0

10'x3 2s

P	17	45	57	60
v	.16	37	52	.73
ρ	.86	87	88	89
c	.27	.26	.285	.28
Q	6.3	9.6	11.9	11.9

10'x 3 4s

P	20	30	38	45
v	.16	37	52	.73
ρ	.86	87	88	89
c	.32	.41	.46	.40
Q	8.0	12.1	14.1	14.5

	11x1			11x2				11x6			
P	55	68	100	17	22	28	41	9.5	13	20	27
✓	37	52	.73	.16	37	52	.73	.16	37	52	73
ρ	.87	88	89	.86	87	88	89	.86	87	88	89
c	.10	.10	.087	.145	.28	.18	.184	.27	.37	.39	.41
Q	12.8	13.8	14.3	10.0	21.6	15.9	19.4	14.1	22.1	28,7	350

The following conditions are for a change from cone [illegible] to no cone [illegible]. The pressure given is the minimum pressure at which a cone [illegible] will be formed.

	12x3 1 slot		12x3 2 slots		12x3 4 slots		12x2		10'x3 1 slot		
P	40	65	35	75	78	122	83	126	8.5	15	25
✓	.37	.52	.37	.52	.37	.52	.37	.52	.37	.52	.73
ρ	.87	.88	.87	.88	.87	.88	.87	.88	.87	.88	.88
c	.44	.49	.48	.58	.63	.67	.69	.67	.19	.19	.20
Q	5.6		10.0		14.7		12.5	14.7	3.1	4.1	5.4

	10'x3 2 slots			10'x3 4 slots			10'x6			11x1			11x2		
P	6.5	10	20	4.5	7.5	16	20	40	80	17	17	39	3.25	5	11
✓	.37	.52	.73	.37	.53	.73	.37	.52	.73	.37	.52	.73	.37	.52	.73
ρ	.87	.88	.88	.87	.88	.88	.87	.88	.88	.87	.88	.88	.87	.88	.88
c	.30	.33	.34	.48	.48	.45	.70	.71	.67	.061	.08	.087	.16	.17	.15
Q	4.2	5.8	8.4	5.7	7.2	10.0	17.5	24.7	33.2	4.2	5.3	9.2	4.9	6.3	8.4

	11x6	
P	3	7
✓	.52	.73
ρ	.88	.88
c	.41	.46
Q	11.6	20.0

MISCELLANEOUS DISCHARGE COEFFICIENTS

Nozzle	12x3 1-s	12x3 2-3	12x3 4-s			12x1	12x2	12x6	10'x3 2-S	10'x3		10'x1	10'x2		
P		120	50	120	300	50	120	50	120	50	120	50	50		
ν		.068	.01	.068	.14	.01	068	.01	.068	.01	.068	.01	.01		
ρ		.855	1.0	.855	.89	1.0	855	1.0	.855	1.0	.855	1.0	1.0		
c		.39	..51	.50	.48	.34	.39	.61	.225	.38	.34	.21	.27		
Q		8.9	6.7	11.0	16.4	4.55	8.6	8.0	13.9	13.6	21.0	7.7	10.0		
	10'6			11x1		11x2			11x6		18x1		18x2		
P	50	120	300	50	120	50	120	300	50	120	50	120	50	120	300
ν	.01	.068	.144	.01	.068	.01	.068	.144	.01	.068	.01	.068	.01	.068	.144
ρ	1.0	.855	.89	1.0	.855	1.0	.855	.89	1.0	.855	1.0	.855	1.0	.855	.89
c	.47	.47	.48	.126	.170	.172	.167	.162	.31	.28	.105	.094	145	.145	.137
Q	17.3	28.8	46	14.0	21.0	19.1	31.3	46	34.0	51.0	17.3	25.8	24.0	40.3	58
	18x6														
P	50	120													
ν	.01	.068													
ρ	1.0	.855													
c	.27	.27													
Q	44.5	73.5													

TABLE VIII

CONE ANGLE AND VORTEX DATA

Lucite Model of T 58x40 (Data from photographs)

Press. p.s.i.	Viscosity $cm^2/sec.$	Cone Angle	r_i/r_o	Comments
7.5	.13			Solid jet
15	.13	67°		Cone but no visible vortex
7.5	.13			Solid jet
11	.13	60		Cone formed but no visible vortex
22.5	.13	55		" " " " " "
30	.13	53	.44	Vortex in tip of nozzle only
45	.13	48	.48	" " " " " "
60	.13	51	.48	" " " " " "
75	.13	55	.48	" " " " " "
105	.13	51	.50	" " " " " "
140	.13	56	.52	Vortex to back of nozzle
140	.13	54	.52	" " " " "
15	.084	40	.34	Vortex in tip of nozzle only
30	.084	49	.50	" " " " " "
45	.084	53	.58	" " " " " "
60	.084	56	.52	Vortex to back of nozzle
105	.084	54	.52	" " " " "
140	.084		.52	" " " " "
15	.032	49	.48	Vortex in tip of nozzle only
30	.032	59	.52	Vortex to back of nozzle
45	.032	61	.54	" " " " "
60	.032	61	.54	" " " " "
105	.032	59	.54	" " " " "
140	.032	61	.60	" " " " "

Table VIII - continued

Lucite model of 10x3 nozzle (photographic data)

Press. p.s.i.	Viscosity $cm^2/sec.$	Cone angle	r_1/r_o front	r_1/r_o back
20	.032	77	.67	.35
40	.032	78.5	.63	.35
80	.032	77.5		
160	.032	80		
20	.058	66	.63	.41
40	.058	80	.55	.38
80	.058	76	.60	.41
10	.12	57.5		
20	.12	67	.54	.38
40	.12	70.5		
80	.12	72		
20	.135	71		
40	.135	73	.55	.36
80	.135	71	.60	.35
160	.135	74	.54	.35
20	.24	55	.44	.19
40	.24	65		
40	.24	65	.51	.22
80	.24	66		
160	.24	66	.51	.27
20	.37	60	.32	0
40	.37	65	.47	.23
80	.37	65		
80	.37	65	.48	.32
20	.50	none	none	none
40	.50	65	0	0
80	.50	62.5	.30	.30
160	.50	62	.45	.26
20	.59	59	0	0
40	.59	62.5	.42	.23
80	.59	63	.45	.26
160	.59	63	.39	.23
80	1.05	none	none	none
120	1.05	70	0	0
160	1.05	60	.32	0

Table VIII - continued

Nozzle	Press.	Vis.	Angle
11x2	50	.01	103°
	140	.10	100
	160	.35	91
	160	1.10	77
	160	.16	103
11x6	50	.01	94
	140	.102	85
	160	.35	77
	160	1.10	64
	160	.16	87
12x3	50	.01	65
	140	.102	61
	165	.35	57
	160	.15	65
	21	.16	62
	25	.16	60
	30	.16	57
12x3-2s	50	.01	80
	140	.102	74
	165	.35	64
	160	.15	65
10x6	50	.01	79
10x3-2s	160	.15	83

Nozzle	Press.	Vis.	Angle
12x2	160	.15	53°
	160	.16	62
12x3-1s	160	.16	56
10x2-1s	160	.15	70
10'x3-2s	160	.16	86
10'x3-4s	160	.16	85
10'x3-1s	50	.01	83
10'x2	160	.16	88
18x1	50	.01	120
18x2	50	.01	106
18x6	50	.01	92

BIOGRAPHICAL NOTE

The author was born in Denver Col. in the year 1918. His preparatory education was obtained in the public schools of Wyoming and California. He received a B.S. degree in Mechanical Engineering from the University of California at Berkeley in May 1940. In September 1940 he enrolled in the Graduate School of Chemical Engineering of the Massachusetts Institute of Technology.

References

1. Kolupaev, P.G. "Atomization of Heavy Fuel Oil"
   Sc.D. Thesis, M.I.T. Course X 1941
2. Snuggs, J.F. "Atomization of Heavy Fuel Oils"
   S.M. Thesis, M.I.T. Course X 1938
3. Kuhn "Uber Die Zerstaubung Flüssiger Brennstoffe"
   Drs. Thesis Technical College Danzig University
   (Information on this work can be found in the book
   "Oil Burning" by Hendrik A. Romp)
4. Houghton Chemical Engineers Handbook by Perry 2-nd edition
5. Chang T.Y. "Combustion of Heavy Fuel Oils"
   Sc. D. Thesis, M.I.T. Course X 1941
6. Hottel, H.C. and Stewart, I. Mc. "Space Requirements
   for the Combustion of Powdered Coal"
   Ind. Eng. Chem., 32 719 (1940)